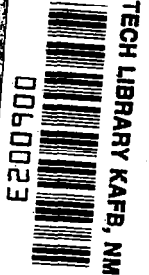
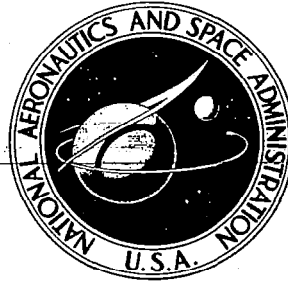


**NASA CONTRACTOR  
REPORT**



**NASA CR-913**

**DEVELOPMENT AND FLIGHT TESTING  
OF A FLUIDIC FLIGHT CONTROL SYSTEM**

*by D. L. Rodgers*

*Prepared by*  
**HONEYWELL INC.**  
**Minneapolis, Minn.**  
*for Flight Research Center*



**DEVELOPMENT AND FLIGHT TESTING OF  
A FLUIDIC FLIGHT CONTROL SYSTEM**

**By D. L. Rodgers**

Distribution of this report is provided in the interest of information exchange. Responsibility for the contents resides in the author or organization that prepared it.

**Issued by Originator as Report No. 20175-FR2**

**Prepared under Contract No. NAS 4-763 by  
HONEYWELL INC.  
Minneapolis, Minn.**

**for Flight Research Center**

**NATIONAL AERONAUTICS AND SPACE ADMINISTRATION**

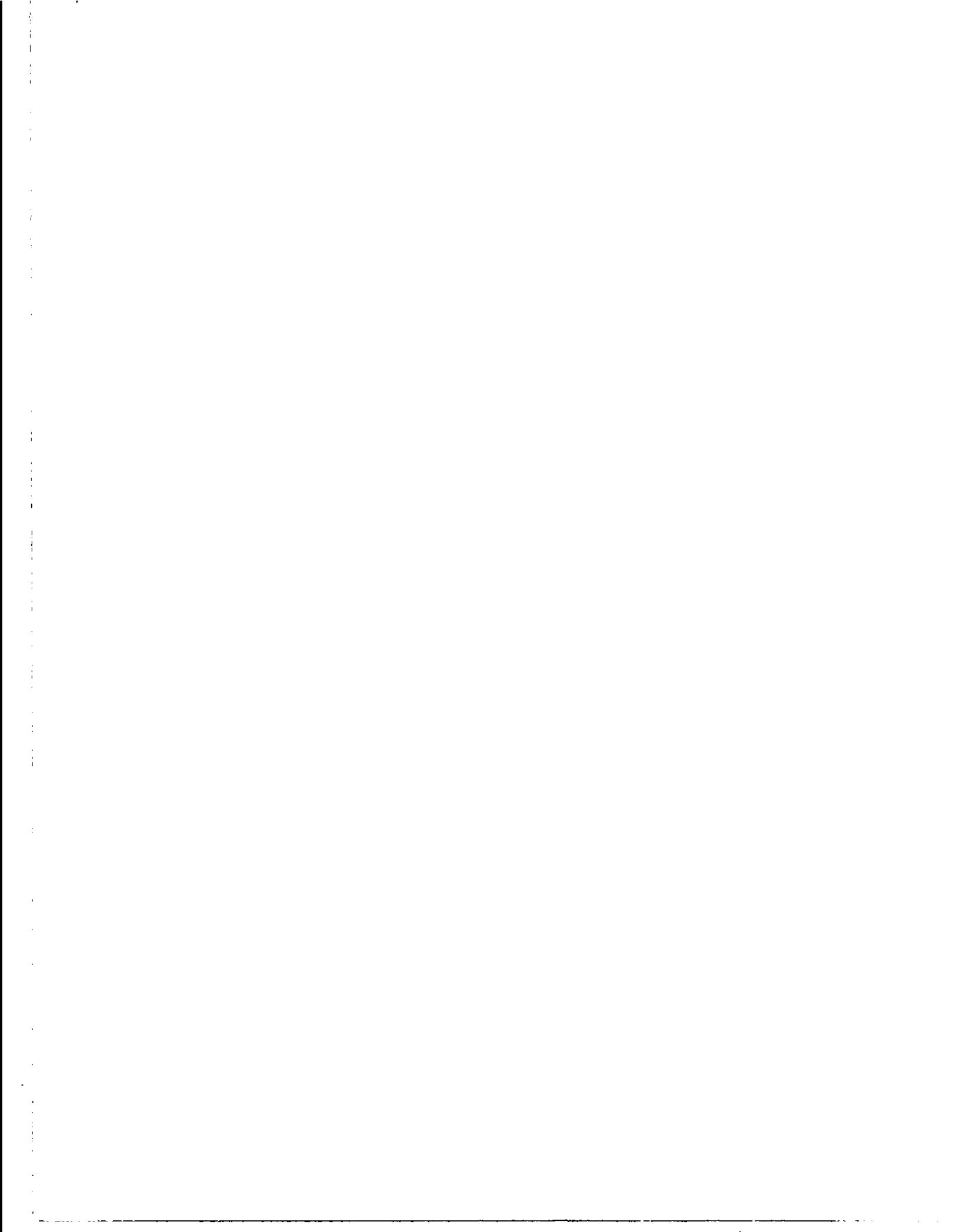


## FOREWORD

This report was prepared by the Fluid Flight Systems Section of Honeywell Inc. It fulfills contract NAS 4-763 Supplemental Agreement No. 3 for the NASA Flight Research Center and constitutes the final engineering report for that contract.

Eleven progress reports have been submitted at monthly intervals as required by Article II (a) of the contract. Copies of the final report are submitted in accordance with Article II(b).

This report covers work performed between 15 July 1965 and 15 December 1966. The work was monitored by Mr. Shu Gee and Mr. Wilton Lock of the NASA Flight Research Center - Edwards, California.



## ABSTRACT

A three-axis fluidic automatic flight control system was developed, installed, and flight tested in an Aero Commander 680 FP aircraft. The results of the analytical studies, system design work, and flight testing are presented in this report. The Honeywell Inc. assigned number for this system is FYG1001A-1.



## CONTENTS

	<b>Page</b>	
<b>SECTION I</b>	<b>INTRODUCTION</b>	<b>4</b>
<b>SECTION II</b>	<b>DESIGN ANALYSIS</b>	<b>6</b>
	Summary	6
	System Description	6
	Data And Assumptions	8
	Lateral Axis Analysis	12
	Longitudinal Axis Analysis	17
<b>SECTION III</b>	<b>DESIGN AND DEVELOPMENT</b>	<b>32</b>
	SUMMARY	32
	TEST AIRCRAFT DESCRIPTION	32
	SYSTEM DESCRIPTION	33
	SYSTEM DESIGN	39
	Stability Derivatives	41
	Roll and Pitch Configurations	42
	Component Locations	43
	Power Supply	45
	Component Design	70
	Developmental Tests	84
	Environmental Tests	96
<b>SECTION IV</b>	<b>FLIGHT TEST</b>	<b>102</b>
	Summary	102
	Installation	103
	Flight Test Instrumentation	108
	Contractor Checkout	111
<b>SECTION V</b>	<b>CONCLUSIONS AND RECOMMENDATIONS</b>	<b>137</b>

## ILLUSTRATIONS

Figure		Page
1	Final Lateral Axis Block Diagram	7
2	Longitudinal Axis Block Diagram	9
3	Lateral Axis Matrix	13
4	Lateral Axis Analog Diagram	15
5	Heading Gyro (Normalized)	16
6	Lateral Axis Performance	18
7	Root Locus Lateral Axis Final Data $T_{rH} = 2 \text{ sec.}, \delta_{r_r} = 0.3 \frac{\circ}{\sqrt{S}}$ Wings Leveler	19
8	Root Locus Lateral Axis Final Data $T_{rH} = 2 \text{ sec.}, \delta_{r_r} = 0.3 \frac{\circ}{\sqrt{S}}$ Heading Hold Autopilot $\delta_{a_r} = 0.5 \frac{\circ}{\sqrt{S}}$	20
9	Pitch Axis Matrix	22a
10	Pitch Axis Analog Computer Diagram	24
11	Pitch Axis Performance, Approach	25
12	Pitch Axis Performance, Approach	26
13	Pitch Axis Performance, Cruise	27
14	Root Locus Longitudinal Axis Cruise A Revised Pitch Rate Damper	30
15	Root Locus Longitudinal Axis Cruise A Revised Altitude Hold Autopilot $\delta_{e_{\dot{\theta}}} = 0.5 \frac{\circ}{\sqrt{S}}$	31
16	Lateral Axis Schematic	34
17	Longitudinal Axis Schematic	35
18	Plan View of Aero Commander Showing Fluid-System Installation	36

## ILLUSTRATIONS (Continued)

Figure		Page
19	Power Supply Schematic	40
20	Airborne Manufacturing Company Pump Model 423 Data	46
21	Pump Absolute Pressure Ratio	48
22	Servo Actuator Schematic	72
23	Servo Actuator Overpower Mechanism	73
24	Mechanization of High Pass Network	77
25	Frequency Response of High Pass Network	78
26	Lead-Lag Block Diagram	80
27	Frequency Response Lead Lag Network	81
28	Directional Gyro Pickoff Schematic	82
29	Directional Gyro Input/Output Relationship	83
30	Altitude Sensor Schematic	85
31	Altitude Sensor Input/Output Relationship	86
32	Yaw Axis Gain Curve	88
33	Roll Axis Gain Curve	89
34	Pitch Axis Gain Curve	90
35	Altitude Hold Frequency Response	92
36	Yaw Damper Frequency Response	93
37	Wing Leveler Frequency Response	94
38	Pitch Damper Frequency Response	95
39	Power Supply Pressure Level	107

## ILLUSTRATIONS (Continued)

<b>Figure</b>		<b>Page</b>
40	Control Flight Summary	112
41	Performance During Contractor Flight Checkout	118
42	Performance During Contractor Flight Checkout	119
43	Performance During Contractor Flight Checkout	120
44	Performance During Contractor Flight Checkout	121
45	Performance During Contractor Flight Checkout	122
46	Performance During Contractor Flight Checkout	123
47	Performance During Contractor Flight Checkout	124
48	Performance During Contractor Flight Checkout	125
49	Performance During Contractor Flight Checkout	126
50	Performance During Contractor Flight Checkout	127
51	Performance During Contractor Flight Checkout	128
52	Performance During Contractor Flight Checkout	129
53	Performance During Contractor Flight Checkout	130
54	Performance During Contractor Flight Checkout	131
55	Performance During Contractor Flight Checkout	132

## TABLES

Table		Page
1	Final Stability Derivatives	10
2	Lateral Transfer Functions, Final Data	14
3	Longitudinal Dimensional Stability Derivatives	22
4	Longitudinal Transfer Functions, "Cruise" Flight Revised (3 Feb. 1966)	29

## SUMMARY

This report covers the work performed in developing and flight testing a three-axis fluidic flight control system. The objectives of the program were to provide developmental and operational experience, and to provide an operating system that could be used as a flight demonstrator and a test bed for future more complex systems.

The control problem was analyzed using analog and digital computers and a system configuration was established. The aircraft was inspected to determine manual control system characteristics, possible component mounting locations, and interfacing system requirements. Component requirements were established.

Components were designed, fabricated, and bench tested. The system was then assembled and static, dynamic, and flightworthiness tests were accomplished.

The system was shipped to the NASA Flight Research Center, Edwards, California where it was installed in an Aero Commander 680 FP aircraft and flight tested.

This was the first aircraft fluidic flight control system, other than a rudimentary pitch damper and wing leveler, to be flight tested.

The system provides yaw damping, wing leveler, turn command, heading and altitude hold modes.

Performance of the lateral axis, yaw damper, wing leveler, heading and turn modes is competitively similar to conventional autopilots of similar configuration. Performance of the longitudinal axis, altitude hold mode, is very good from sea level to 6,000 feet. Above 6,000 feet, performance deteriorates as altitude is increased.

## SYMBOLS

$G$	Pressure gain
$\delta_{a_r}$	Wings-leveler gain, $\frac{\text{deg aileron}}{\text{deg/sec yaw rate}}$
$G_{\delta_{a_r}}$	Wings-leveler pressure gain, $\frac{\text{PSI}}{\text{PSI}}$
$\delta_{a_\psi}$	Heading gain, $\frac{\text{deg aileron}}{\text{deg heading}}$
$G_{\delta_{a_\psi}}$	Heading pressure gain, $\frac{\text{PSI}}{\text{PSI}}$
$\delta_{e_{\Delta h}}$	Altitude gain, $\frac{\text{deg elevator}}{\text{ft}}$
$G_{\delta_{e_{\Delta h}}}$	Altitude pressure gain, $\frac{\text{PSI}}{\text{PSI}}$
$\delta_{e_{\dot{\theta}}}$	Pitch-rate gain, $\frac{\text{deg elevator}}{\text{deg/sec pitch rate}}$
$G_{\delta_{e_{\dot{\theta}}}}$	Pitch-rate pressure gain, $\frac{\text{PSI}}{\text{PSI}}$
$\delta_{r_r}$	Yaw-damper gain, $\frac{\text{deg rudder}}{\text{deg/sec yaw rate}}$
$G_{\delta_{r_r}}$	Yaw-damper pressure gain, $\frac{\text{PSI}}{\text{PSI}}$
$g$	Acceleration due to gravity, $\text{ft/sec}^2$
$K$	transfer-function constant
$r$	Yaw rate, $\text{deg/sec}$
$s$	Laplace transform variable
$t$	time, $\text{sec}$

V	True airspeed, ft/sec
$\Delta h$	Altitude error, ft
$\Delta p$	Pressure differential, psig
$\delta_a$	Aileron-surface deflection, deg
$\epsilon$	Error
$\delta_e$	Elevator-surface deflection, deg
$\delta_r$	Rudder-surface deflection, deg
$\theta$	Pitch attitude, deg
$\dot{\theta}$	Pitch rate, deg/sec
$\tau$	Time constant, sec
$\phi$	Roll-attitude angle, deg
$\dot{\phi}$	Aircraft roll rate, deg/sec
$\psi_{ac}$	Aircraft heading, deg
$\psi_c$	Heading command, deg
$\psi$	Aircraft heading, deg
$\dot{\psi}$	Aircraft yaw rate, deg/sec
q	Aircraft pitch rate, deg/sec
$\bar{q}$	Dynamic pressure, $\frac{lb}{ft^2}$
j	$= \sqrt{-1}$
$U_1$	Steady state forward velocity ft/sec
p	Aircraft roll rate, deg/sec
$\beta$	Side slip angle, deg
$\psi_g$	Directional gyro heading scale factor, $\frac{PSI}{deg\psi}$

## SECTION I INTRODUCTION

Higher priced aircraft have long been equipped with automatic flight control systems which improved their handling qualities, stability, and flight safety. Low cost aircraft have generally not been equipped with such systems because of their prohibitive cost.

Recent fluidic technology developments give the potential for providing low cost of ownership automatic flight control systems to the light aircraft operator.

Most of the fluidic development to date has been on single components. Very few complete fluidic flight control systems have been mechanized and these have been very simple, single-axis designs.

Recognizing the need for low cost, reliable flight control systems, and the potential of the new fluidic technology, NASA sponsored a program to investigate and develop a fluidic autopilot.

The program began with a feasibility study contract to investigate various flight path control concepts that were suitable for fluidic mechanization. This work resulted in a contract amendment to design, develop, and fabricate the system discussed in this report.

The objectives of this phase of the program were:

- To provide development experience with fluidic flight control systems which would aid light aircraft pilots under adverse flying conditions.
- To provide operational experience with a fluidic system to determine its reliability.
- To provide an installation to be used to demonstrate fluidic system performance in flight.
- To provide a fluidic system test bed which could be modified to investigate more complex control functions.

The long range goal is to develop a flight control system providing full time stability augmentation and pilot relief. The Stability Augmentation System would be operative at all times; the pilot would fly the aircraft conventionally through manual controls with the control system providing augmented response. Upon release of control by the pilot, the system would return the aircraft to wings level and, if selected, altitude hold.

## SECTION II DESIGN ANALYSIS

### SUMMARY

This section describes the analytical design effort for the lateral and longitudinal axes of the control system.

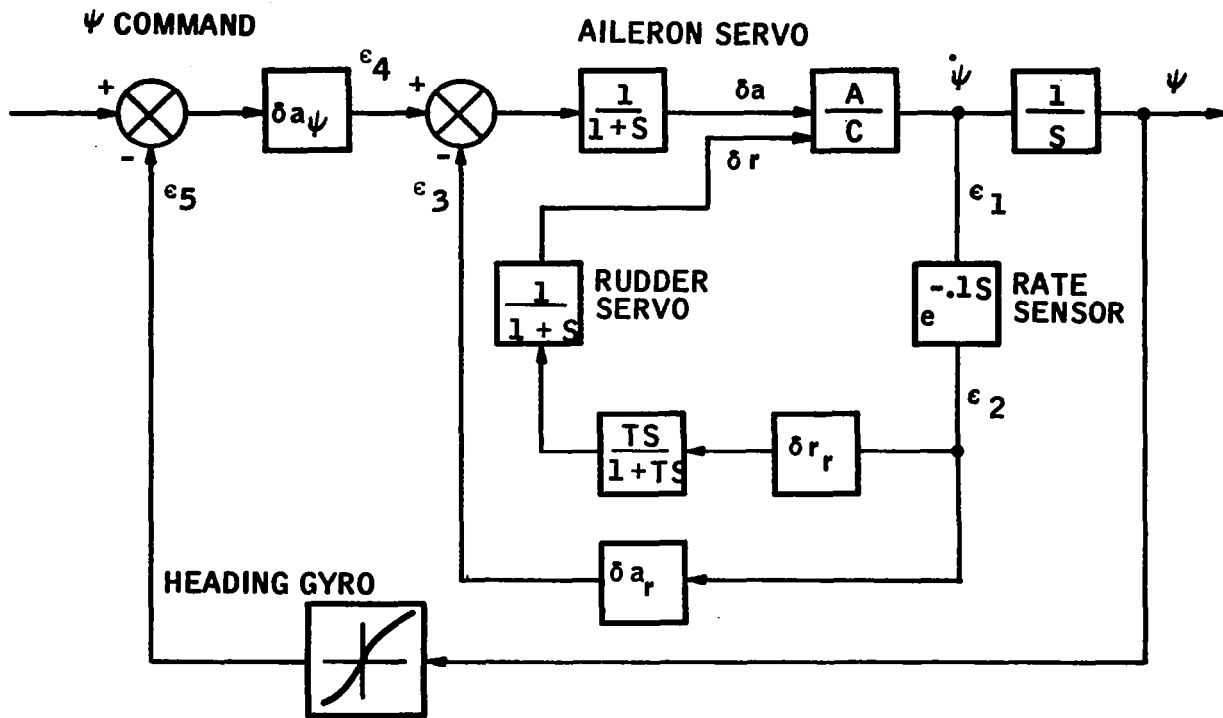
A preliminary control system was defined using estimated aerodynamic stability derivatives for the Aero Commander 680 FP airplane.

The preliminary lateral system provided aileron control only. A final lateral control system was defined based on aerodynamic stability derivatives provided by NASA. The final system provided rudder as well as aileron control. The heading hold control could not be achieved with aileron control only because of the undesirable adverse aileron yaw characteristics of the Aero Commander.

### SYSTEM DESCRIPTION

The block diagram for the final lateral control system is shown in Figure 1.

Yaw rate is sensed by a fluidic vortex rate sensor and summed at the aileron servo to form an inner damping loop. This control loop, yaw rate feedback to ailerons, is sometimes referred to as a "wing leveler" mode. Aircraft heading is sensed with a directional gyroscope and summed with yaw rate to form an outer heading loop. The gyroscope has a heading select feature which permits heading commands to be inserted by the pilot. The lateral system also has a yaw damper (yaw rate feedback to rudder). The aircraft yaw rate signal from the fluidic vortex rate sensor is shaped by a two second high pass network and fed to the rudder servo.



$$T = 2 \text{ SEC}$$

$$\delta r_r = 0.3 \frac{\text{°}\delta r}{\text{SEC}} \dot{\psi}$$

$$\delta a_r = 0.5 \frac{\text{°}\delta a}{\text{SEC}} \dot{\psi}$$

$$\delta a_\psi = 0.1 \text{°}\delta a / \psi$$

Figure 1. Final Lateral Axis Block Diagram

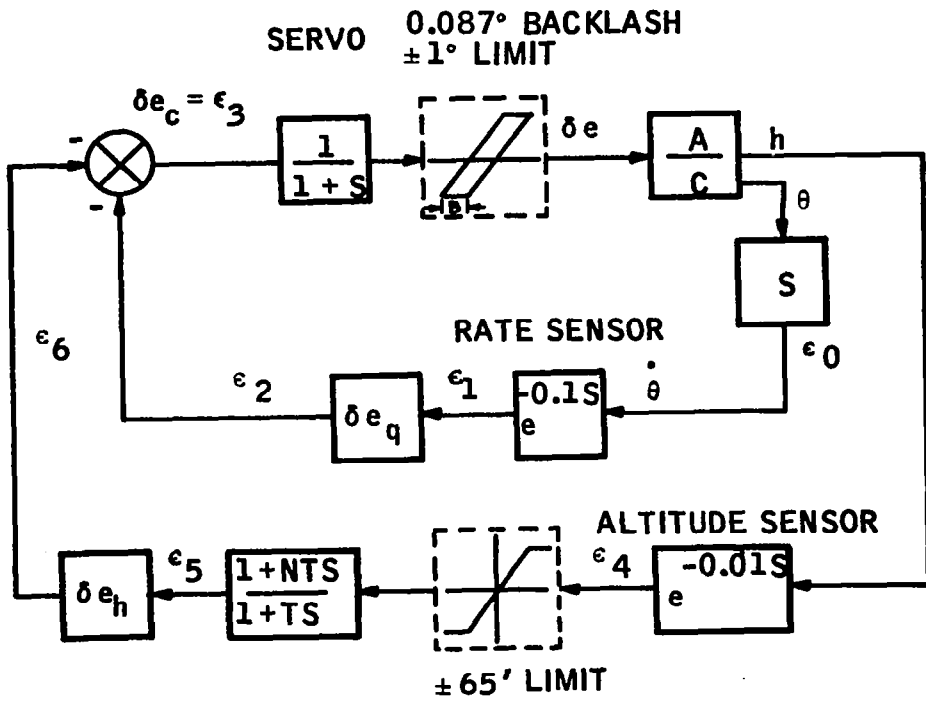
The block diagram of the longitudinal control system is shown in Figure 2.

Pitch rate is sensed with a fluidic vortex rate sensor and summed at the elevator servo to form the inner damping loop. Pressure altitude is sensed, shaped with a 10 to 1 lead network, and summed with the pitch rate signal at the elevator servo to complete the altitude hold autopilot. A feature of the system is that neither pitch attitude nor altitude rate is employed.

## DATA AND ASSUMPTIONS

The Aero Commander 680 FP was designated by NASA as the test aircraft. The aerodynamic stability derivatives for this aircraft had never been determined. These derivatives were required to analyze the control system requirements. It was necessary to estimate the derivatives by comparing the test aircraft configuration and dimensions to similar aircraft with known stability characteristics. The Cessna 310 and Jet Commander 1121 were used as "similar" mathematical models. Subsequently, flight test performance data obtained from the NASA Flight Research Center were used to verify or modify the estimated derivatives.

The final stability derivatives are given in Table 1, in radian-foot-second units. The control deflections follow the convention that a negative control deflection produces a positive moment. Positive aircraft motion is defined as a climbing, right-hand turn.



$$T = 0.5 \text{ SEC}$$

$$N = 10$$

$$\delta e_q = 0.5 \frac{\text{°}\delta e}{\text{SEC } \delta}$$

$$\delta e_h = 0.03 \frac{\text{°}\delta e}{\text{FT } h}$$

Figure 2. Longitudinal Axis Block Diagram

Table 1. Final Stability Derivatives

Yaw

Change in Side Force with Changing Sideslip Angle ( $C_{Y\beta}$ ) = -0.462

Change in Side Force with Change in Rudder Deflection ( $C_{Y\delta_r}$ ) = +0.205

Change in Side Force with Yawing Velocity Change ( $C_{Y_r}$ ) = 0.48

Change in Yawing Moment with Change in Sideslip ( $C_{n\beta}$ ) = 0.040

Change in Yawing Moment with Rudder Deflection Change ( $C_{n\delta_r}$ ) = -0.065

Change in Yawing Moment with Change in Yawing Velocity ( $C_{n_r}$ ) = -0.132

Change in Yawing Moment with Change in Rolling Velocity ( $C_{n_p}$ ) = 0.054

Change in Yawing Moment with Aileron Deflection Change ( $C_{n\delta_a}$ ) = 0.0123

Pitch

Pitching Moment Change with Angle of Attack Change ( $C_{m\alpha}$ ) = -0.624

Pitching Moment Change with Elevator Deflection Change ( $C_{m\delta_e}$ ) = -0.941

Pitching Moment Change with Varying Pitch Velocity ( $C_{m_q}$ ) = -12.02

Pitching Moment Change with Rate of Change of Angle of Attack ( $C_{m\dot{\alpha}}$ ) = -11.78

**Table 1. Final Stability Derivatives (Continued)**

Roll

Change in Rolling Moment with Aileron Deflection Change ( $C_{l_{\delta_a}}$ ) = -0.179

Change in Rolling Moment with Variation in Rudder Deflection ( $C_{l_{\delta_r}}$ ) = 0.024

Change in Rolling Moment with Change in Rolling Velocity ( $C_{l_p}$ ) = -0.581

Change in Rolling Moment with Yawing Velocity Change ( $C_{l_r}$ ) = 0.118

Change in Rolling Moment with Variation in Sideslip ( $C_{l_{\beta}}$ ) = -0.114

The moments of inertia used in the analysis are:

$$I_x = 9,200 \text{ slug ft.}^2$$

$$I_y = 6,800 \text{ slug ft.}^2$$

$$I_z = 15,000 \text{ slug ft.}^2$$

$$I_{yz} = 302 \text{ slug ft.}^2$$

The flight conditions used for the "cruise" flight condition were:

aircraft weight - 7,500 pounds

true airspeed - 230 mph

altitude - 8,000 feet

## LATERAL AXIS ANALYSIS

The equations of motion of the aircraft and the control equations lateral system are shown in matrix form in Figure 3. The lateral transfer functions for the free aircraft were calculated from this matrix and are shown on Table 2, using final values of the derivatives. A root locus analysis and an analog simulation were made using the matrix of Figure 4.

Inspection of the Table 2 transfer functions shows the yaw rate to aileron transfer function ( $r/\delta_a$ ) to contain a right hand plane zero. As a consequence, a stability problem exists which does not occur in the usual autopilot where the ailerons are normally controlled by roll axis, not yaw axis inputs. Deliberate cross-coupling of the roll and yaw axis is one consequence of using yaw rate and heading as aileron inputs.

The analog computer diagram is shown on Figure 4. Figure 5 shows the normalized non-linear heading gyroscope characteristics which were set up on a function generator as a part of the analog simulation. The simulation is time scaled to run 10 times as fast as real time. Aileron steps, beta gusts, and heading commands were used in evaluating performance.

The analog simulation was checked against the root locus plots by measuring critical gains and frequencies. Agreement was reached within 5 percent of the root locus predictions. The initial lateral axis configuration, no yaw damper, had the following characteristics:

- The yaw rate to aileron gain undamps the dutch roll mode, so a high gain wing leveler mode cannot be used except with aircraft having well damped, large  $N_r$ , or high frequency, large  $N_\beta$ , dutch roll roots.
- Closing the heading loop introduces a "lateral phugoid" which goes divergent at low frequencies due to adverse yaw phenomena;  $N_{\delta_a} > 0$  gives a right hand plane zero, a non-minimum phase system.

	1	2	3	4	5	6	7	8	9	10	
1	$-S$ -.1593	-.98875	.09	0	.0784						$\beta$
2	3.41	$-S^2$ -.8255	-.4695	.607	-6.17						$\psi$
3	-17.37	1.2145	$-S^2$ -6.125	-27	3.50						$\phi$
4				$-S-1$				1	1		$\delta_a$
5					$2S^2 + 3S + 1$		$\delta_r T_r S$				$\delta_r$
6		S				-1					$e_1 = 0$
7						$S^2$ -60S+ 1200	$-S^2$ -60S -1200				$e_2$
8							$\delta a_r$	1			$e_3$
9									1	$\delta a_\psi$	$e_4$
10		$S^2$ -60S 1200								$-S^2$ -60S -1200	$e_5$

x

= 0

Figure 3. Lateral Axis Matrix

Table 2. Lateral Transfer Functions, Final Data

$$\begin{aligned}
 p/\delta_a &= \frac{s (s + 0.4869 \pm 17098j) (27.66)}{D} \\
 r/\delta_a &= \frac{(s - 0.5857) (s + 7.81) (s + 0.7611) (-0.614)}{D} \\
 \beta/\delta_a &= \frac{(s + 0.1047) (s + 31.81) (0.607)}{D} \\
 Y/\delta_a &= \frac{(s + 0.07602) (s + 20.85 \pm 2.597j) (-0.0781)}{D} \\
 p/\delta_r &= \frac{(s + 4.517) (s - 6.013) (-3.512)}{D} \\
 r/\delta_r &= \frac{(s + 6.435) (s + 0.03362 \pm 0.4634j)}{D} \\
 \beta/\delta_r &= \frac{(s - 0.01026) (s + 86.02) (s + 6.588) (-0.0706)}{D} \\
 Y/\delta_r &= \frac{(s - 0.00833) (s + 6.328) (s - 3.176) (s + 2.928) (-0.787)}{D} \\
 D &= (s + 0.02969) (s + 6.378) (s + 0.4057 \pm 2.194j)
 \end{aligned}$$

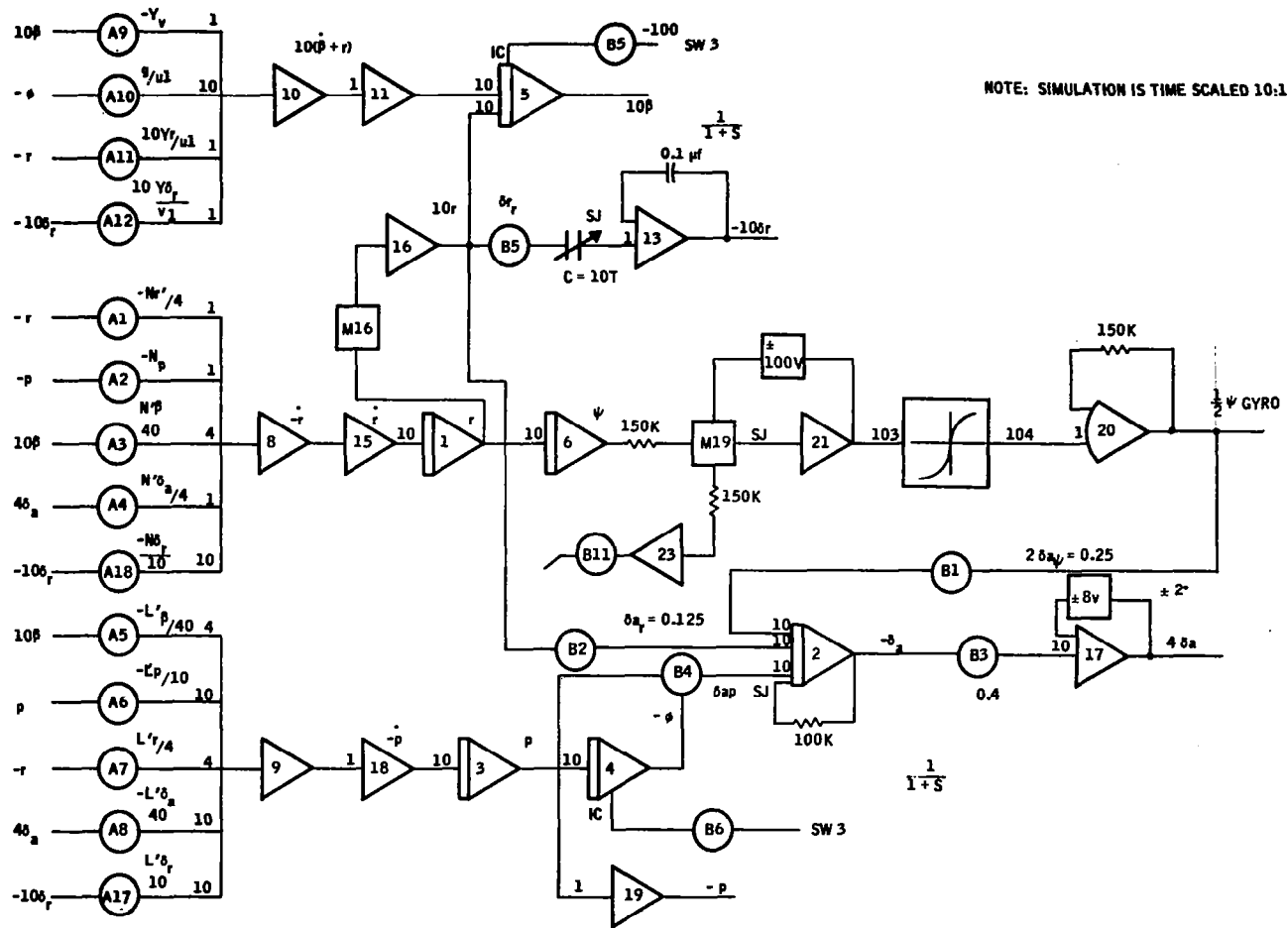


Figure 4. Lateral Axis Analog Diagram

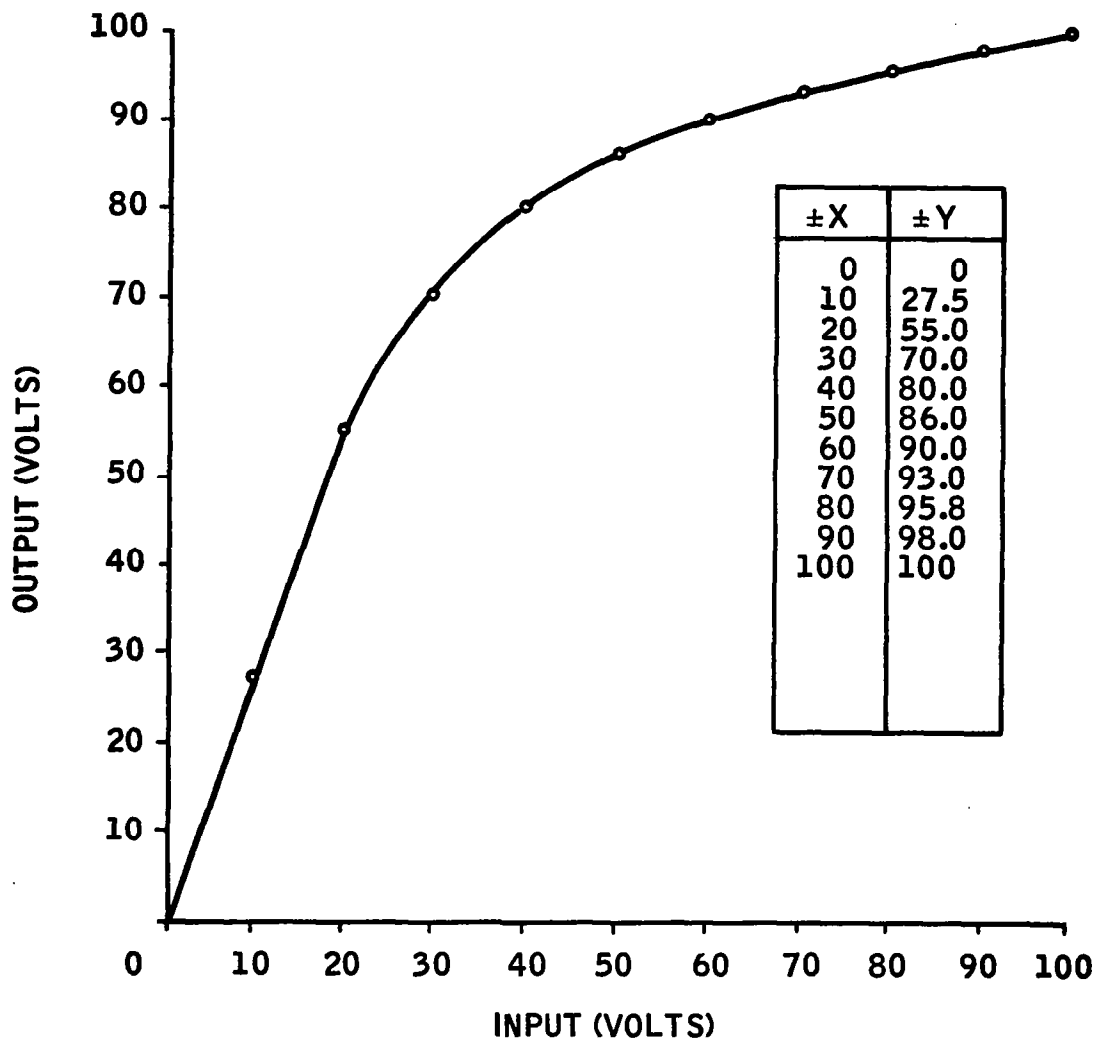


Figure 5. Heading Gyro (Normalized)

- Increasing the wing leveler gain tends to stabilize the "phugoid" but only at the price of undamping the dutch roll mode. The result is that both a minimum and a maximum stable yaw rate to aileron gain exists.

Analog results show performance of the aircraft without yaw damping to be unacceptable; both low frequency and dutch roll frequency damping are excessively low for anything approaching the desired response speed (3 degrees per second heading rate). When the non-linear gain of the heading sensor (Figure 5) is included, damping becomes totally unacceptable in level flight.

Tilting the rate sensor adds a roll rate component to the aileron signal which increases damping of the dutch roll mode but also tends to reduce the heading angle response speed. An optimum gain combination which slightly improves system damping does exist, but this improvement is not sufficient to yield acceptable performance.

The effect of a yaw damper in this application is to add lead at the dutch roll frequency sufficient to permit increasing the yaw rate to aileron gain such that the "phugoid" can be successfully damped. In addition, the yaw damper makes possible a significant improvement in response speed.

The yaw damper was added to the system for the above reasons. The final lateral axis configuration is as shown in Figure 1. Analog simulation results are shown in Figure 6. Figures 7 and 8 are the root locus plots for the final lateral axis configuration.

## LONGITUDINAL AXIS ANALYSIS

Figure 2 is the block diagram of the longitudinal axis control system.

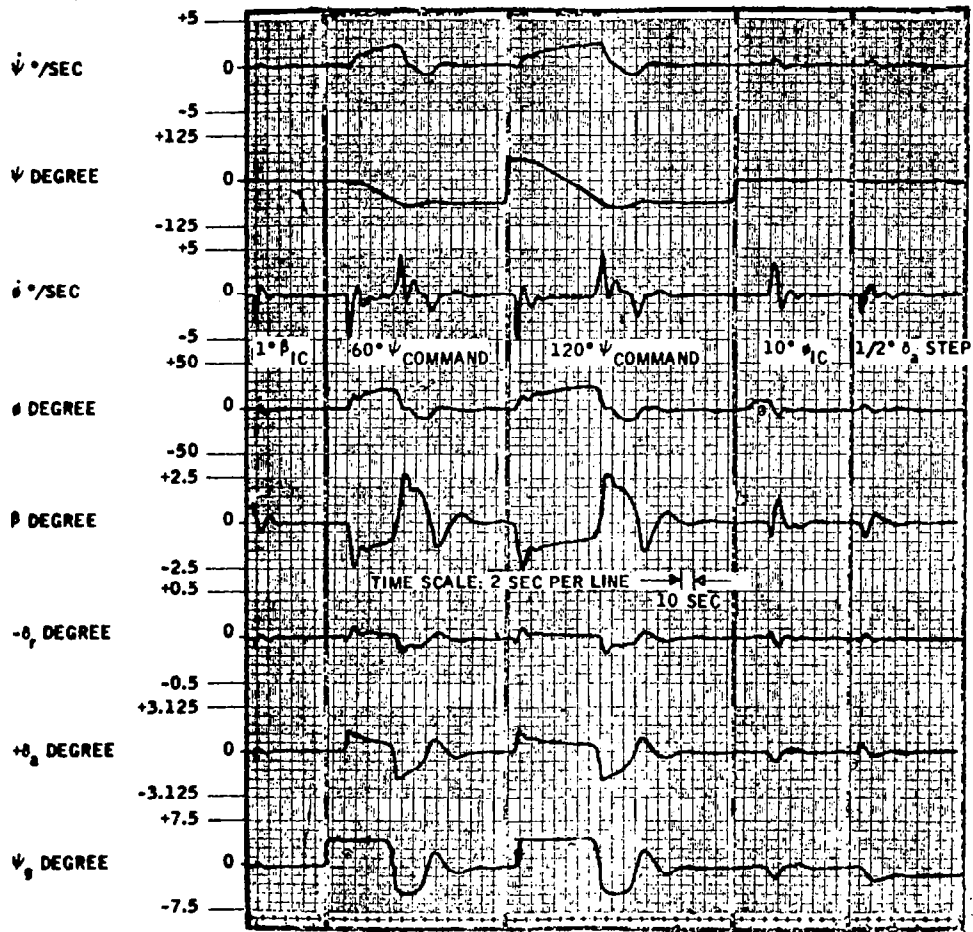


Figure 6 Lateral Axis Performance



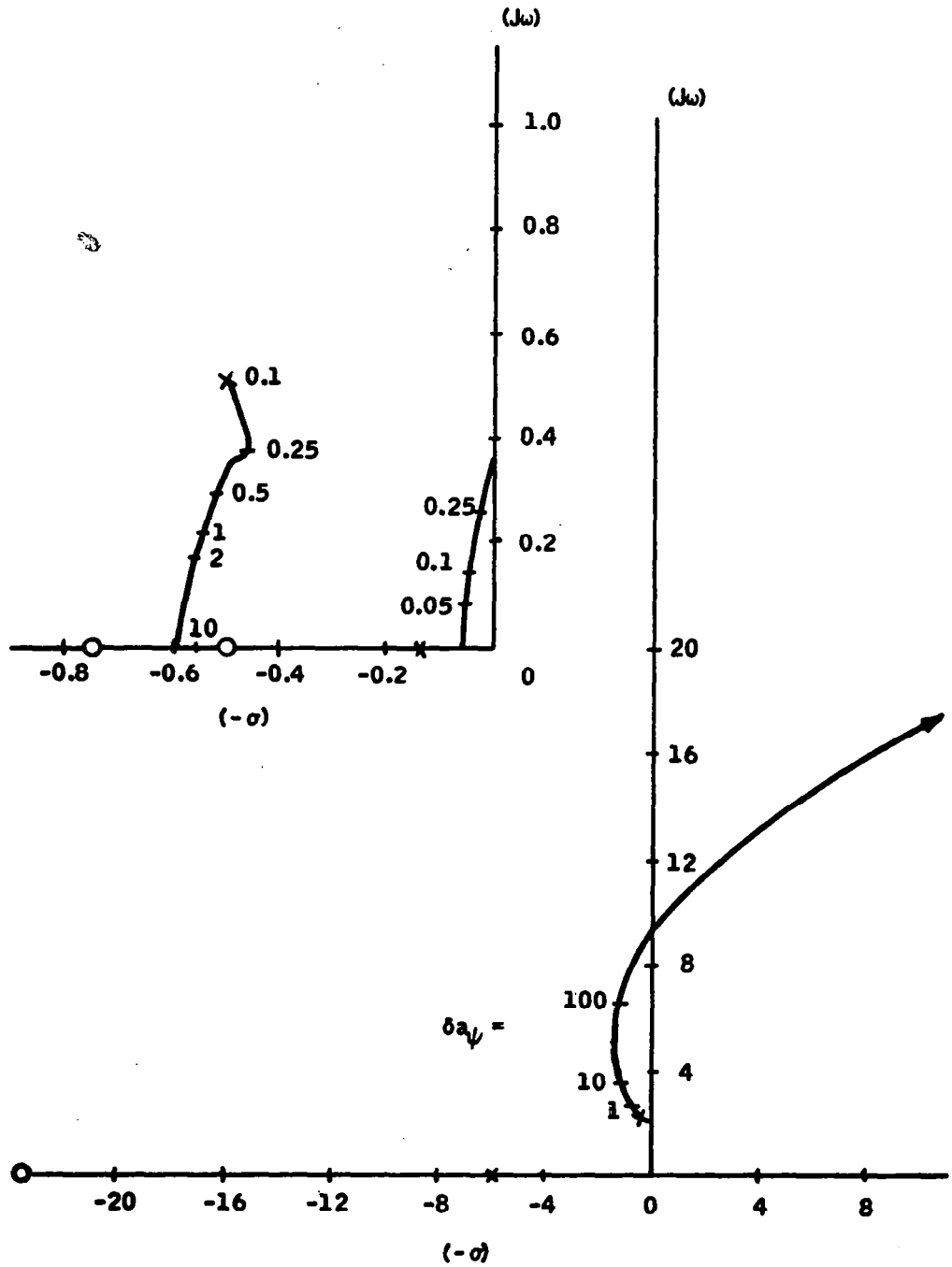


Figure 8. Root Locus Lateral Axis Final Data

$$T_{r_H} = 2 \text{ sec.}, \delta_{r_r} = 0.3 \frac{\circ}{S}$$

$$\text{Heading Hold Autopilot } \delta_{a_r} = 0.5 \frac{\circ}{S}$$

Aerodynamic stability derivatives provided by NASA are given in Table 1. A pitch axis analysis using these derivatives showed that short period performance was good with an altitude error response time of under three seconds and a 0.4 damping ratio. However, there was a long period altitude divergence, apparently caused by inaccuracies in the airspeed derivatives. This long period divergence did not occur if airspeed was constant, nor had it been observed in flight. Consequently, it was ignored in optimizing the gains. A restudy of the airspeed derivatives,  $X_u$  and  $Z_u$ , was made and they were found to be in error.

The dimensional stability derivatives used for the restudy are shown on Table 3. The final values provided by NASA are "approach" and "Cruise A". A matrix of the equations of motion and of the autopilot control equations are shown on Figure 9. Servo backlash is not included in the matrix for the digital computer analysis but was simulated in the analog computer study. The rate sensor is represented by a second order approximation valid up to approximately two cycles per second. The altitude sensor is also represented by a second order approximation.

Root locus plots of the system were made using digital computer solutions of the Figure 9 matrix and the stability derivatives of Table 3. The 100 millisecond rate sensor was approximated as

$$e^{-0.1s} = \frac{s^2 - 60s + 1200}{s^2 + 60s + 1200}$$

and the 10 millisecond altitude sensor was approximated as

$$e^{-0.01s} = \frac{s^2 - 600s + 1,440,000}{s^2 + 600s + 1,440,000}$$

The servo was assumed to be a one second first order lag, i. e. ,

$$\frac{\delta_e}{\delta e_c} = \frac{1}{1 + s}$$

Table 3. Longitudinal Dimensional Stability Derivatives

Parameter Description	Condition Approach Set	Condition Cruise A Set
$\bar{q}$ (PSF)	31.42	50.91
$U_1$ (FPS)	183.0	234.0
W (LBS)	7770.0	7220.0
$M_{\delta_e}$ sec <sup>-2</sup>	- 9.0	- 10.4
$M_q$ sec <sup>-2</sup>	- 1.45	- 1.65
$M_\alpha$ sec <sup>-2</sup>	- 4.21	- 6.90
$M_{\dot{\alpha}}$ sec <sup>-2</sup>	- 1.83	- 1.62
$Z_u$ sec <sup>-1</sup>	- 0.352	- 0.278
$Z_w$ sec <sup>-1</sup>	- 1.11	- 1.12
$Z_{\delta_e}$ sec <sup>-1</sup>	- 12.0	- 19.4
$X_u$ sec <sup>-1</sup>	- 0.040	- 0.015
$X_w$ sec <sup>-1</sup>	+ 0.026	+ 0.035





and the altitude shaping network was assumed to be

$$\frac{1 + 5s}{1 + 0.5s}$$

Root locus plots were made for both approach and cruise flight conditions, as well as for the inner rate loop and for the complete altitude loop using a nominal rate gain of unity, respectively.

An analog computer simulation of the Figure 9 equations of motion was made and is shown on Figure 10. The altitude sensor time delay was not mechanized but a servo backlash simulation was inserted. The root locus plots were verified by measuring aircraft short period and long period natural frequencies and damping ratios as well as closed loop maximum and minimum critical gains and frequencies. Agreement was within 5 percent.

Selected analog results are shown on Figures 11, 12 and 13. In these cases, the pitch rate gain was unity. Figure 11 shows the altitude loop response to a 5 degree initial condition on angle of attack,  $\alpha$ . The elevator per altitude gain is 0.015 degree per foot and the change in airspeed rather than elevator angle is shown on the last recorder channel to point out the unusual backside of the power curve altitude and airspeed behavior.

Figure 12 shows 2 degrees and 50-foot altitude initial condition responses for the same flight condition as Figure 11 but the altitude gain has been doubled, a  $\pm 1$  degree limit has been placed on elevator displacement, and 0.087 degree backlash has been inserted.

Figure 13 is the same as Figure 12 except that the cruise flight condition is displayed.

The short period performance of this mode is good. In response to a 50-foot initial condition on altitude, the time to 90 percent of the short period final



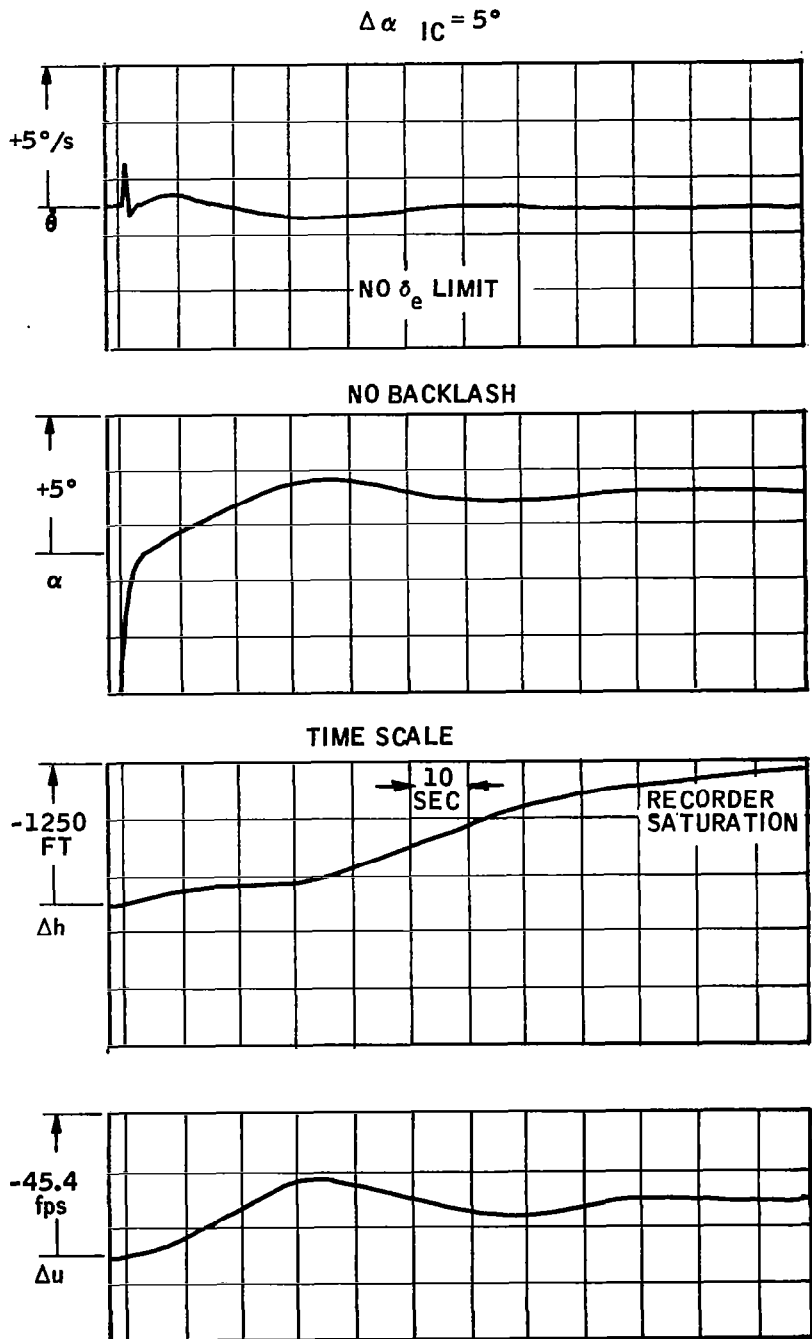


Figure 11. Pitch Axis Performance, Approach

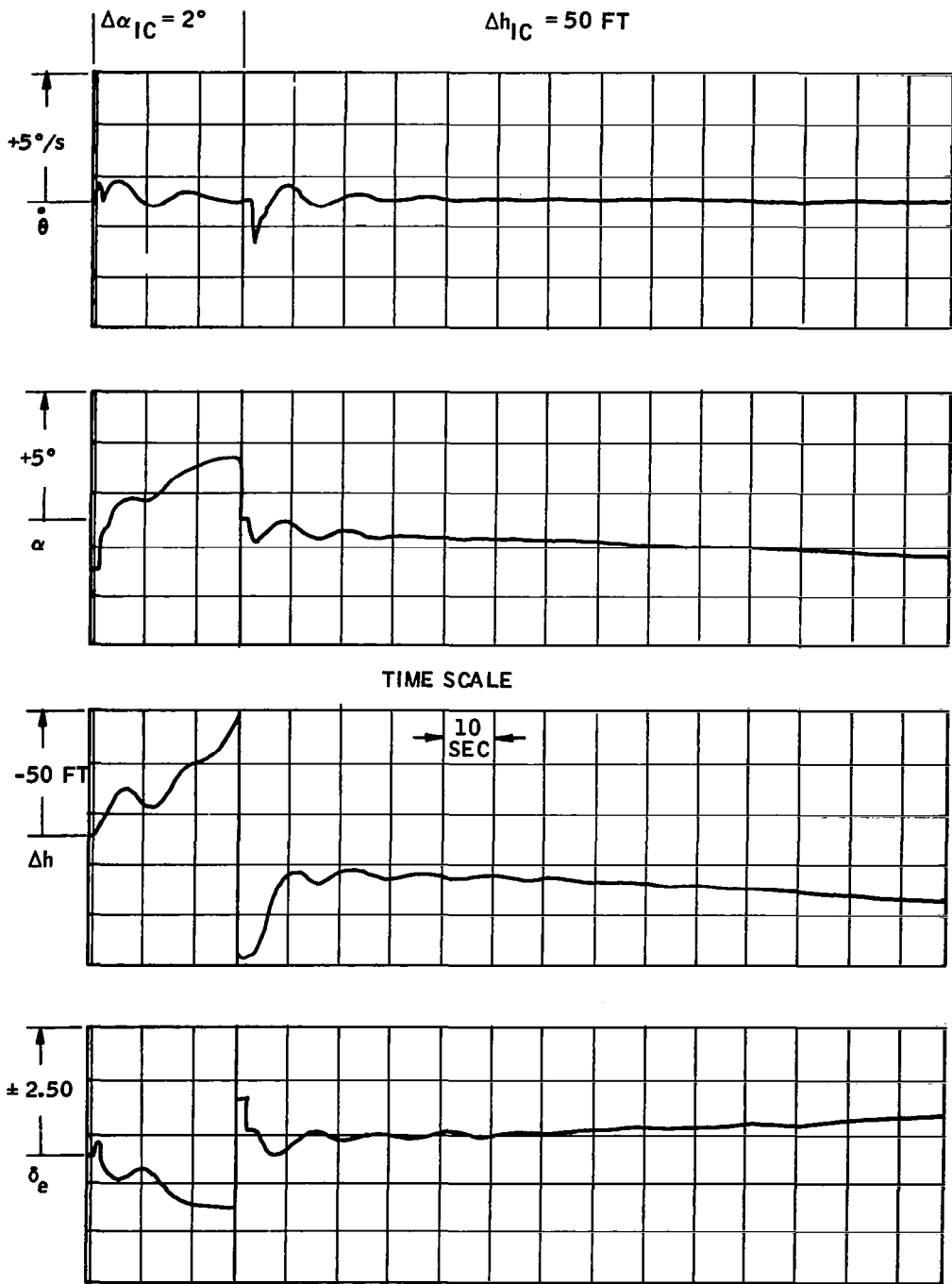


Figure 12. Pitch Axis Performance, Approach

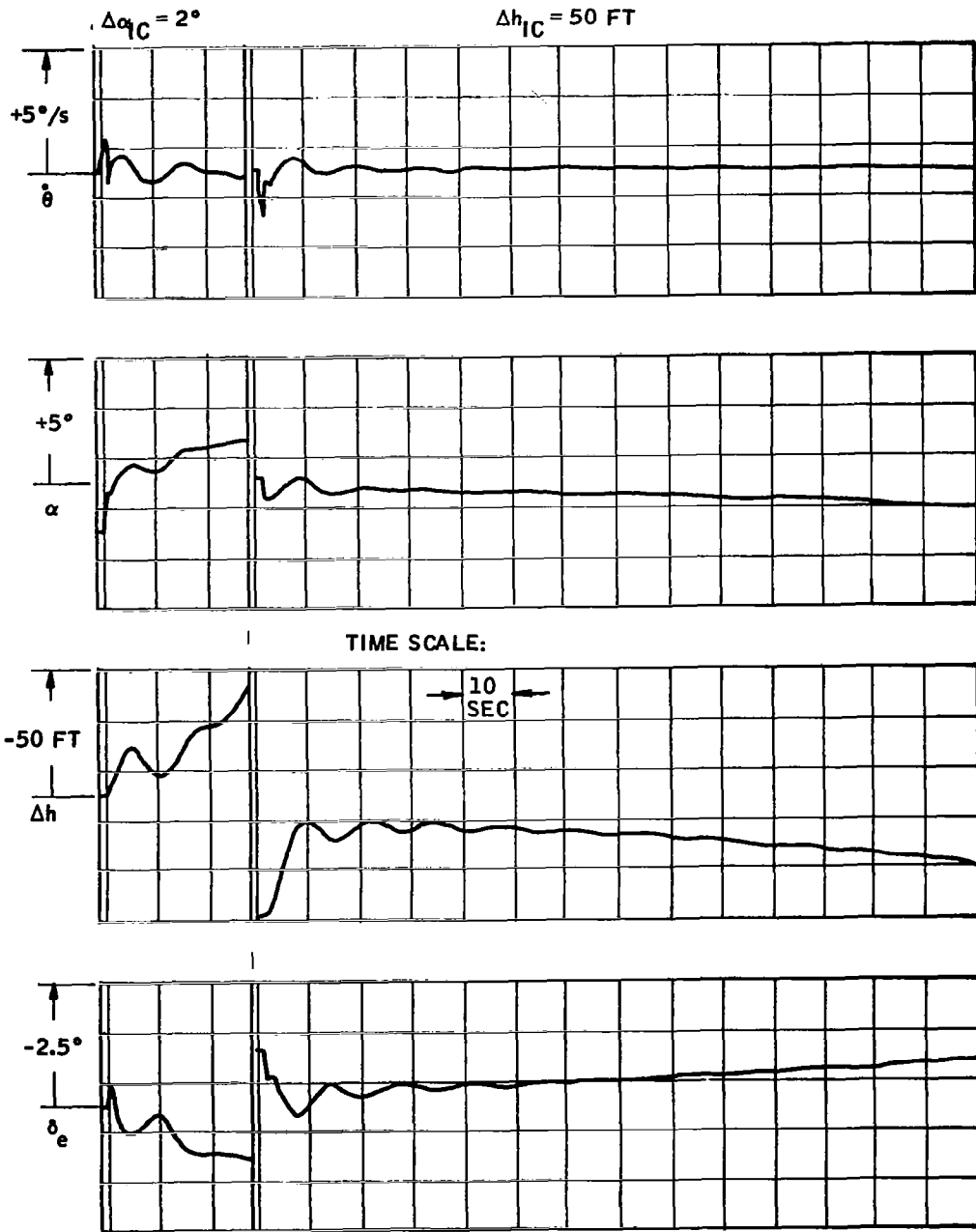


Figure 13. Pitch Axis Performance, Cruise

value is less than 10 seconds with a frequency of 0.4 radian per second and a damping ratio of 0.4. However, the unstable root begins to dominate the response within a minute and the elevator begins slowly moving in a direction which increases altitude error. Airspeed moves in the same direction as altitude, a "back-side of the power curve" characteristic.

If airspeed is held constant, the altitude hold mode behaves quite normally.

The effect of backlash in the servo is an apparent underdamping of the small amplitude performance. A comparison of pitch rate and angle of attack on Figures 11, 12 and 13 shows a 15-second period oscillation with an amplitude of about two feet to be superimposed upon the major response of Figures 11 and 12.

The  $\pm 1$  degree servo authority seems quite adequate to handle the disturbance used here, i. e., a 50-foot altitude command will initially saturate the servo but this only increases the response time. A 5 degree initial condition on angle of attack, corresponding to at least a 16-foot per second sharp edge gust will initially saturate the servo.

The restudy of the airspeed derivatives resulted in new values. For "Cruise A" configuration the revised numbers are:

$$Z_u = -0.24$$

$$X_u = -0.054$$

The pitch axis transfer functions were recalculated and are shown on Table 4.

With this revision of the airspeed derivatives the altitude hold autopilot is stable, i. e., the long period aperiodic divergence is not present, and demonstrates the same response otherwise as previously documented above. The root locus plots for the Cruise A revised data are shown as Figures 14 and 15.

Table 4. Longitudinal Transfer Functions, "Cruise"  
Flight Revised (3 Feb. 1966)

$$\frac{\alpha}{\delta_e} = \frac{-0.0829 (s + 0.02687 \pm 0.1785j) (s + 127.1)}{D}$$

$$\frac{\theta}{\delta_e} = \frac{-10.27 (s + 0.06237) (s + 1.071)}{D}$$

$$\frac{u}{\delta_e} = \frac{0.0029015 (s + 1.454) (s - 361.2)}{D}$$

$$D = (s + 0.02429 \pm 0.1595j) (s + 2.197 \pm 1.981j)$$

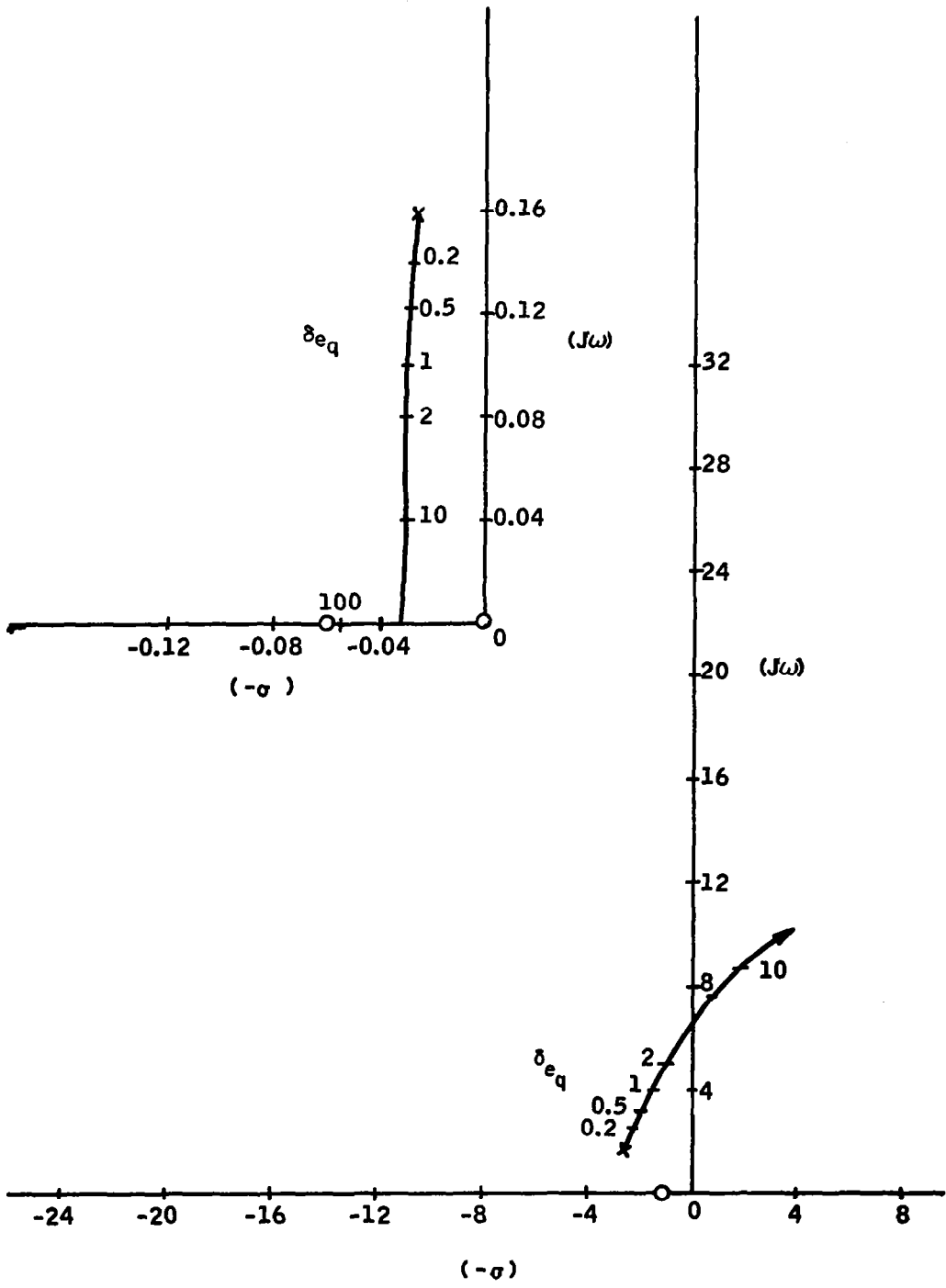


Figure 14. Root Locus Longitudinal Axis Cruise A Revised Pitch Rate Damper

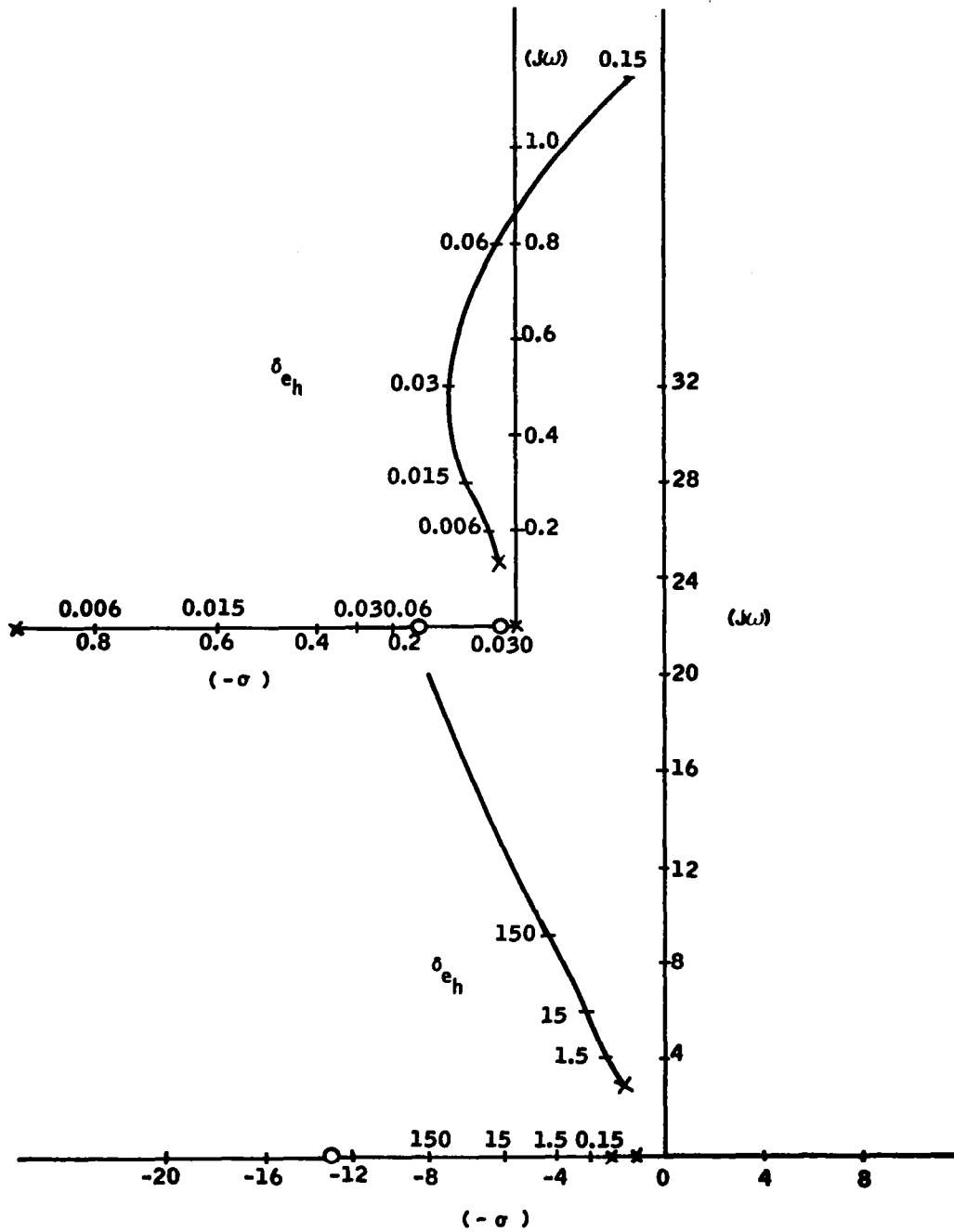


Figure 15. Root Locus Longitudinal Axis Cruise A  
 Revised Altitude Hold Autopilot  $\delta_{e\dot{\theta}} = 0.5 \frac{\dot{\theta}}{s}$

## SECTION III DESIGN AND DEVELOPMENT

### SUMMARY

A three-axis fluidic automatic flight control system was defined based on the block diagrams that resulted from the analytical studies. The analog studies provided performance predictions which were useful in the subsequent flight test program.

### TEST AIRCRAFT DESCRIPTION

An Aero Commander 680 FP aircraft was chosen by the NASA as the test aircraft for the fluid control system. This aircraft is used by the NASA FRC as a general utility vehicle which enabled the system to be evaluated under typical operating conditions. The 680 FP is a seven-place, high-wing aircraft with two Lycoming IGSO-540-B1A engines. It is equipped with landing flaps, retractable tricycle landing gear, and has a pressurized cabin and a deicing system.

The wing span is 49 feet and the maximum gross weight is 8,000 pounds.

The airplane has a fixed horizontal-stabilizer and conventional aileron, rudder, and elevator control surfaces. The cockpit controls consist of a wheel (for pitch and roll control) and rudder pedals (for yaw control).

## SYSTEM DESCRIPTION

The block diagrams for the fluidic system are shown on Figures 1 and 2. The circuit schematics for the lateral and longitudinal control axes are shown on Figures 16 and 17, respectively. Figure 18 shows all the major components of the system.

The system provides three-axis control--yaw, roll, and pitch. The aircraft parameters that are sensed are yaw rate, pitch rate, altitude error, and aircraft heading. The control system provides yaw damping, wing-leveling, heading hold, and altitude hold modes.

Yaw rate is sensed by a vortex rate sensor for both the yaw and roll control axes. Yaw axis control is achieved by shaping the yaw rate signal with a 2-second high pass network, amplifying it, and then feeding it into the rudder servo. The calculated gain of the yaw axis is  $0.3 \frac{\delta_r}{\text{sec } r}$ ; 0.3 degree of rudder is commanded for each degree per second of yaw rate. The 2-second high pass network blocks steady state yaw rate signals which allows the aircraft to make constant rate heading changes unopposed by the rudder. The rudder servo is connected in parallel with the normal rudder controls. Any servo output is reflected in rudder pedal motion.

The pilot has a yaw trim control with which biases and null shifts in the yaw axis can be eliminated.

A cockpit trim indicator displays the presence of an error signal at the output of the pulse width modulator. By observation of the yaw trim indicator and use of the yaw trim control, the pilot can accomplish pre-engage trimming of the yaw axis as well as trimming after engagement. This permits elimination of engage transients as well as balancing of aircraft surface asymmetries.

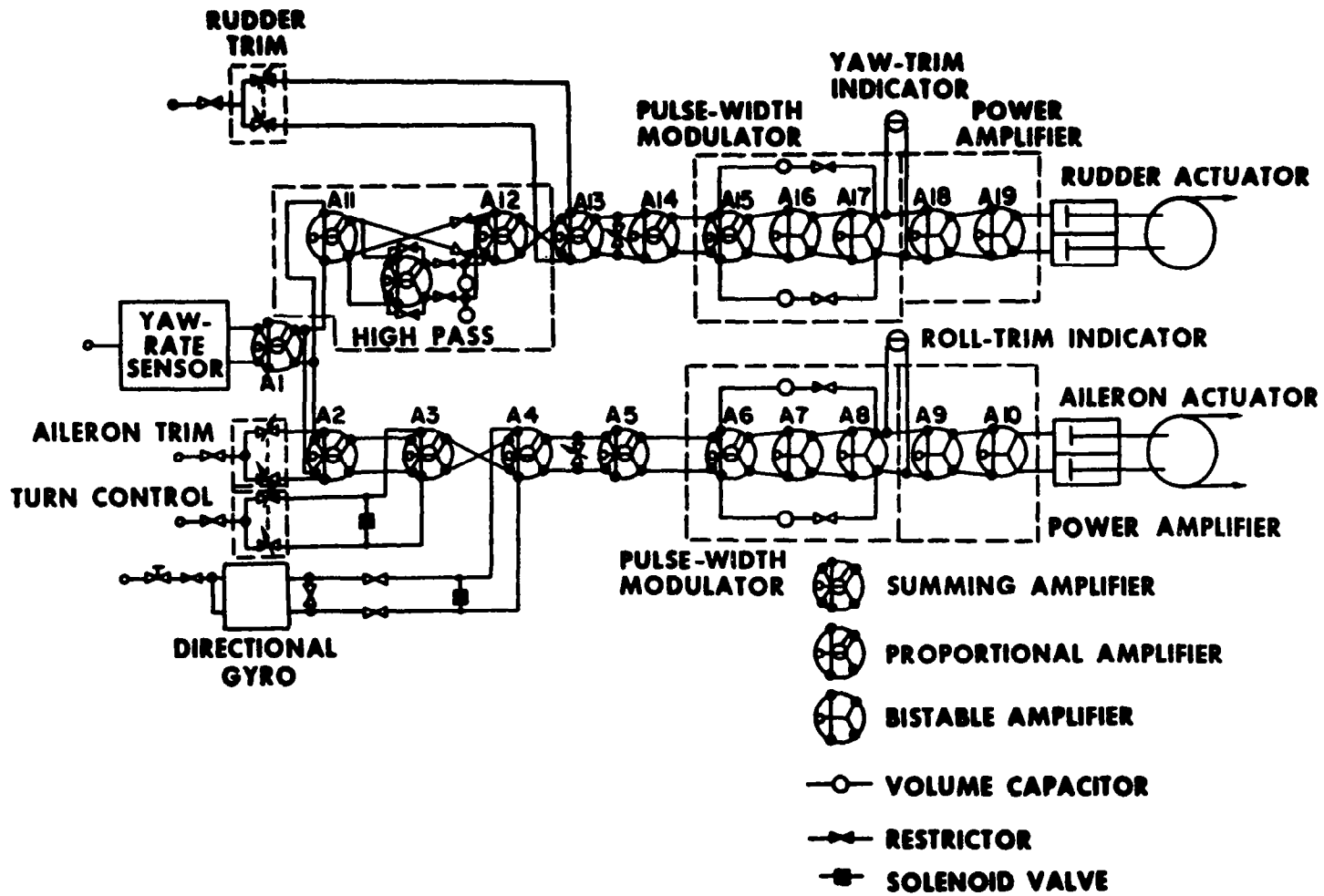


Figure 16. Lateral Axis Schematic

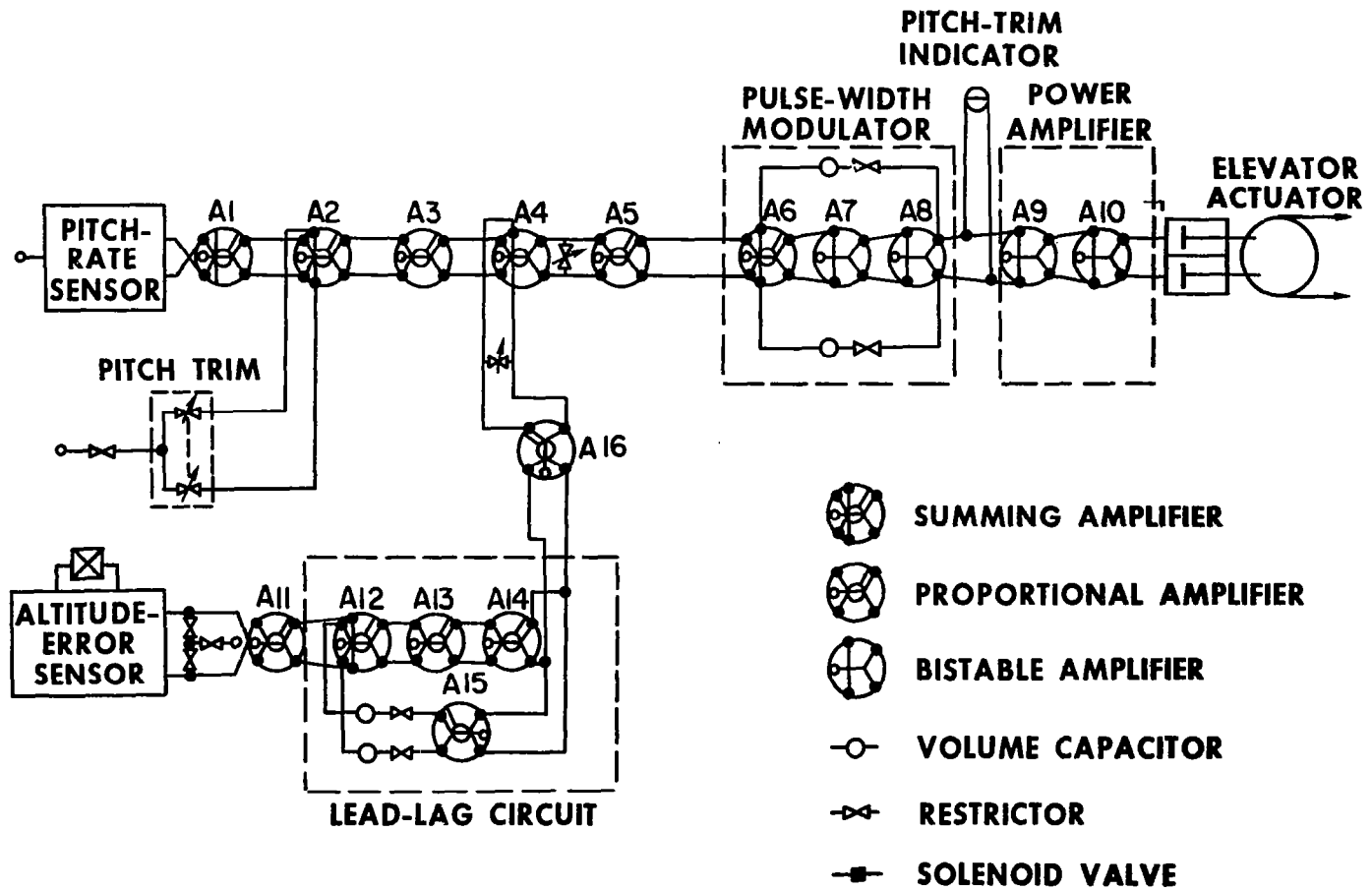


Figure 17. Longitudinal Axis Schematic

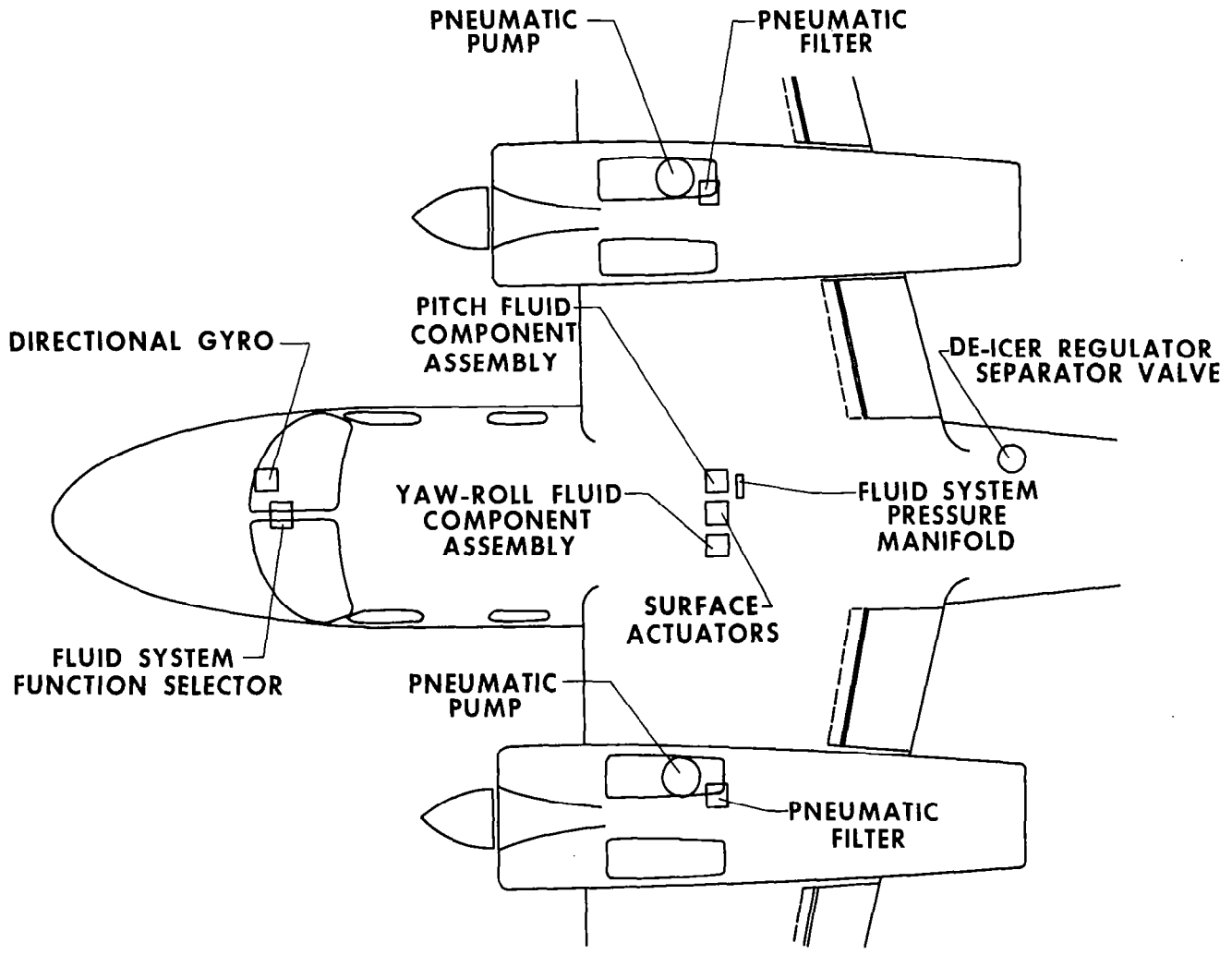


Figure 18. Plan View of Aero Commander Showing Fluid System Installation

Roll axis control is achieved by amplifying the yaw rate signal and feeding it into a servo connected to the ailerons. This control mode is called "Wing-leveler". Roll angle is directly proportional to yaw rate for a constant airspeed and altitude.

By keeping yaw rate at zero, roll attitude is maintained without a roll attitude reference. The calculated gain for the wing-leveler mode is  $0.5 \frac{\delta_a}{\text{°/sec } r}$ ; 0.5 degree of differential aileron is commanded for each degree per second of yaw rate. The aileron servo is connected in parallel with the aileron control cables. Any servo output results in rotation of the pilot's control wheel.

The roll axis also has a heading and a turn mode. Heading error is sensed by a directional gyroscope and summed with the yaw rate signal such that a fixed yaw rate is commanded for each degree of heading error. The calculated heading gain is  $0.1 \frac{\delta_a}{\text{°}\psi}$ . The calculated wing-leveler gain is  $0.5 \frac{\delta_a}{\text{°/sec } r}$ . The ratio of the gains,  $0.1 \frac{\delta_a}{\text{°}\psi}$  to  $0.5 \frac{\delta_a}{\text{°/sec } r}$ , is  $0.2 \frac{\text{°/sec } r}{1\text{°}\psi}$ .

A heading select capability is provided with a gain of 0.2 deg/sec r per degree of heading selected.

Excessive bank angles do not occur, since the heading signal generated by the directional gyroscope is limited to approximately 15 degrees.

The roll axis turn mode is mechanized by providing the pilot with the capability of commanding yaw rate by biasing the wing-leveler mode. Thus turn control knob positions correspond to turn rates.

The pilot has a roll trim control and roll trim indicator which are mechanized and function in the same manner as the previously described yaw trim control.

Pitch axis control is achieved by a pitch rate damper inner loop and an altitude control outer loop. Mode switching of the system was set up such that pilot selection of pitch engaged both the pitch rate damper and altitude hold. The pitch rate damper, therefore, cannot be selected alone. This was done because a damper mode would have little utility in the Aero Commander aircraft.

Aircraft pitch rate is sensed by a vortex rate sensor, amplified, and fed into an elevator servo. The calculated gain for the pitch damper is  $0.5 \frac{\delta_e}{\text{sec } q}$ ; 0.5 degree of elevator is commanded for each degree per second of pitch rate.

Altitude control is achieved by trapping a reference sample of air at the desired altitude and generating an altitude error signal if altitude deviations occur. The error signal is shaped by a 5 second, 10 to 1 lead lag network, amplified and fed to a servo connected to the elevator. The calculated gain of the altitude control loop is  $0.03 \frac{\delta_e}{\text{FT}}$ ; 0.03 degree of elevator is commanded for each foot of altitude error. The servo is connected in parallel with the elevator control cables. Any servo output results in movement of the pilot's control column. The pilot has a pitch trim control and pitch trim indicator which are mechanized and function in the same manner as the previously described yaw trim control and indicator.

Pilot controls are all located in a function selector unit located in the cockpit. This unit has function switches labeled "Master", "Roll-Yaw", "Heading", and "Pitch". These switches engage the modes in combination as desired by the pilot. Trim controls, trim indicators and the turn control are also located on this panel.

Mode switching and control of power is accomplished by solenoid controlled valves. To control and switch power mechanically would have required either routing all lines through the cabin or routing mechanical controls back through the cabin to the power source in the aft section of the fuselage. The cabin is pressurized and all connections to the cockpit require penetrating a pressure bulkhead.

The system is powered from the pressure side of two engine-driven pneumatic pumps. Figure 19 is a schematic of the power supply. The output of the pumps is filtered, routed through a check valve, and summed with the output of the other pump. Each pump is fitted with a relief valve for safety purposes. The air is then routed to the deicer regulator separator unit which provides 17.5 psig air to the selected system. When neither the deicer system nor the autopilot is engaged, the air is dumped to the atmosphere. The deicer and autopilot cannot be used simultaneously because the deicer cycling action causes pressure transients in the power supply.

## SYSTEM DESIGN

The major potential design problems recognized at program start are given below. The design considerations involved in solving these problems are discussed in this section.

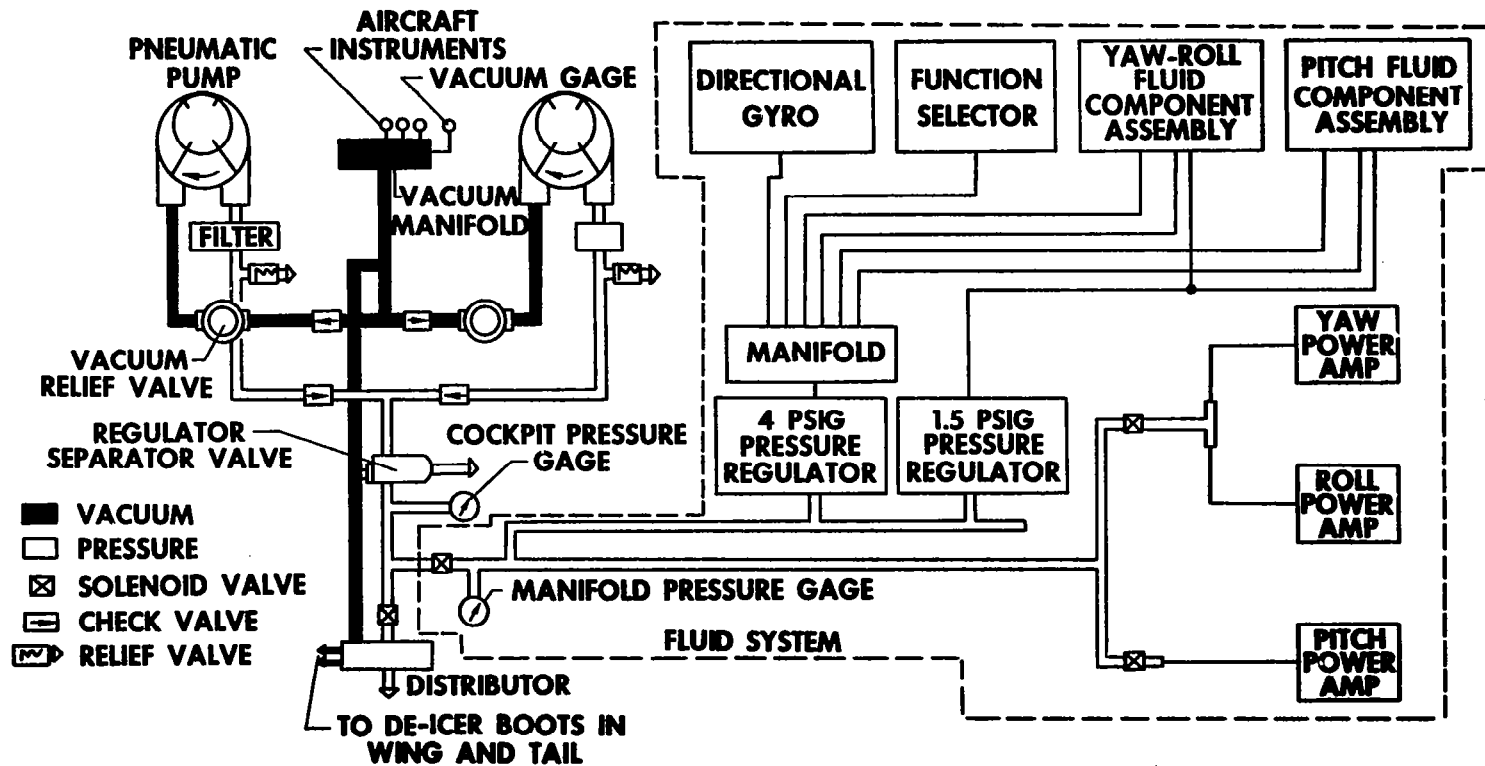


Figure 19. Power Supply Schematic

- Aircraft aerodynamic stability derivative inaccuracy
- Unique roll and pitch axis control configuration
- Component layout in aircraft
- Power supply and interfaces

## STABILITY DERIVATIVES

The stability derivatives for the Aero Commander 680 FP were generated jointly by NASA and Honeywell during this program, as discussed previously in this report. The numbers were defined as accurately as possible within the time available and methods used. Errors, however, resulted in changes being required in control loop gain.

For this reason, a  $\pm 100$  percent gain adjust capability was built into each control loop and the time constants mechanized with adjust capability.

The amplifier cascades were built by mounting the individual amplifier stages on circuit boards and interconnecting them with plastic tubing. This provided flexibility in circuit configuration and ease of adding instrumentation test points between stages. Individual amplifiers can be replaced and amplifiers can be nulled by shifting cover plates.

The disadvantage of individual mounting of stages is in the added signal transmission length and the extra volume of the completed package. However, it was felt that flexibility of circuit configuration and ease of testing were more significant, since there were questions on the validity of the stability derivatives.

## ROLL AND PITCH CONFIGURATIONS

The uniqueness of the roll and pitch axis control configurations was a major design consideration. Neither roll attitude nor pitch attitude are used as feedbacks, even though a pseudo roll attitude mode and an altitude hold mode are mechanized.

The pseudo roll attitude mode is the "wing-leveler" mode. Roll attitude is directly proportional to yaw rate for a constant true airspeed and altitude. The relationship is given by:

$$r = \frac{180}{\pi} \frac{g}{V} \tan \phi,$$

The wing-leveler mode function is based on this relationship between yaw rate and roll attitude.

The yaw rate sensor threshold is important since it sets the roll attitude threshold in this system. Rate-sensor diameter and the operating pressure are key performance tradeoff factors. The diameter of the unit for a given supply pressure determines the sensor threshold and sensor transportation delay time. As the diameter is increased, transportation time is increased and threshold is decreased. With 4 psi supply pressure and a 6-inch diameter unit, a transportation time of less than 0.1 second and a threshold of 0.1 deg/sec can be obtained. The roll attitude threshold at a typical airspeed, 150 mph, with such a unit is approximately 2/3 degree. The aircraft control cable friction and surface actuator deadband are the other significant contributors to the roll attitude deadband. The control column forces required, due to cable friction, were measured to be approximately 4 pounds for the aileron and 10 pounds for the rudder.

The elevator has a downspring which must be overcome to make friction measurements. These measurements indicated heavy control cable friction which would appear as system threshold.

The aircraft surface hinge force was simulated on a load fixture with a prototype servo and driven by both analog and pulse width modulated power amplifiers. The pulse width modulation dither reduced the threshold of the actuator by a factor of 4.

Frequency response of both the analog and pulse width modulated test setups was determined. There was no phase advantage within measurement accuracy, over the control frequencies tested for either the analog or pulse width modulation mechanizations. The pressure recovery was found to be approximately 40 percent of the supply pressure for the bistable amplifiers used in the pulse width modulation system. The proportional power amplifiers used in the analog mechanization had approximately 30 percent pressure recovery. Thus, for a given operating pressure, the pulse width modulation system would have greater authority. To achieve as small a roll attitude threshold as feasible, the rate sensor threshold design aim was set at 0.1 deg/sec and pulse width modulator mechanization was used instead of a proportional type mechanization.

## COMPONENT LOCATIONS

Component layout was complicated in that there was an existing autopilot and a pressurization system in the aircraft. NASA desired to keep the existing autopilot operational and this required leaving the electric servos in place, connected to the aircraft cabling. These servos were at the best location in terms of accessibility and smoothness

of operation, which meant a less desirable location for the fluid servos. The aft section of the fuselage was occupied by the cabin pressurization system. This left very little space for servo installation or placing of components in the aft fuselage area.

These problems were solved by placing the three servos, the pitch fluid component assembly, the yaw-roll fluid component assembly, the regulators, manifolds and power distribution plumbing in the baggage compartment. The three servos were mounted on the aft cabin vertical pressure bulkhead. The fluid component assemblies were mounted on the same bulkhead.

A rearrangement of the copilot's instrument panel was made to permit installation of the directional gyroscope. The function selector was located in a map case, between the pilots.

Interconnection of the components in the cabin with the components in the baggage compartment required routing all pneumatic lines and electrical wiring through the cabin pressure bulkhead. The tubing interconnect through the pressure bulkhead was made by drilling out an electrical connector and replacing the pins with brass tubes. Twenty-two tygon tubes, 173 inches long, were needed from bulkhead to function selector and directional gyro. Protection of this tubing from cuts and blockages was provided by bundling the small tubes and putting them in a large plastic tube. At points of possible external pressure, metal standoffs were placed around the tube bundle. Figure 18 shows the placing of the various components in the aircraft.

## POWER SUPPLY

The power supply for the system presented several problems; pressure and flow limitations, contamination, and interfacing with the aircraft deicer system and flight instruments.

The deicer regulator separator valve originally was set to operate at 15 psig. The vacuum relief valves are set to maintain 5 inches Hg for the flight instruments. It was desired to keep both the deicer system and the flight instruments in operation without modification. The deicer system alternately pressurizes and applies vacuum to the boots. The pressure cycle causes a sharp transient in the pressure which the fluid system could not tolerate. Therefore, the system was mechanized so that either the fluid system or the deicer could be operated but not both at the same time.

The original equipment ARO 505 pumps were oil lubricated and the output had to be filtered to remove oil droplets. For this program, the wet pumps were replaced by Airborne Manufacturing Company model 423CC carbon vane type pumps. Filtration was added to prevent carbon particle contamination. Figure 19 is the final power supply schematic.

Figure 20 is a plot of the pressure flow characteristics of the 423 pumps as installed on the Aero Commander 680 FP. The data is for 16,800 foot altitude and includes 6 inches Hg vacuum load in the differential pressure, which is 2800 feet higher than maximum system operating altitude. The system was designed to take 10 SCFM when operated at 15 psig. Figure 20 shows that with those operating conditions, about 5 psi can be dropped in line loss between the pump and the system.

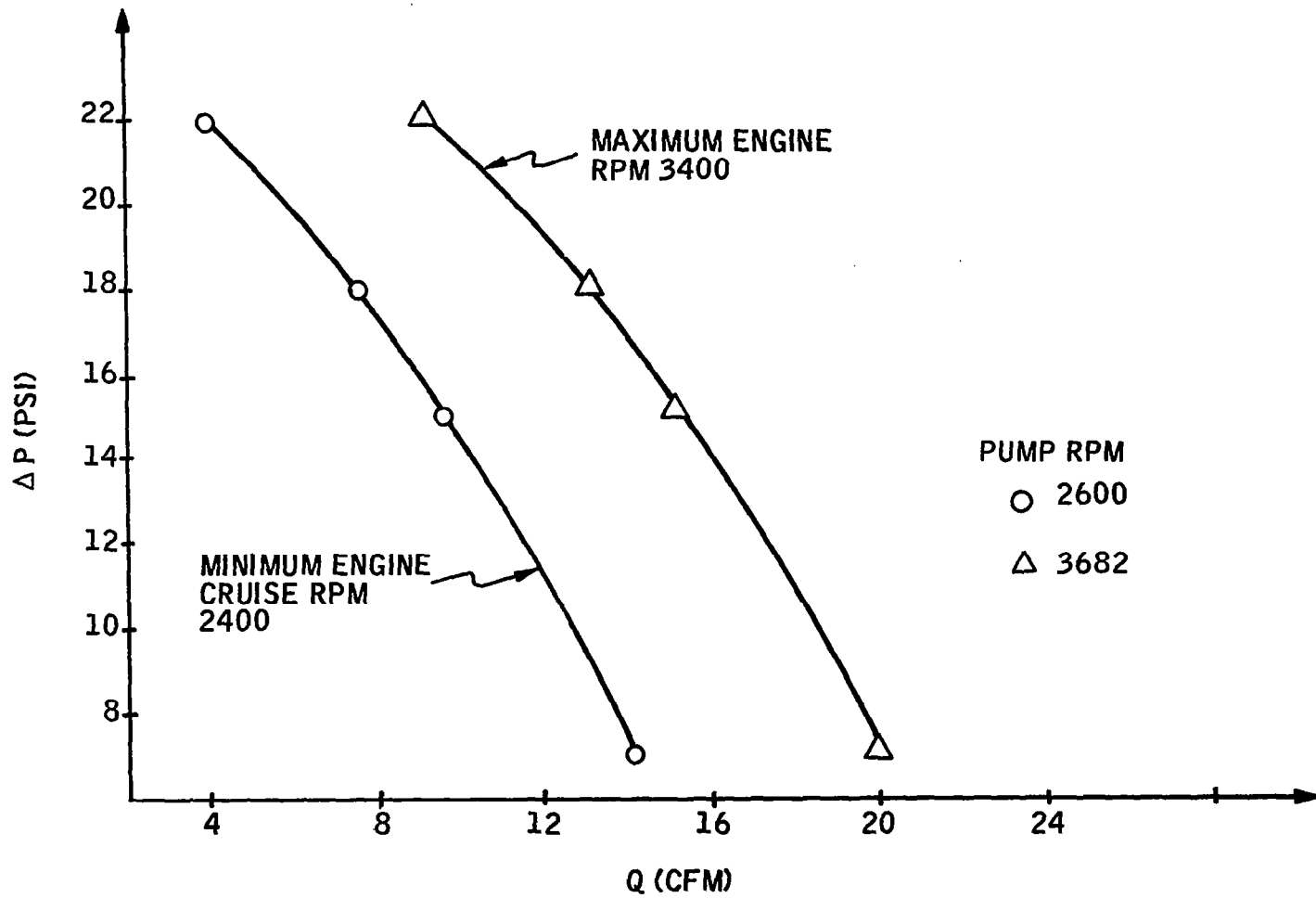


Figure 20. Airborne Manufacturing Company Pump Model 423 Data

The deicer regulator-separator valve sets the operating pressure for both deicer and fluid system. To obtain satisfactory control authority, it was desirable to operate the fluid system to obtain at least  $\pm 5$  psid power amp output. After system installation in the aircraft, it was found that 3.5 psi was dropped in line loss between the deicer regulator and the system power amplifiers. Therefore, the deicer regulator was adjusted from the initial 15 psig to 17.5 psig to provide the minimum  $\pm 5$  psid power amp control range.

The pulse width modulated mechanization, with 40 percent supply pressure recovery, requires approximately 14 psig power amp supply pressure. In operation, the system required 18.5 psig at the pump output to provide the 17.5 psig at the regulator and subsequently 14 psig at the power amplifiers.

The key pump life determinant is absolute pressure ratio (pump output absolute pressure divided by pump input absolute pressure). Pump life is inversely related to this ratio. Figure 21 illustrates this ratio over the operating envelope of the system.

The method of regulating supply pressure has a significant effect on system performance. Variations in fluid amplifier supply pressure cause variations in output range and pressure recovery, gain, output noise, and power consumption. Amplifier null is also changed by supply-pressure variation. However, careful design of the amplifier and selection of proper operating pressure minimize null shift with supply-pressure variation. The effect of atmospheric-pressure changes on a vented fluid amplifier depends on the type of regulation used in the power supply.

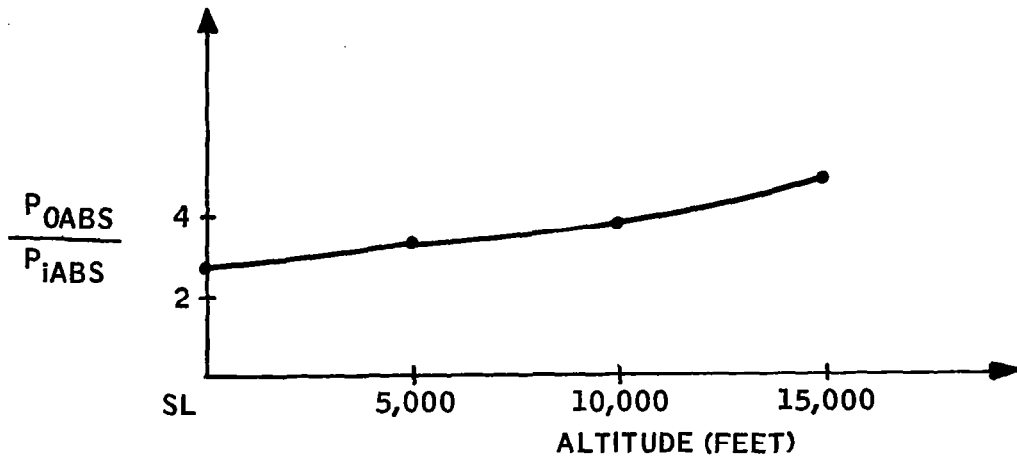
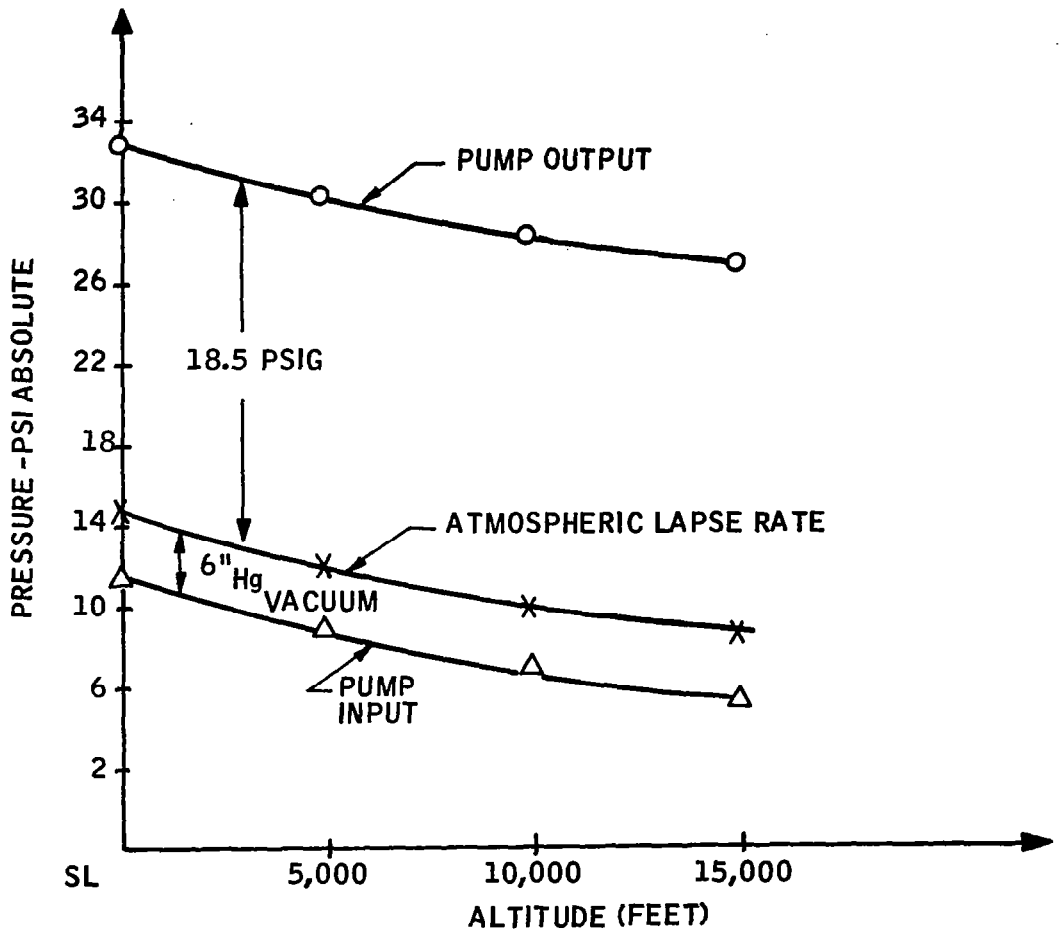


Figure 21. Pump Absolute Pressure Ratio

Three types of regulation were considered: absolute pressure, gage pressure, and differential pressure (constant absolute-pressure system environment).

The first method, absolute pressure, would provide the poorest operating conditions, since the pressure across the amplifiers would vary with changes in altitude. The second method, gage pressure supply, would supply a constant pressure across the amplifiers but would also introduce adverse mass-flow variations due to air-density change with altitude. The last type, differential pressure, would result in the best operating condition. However, differential pressure is also the most costly, since both an absolute regulator and a pressure-tight container for the system are required.

The gage pressure-regulation system was selected, and each control loop was designed with a pilot-operated trimming device to ensure that null shifts due to altitude change could always be cancelled.

The deicer regulator separator valve dumps the pump output when neither deicer nor fluid system is engaged. A solenoid valve controls this switching.

### Autopilot Switching

The fluid autopilot control panel has the following modes of operation:

- Master: Air to system.
- Roll-yaw: Engagement of roll servo and of yaw servo; wing leveler and yaw damper.

- **Heading:** Adds heading signal and removes turn control capability.
- **Pitch:** Engagement of elevator servo; altitude hold mode.

Since the components were all located 20 feet away in the baggage compartment and separated from the pilot operated function selector by a pressure bulkhead, all switching was accomplished with solenoid valves. To prevent simultaneous deicer and fluid system operation, a manual toggle switch was put on the copilot's instrument panel which armed the fluid system master switch electrically. Electrical power to engage solenoids is present in the function selector only when AFCS is selected with the toggle switch. The AFCS master switch then was connected in parallel with the deicer for operation of the deicer regulator separator valve.

Servos are engaged and disengaged by activating the power amplifier power supply by a solenoid valve in the line. This method provides open circuit fail safe operation of servo engagement.

Aircraft 15 psig pneumatic power is connected to each of three servo-amplifiers and to the AFCS 4 psig regulator. Flow required in standard cubic feet per minute is as follows:

Pitch Rate Sensor	0.750	
Altitude Sensor	0.125	
Pitch Axis Circuitry	<u>1.185</u>	
Pitch FCA		2,060
Pitch Servo Amp		<u>1.130</u>
Pitch Axis		3,190 SCFM
Yaw Rate Sensor	0.850	

Yaw Axis Circuitry	1.185	
Yaw Servo Amp		1.130
Yaw Axis		3.165 SCFM
Directional Gyro	0.80	
Roll Axis Circuitry	1.185	
Roll Servo Amp	1.130	
Roll Axis		3.115 SCFM
Yaw/Roll FCA	3.22	
		<hr/>
		9.470 SCFM

The following devices were used to modify the existing pneumatic system on the aircraft:

1. Pneumatic Pump (2 each) - Airborne Manufacturing Company Model 423CC.
2. Filter (2 each) - Air Maze Model 201963.
3. Pressure Regulator (2 each) - Moore Products Model 40H-50.
4. Deicer Cutoff Solenoid (normally open) - Valcor Model V36100.
5. AFCS Turn On Solenoid (normally closed) - Skinner Model L2 DB5150.
6. Yaw/Roll Axes Engage Solenoid (normally closed) - Skinner Model LC2 DB4150.
7. Pitch Axis Engage Solenoid (normally closed) - Skinner Model LC2 DB4150.

Aircraft 28 vdc is used for powering solenoid valves used for AFCS switching. Listed below are solenoids and hold currents required.

<u>Solenoid</u>	<u>Holding Current</u>
Deicer Cutoff Solenoid (normally open) - Valcor V36100, 30 Watt	1.0
AFCS Turn On Solenoid (normally closed) - Skinner L2 DB5150, 10 Watt	0.396
Yaw/Roll Axes Engage Solenoid (normally closed) - Skinner LC2 DB4150, 8 Watt	0.292
Pitch Axis Engage Solenoid (normally closed) - Skinner LC2 DB4150, 8 Watt	0.292
Heading Solenoid (normally open) (Yaw/Roll FCA) - Skinner	0.396
Turn Solenoid (normally closed) (Yaw/Roll FCA) - Skinner	0.396
Altitude Solenoid (normally open) (Pitch FCA) - Eckel	<u>0.396</u>
Total	3.168
Existing Deicer Regulator - Separator Valve	<u>0.500</u>
Total	3.668

## Servo Actuators

The MG113 type pneumatic servo was chosen for this application because it is a proven flightworthy device. To utilize it for the fluid system required design of a new piston and cylinder assembly and cable drum. A description of the servo is given in the Component Design section of this report.

The servo cable drum minimum size is set by the surface cable travel. The servo cable drum maximum size is determined by the desired surface authority for a given torque capability servo.

The surface hinge moments were calculated using the coefficients supplied by NASA for the ailerons and elevator. The coefficient for the rudder was not available so flight test pedal force and displacement data were used. The calculation of the aileron hinge moment is as follows:

$$HM_{\delta_a} = C_{H_{\delta_a}} q S \bar{C}$$

$$HM_{\delta_a} = \text{hinge moment per degree of aileron}$$

$$C_{H_{\delta_a}} = \text{hinge moment coefficient, 0.258}$$

$$\bar{q} = \text{dynamic pressure}$$

$$S = \text{area of surface}$$

$$\bar{C} = \text{chord of surface}$$

$$HM_{\delta_a} = \frac{39 \text{ inch pounds}}{\text{degree of differential aileron}}$$

$$\bar{q} = 112 \text{ psf cruise}$$

The calculation of the elevator hinge moment is as follows:

$$HM_{\delta_e} = C_{H_{\delta_e}} \bar{q} S \bar{C}$$

$HM_{\delta_e}$  = hinge moment per degree of elevator

$C_{H_{\delta_e}}$  = hinge moment coefficient, 0.36

$\bar{q}$  = dynamic pressure

S = area of surface

$\bar{C}$  = chord of surface

$$HM_{\delta_e} = 146 \frac{\text{inch pounds}}{\text{degree of elevator}}$$

$\bar{q}$  = 112 psf cruise

Rudder deflection was measured at cruise and found that:

$$10^\circ \delta_r = 78 \text{ pounds at the pedals}$$

7 inches of pedal travel = 2.9 inches of cable travel

$$\text{Cable force} = \text{pedal force} \left( \frac{7}{2.9} \right)$$

$$1^\circ \delta_r = 7.8 \left( \frac{7}{2.9} \right) \text{ pounds of cable force}$$

Using the data shown in Table 5, the calculations for sizing the aileron servos are as follows:

1. Minimum cable drum radius

$$S = R \delta$$

$$R = \frac{7.5 \text{ inches}}{2} = 3.25 \text{ inches}$$

S = arc length, in.

R = radius, in.

$\theta$  = angle, radians

Use 4" radius

2. Hinge moment referred to servo is:

7.5 inches of cable motion =  $76^\circ \delta_a$  D. A.

Servo cable drum is 4 inch radius.  $1^\circ \delta_a = \frac{7.5}{76}$  inches of cable motion.

Hinge moment referred to servo drum:

$$39 \frac{\frac{4}{7.5 \times 57.3}}{76} = \frac{28 \text{ inch pounds}}{\delta_a}$$

3.  $4^\circ \delta_a$  control authority is desired at cruise.

Desired servo torque output then is  $(4^\circ \delta_a) \frac{28 \text{ inch pounds}}{\delta_a} = 112 \text{ in. lbs.}$

Cable friction moment =  $3 \times 4 = 12 \text{ inch pounds}$

$\therefore$  124 inch pound device is required

Servo torque = (P) Area (arm)

$$\text{area} = \frac{124}{P(\text{arm})}$$

$\pm 5$  psid was determined as the control signal range. Using a

2.5 inch arm:

$$\text{area} = \frac{124}{(5)(2.5)} = 10 \text{ inches square}$$

Table 5. Aero Commander 680 FP Manual Control System Data

AILERONS

Wheel Rotation: 180 degrees; Wheel diameter 12 inches  
Wheel Travel: 18.85 inches  
Cable Travel: 7.5 inches for  $\pm 38$  degrees D. A. Aileron  
Surface Travel: 38 degrees D. A.; 23 degrees up and 15 degrees down

ELEVATOR

Control Column Travel: 6.5 inches; 15 degrees  
Cable Travel: 4.25 inches  
Surface Travel: 30 degrees up and 10 degrees down

RUDDER

Pedal Travel: 7 inches  
Cable Travel: 2.875 inches  
Surface Travel: 20 degrees left and right

4. The transfer function of the aileron servo is then:

$$\frac{4^\circ \delta_a}{5 \text{ psid}} = 0.8 \frac{^\circ \delta_a}{\text{psid}}$$

The servo is a force limited device and as the spring rate, i. e., the dynamic pressure seen by the surface, changes the transfer function changes. This relationship then is:

$$\frac{\delta_a}{\text{psid}} = \frac{112}{q} \quad (0.8)$$

The calculations for sizing the elevator servo are:

1. Minimum cable drum radius

$$S = R\phi$$

$$R = \frac{S}{\phi} = \frac{4.5}{2} = 2.25 \text{ inches}$$

Use 3.25 inches radius

2. Hinge moment referred to servo is:

4.25 inches of cable motion is 40 degrees  $\delta_e$  servo cable drum is 3.25 inches in radius

$$1^\circ \delta_e = \frac{4.25}{40} \text{ inches of cable motion}$$

hinge moment referred to servo drum:

$$(146) \quad \frac{\frac{3.25}{4.25 \times 57.3}}{40} = \frac{78 \text{ inch pounds}}{\delta_e}$$

3.  $1.5^\circ \delta_e$  control authority is desired at cruise.

Desired servo torque output then is  $(1.5^\circ \delta_e) \frac{78 \text{ inch pounds}}{\delta_e} = 117 \text{ in. lbs.}$

Since this is very near the torque required for the aileron unit the same area, 10 square inches is used, making the units identical.

4. The transfer function of the elevator servo is then:

$$\frac{1.5^\circ \delta_e}{5 \text{ psid}} = \frac{0.3^\circ \delta_e}{1 \text{ psid}}$$

The servo is a force limited device and as the spring rate, i. e., the dynamic pressure seen by the surface, changes the transfer function changes. The relationship is:

$$\frac{\delta_e}{\text{psid}} = \frac{112}{\bar{q}} \quad (0.3)$$

The calculations for sizing the rudder servo are:

1. Minimum cable drum radius

$$S = R\alpha$$

$$R = \frac{S}{\alpha} = \frac{2.9}{2} = 1.45 \text{ inches}$$

Use 1.5 inch radius

2.  $1^\circ \delta_r = 7.8 \left( \frac{7}{2.9} \right)$  pounds of cable

$1.75^\circ \delta_r$  control authority is desired.

$1.75 (7.8) \left(\frac{7}{2.9}\right) (1.5) = 49.5$  inch pounds of torque required for control authority

rudder cable friction 10 pounds;

friction torque  $10 \times 1.5 = 15$  inch pounds

Total torque servo must provide is 64.5 inch pounds.

3. Servo area is determined by:

Servo torque = P area (arm)

$$\text{area} = \frac{(65 \text{ inch pounds})}{5 (2)} = 6.5 \text{ square inches}$$

4. The transfer function of the rudder servo is then:

$$\frac{1.75^\circ \delta_r}{5} = \frac{0.35^\circ \delta_r}{\text{psid}}$$

The servo is force limited as are the aileron and elevator. The transfer function at any dynamic pressure is determined by:

$$\frac{\delta_r^\circ}{\text{psid}} = \frac{112}{\bar{q}} \quad (0.35)$$

The servos have a fixed control torque capability. A feedback or follow-up around the servo is not used. The control system is a "torque limited" type system. The basis for this type system can be seen by examining the pitching moment due to elevator deflection,  $M_{\delta_e}$ , and hinge moment due to elevator deflection  $HM_{\delta_e}$ .

$$M_{\delta_e} = C_{M_{\delta_e}} \bar{q} S \bar{C}$$

$$HM_{\delta_e} = C_{h_{\delta_e}} \bar{q} S \bar{C}$$

The ratio of aircraft pitching moment to applied hinge moment is:

$$\frac{M_{\delta_e}}{HM_{\delta_e}} = \frac{C_{m_{\delta_e}} \bar{q} S \bar{C}}{C_{h_{\delta_e}} \bar{q} S \bar{C}} = \frac{C_{M_{\delta_e}}}{C_{h_{\delta_e}}}$$

The relationship is a function of the dimensionless coefficients and not a function of dynamic pressure. In theory the loop gains are relatively constant with changes in flight condition and reduce the need for scheduling of gains with dynamic pressure, i. e., surface effectiveness.

The servo overpower force for each surface is calculated as follows:

For the following equations of the overpower force on the ailerons, elevator and rudder, this symbology applies:

$F_c$  = Force of cable

$T_c$  = Travel of cable

$F_w$  = Force on wheel

$T_w$  = Travel of wheel

$F_c$  = Force on control column

$T_c$  = Travel of control column

$F_p$  = Force on pedals

$T_p$  = Travel of pedals

- Ailerons

(Force Wheel) (Wheel travel) = (Force cable) (Cable travel)

$$F_W = \frac{F_c T_c}{T_W}$$

$$F_c = \frac{\text{servo torque}}{\text{cable drum radius}} = \frac{124}{4} = 31 \text{ pounds}$$

overpower force at control wheel, FW:

$$F_W = \frac{(31) 7.5}{18.85} = 12.4 \text{ pounds}$$

- Elevator

$$F_e = \frac{F_c T_c}{T_e}$$

$$F_c = \frac{124}{3.25} = 38.2 \text{ pounds}$$

overpower force at control column,  $F_e$ :

$$F_e = \frac{(38.2) 4.25}{6.5 (2)} = 12.5 \text{ pounds}$$

- Rudder

$$F_p = \frac{F_c T_c}{T_p}$$

$$F_c = \frac{65}{1.5} = 43.2 \text{ pounds}$$

overpower force at control pedals,  $F_p$ :

$$F_p = \frac{43.2 (2.875)}{7} = 17.8 \text{ pounds}$$

### Control Loop Pressure Gain Determination

The control loop gains required were established during the analysis and are:

- Lateral Axis

$$\text{Yaw rate to aileron, } \delta_{a_r} = 0.5 \frac{\text{° Aileron (Differential)}}{\text{°/sec yaw rate}}$$

$$\text{Heading to aileron, } \delta_{a_\psi} = 0.1 \frac{\text{° Aileron (Differential)}}{\text{°/Heading error}}$$

$$\text{Yaw rate to rudder, } \delta_{r_r} = 0.3 \frac{\text{° Rudder}}{\text{°/sec}}$$

- Longitudinal Axis

$$\text{Pitch rate to elevator, } \delta_{e_q} = 0.5 \frac{\text{° Elevator}}{\text{°/sec}}$$

$$\text{Altitude error to elevator, } \delta_{e_h} = 0.03 \frac{\text{° Elevator}}{\text{Foot}}$$

The scale factor of the vortex rate sensor is directly proportional to mass flow of the fluid through the sensor. The vortex rate sensor scale factor at sea level is 0.065 " H<sub>2</sub>O/°/sec. The scale factor then at any atmospheric pressure is:

$$S. F. = 0.0028 \sqrt{111 + Patmos}$$

111 is sensor supply in inches of H<sub>2</sub>O

Patmos is atmospheric pressure in inches of H<sub>2</sub>O.

$$S. F. / 10K = 0.0028 \sqrt{111 + 280}$$

$$= 0.055 \text{ " H}_2\text{O}/^\circ/\text{sec.}, 0.004 \text{ "Hg}/^\circ/\text{sec.}$$

At a dynamic pressure of 112 pounds per square feet, the 3 servo actuator transfer functions are:

$$\text{Elevator} \quad 0.15 \quad \frac{\delta_e^\circ}{1 \text{ "Hg}}$$

$$\text{Aileron} \quad 0.4 \quad \frac{\delta_a^\circ}{1 \text{ "Hg}}$$

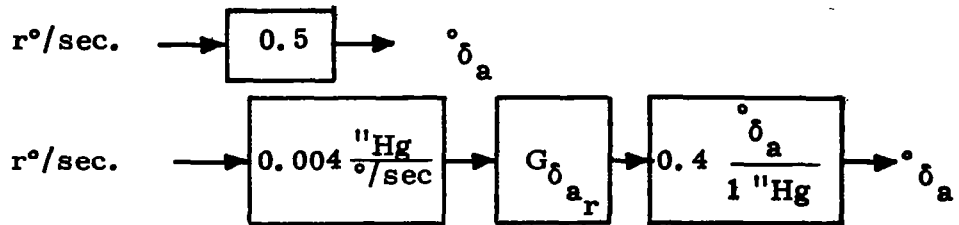
$$\text{Rudder} \quad 0.175 \quad \frac{\delta_r^\circ}{1 \text{ "Hg}}$$

The pressure gain required for each loop is calculated as follows:

Pressure gain as used here means the number of units of pressure output for 1 unit of pressure input.

- Yaw Rate to Aileron (Wing-Leveler)

Desired:

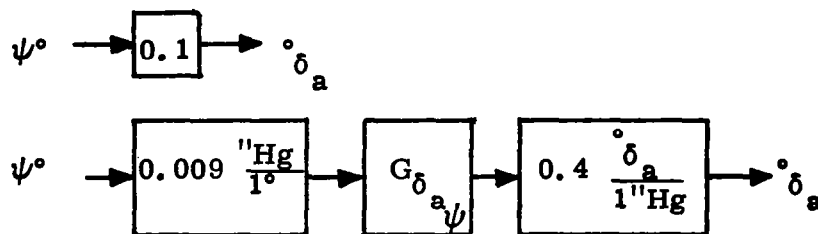


$$(0.004) G_{\delta_{a_r}} (0.4) = 0.5$$

$$G_{\delta_{a_r}} = \frac{0.5}{0.0016} = 312$$

- Heading to Aileron

Desired:

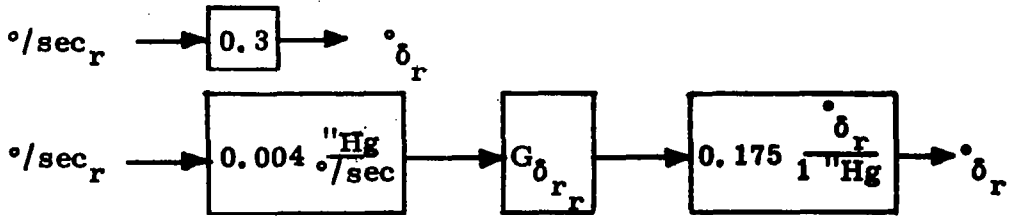


$$(0.009) G_{\delta_{a_\psi}} = \frac{0.1}{0.0036} = 28$$

0.009'' Hg/1° is the directional gyro scale factor.

- Yaw Rate to Rudder (Yaw Damper)

Desired:

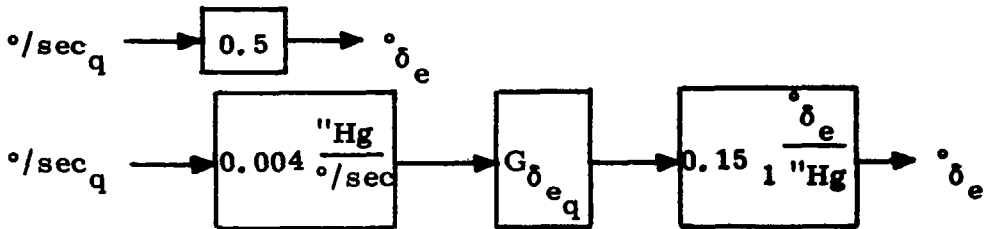


$$(0.004) \quad G_{\delta_{r_r}} \quad (0.175) = 0.3$$

$$G_{\delta_{r_r}} = \frac{0.3}{0.007} = 428$$

- Pitch Rate to Elevator

Desired:

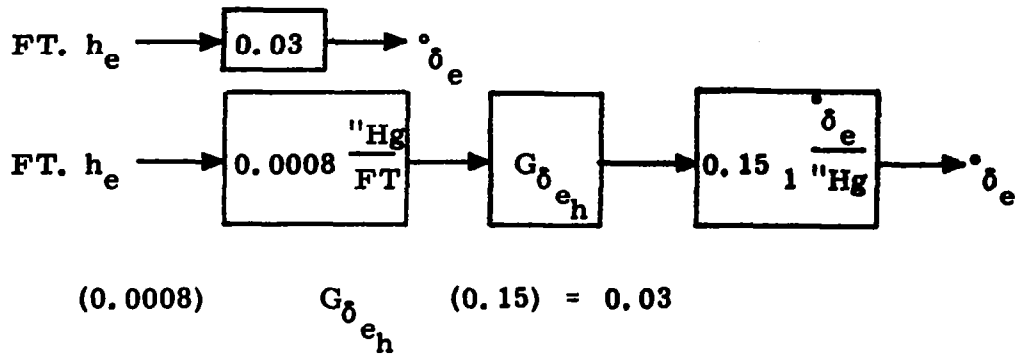


$$(0.004) \quad G_{\delta_{e_q}} \quad (0.15) = 0.5$$

$$G_{\delta_{e_q}} = \frac{0.5}{0.0060} = 832$$

- Altitude to Elevator

Desired:



$$G_{\delta_{e_h}} = \frac{0.03}{0.000120} = 250$$

0.0008 inch Hg/FT is the NASA Standard Atmosphere pressure lapse rate about the 10,000 foot altitude level.

### Control Loop Mechanization

Mechanization is used here to mean selection and cascading of amplifiers to provide required pressure gain and control range for the control loop from the sensor output to the servo input.

Determination of required nominal, maximum and minimum adjustment range, pressure gain for each loop was discussed previously. Control range was set by the loop gains and surface authority required. Roll axis gain,  $\delta a_r$ , is  $0.5 \delta_a$  per  $^\circ/\text{sec } r$ . Aileron authority desired is  $4^\circ \delta_a$ .

Control range is:

$$\text{range} = \frac{4^\circ \delta_a}{\frac{0.5^\circ \delta_a}{\text{°/sec}}} = 8 \text{ degrees per second}$$

Each range of the other control loops is calculated by using the same technique.

Open amplifiers were selected for this system because of the impedance matching difficulty with closed amplifiers. Closed amplifiers lack isolation between input and output; variation in output load affects the input characteristic of the amplifier. Changes in a closed amplifier cascade output load would be reflected back through the cascade having an effect on each stage.

The amplifier operating pressures are 4 psig and 1.5 psig. These values were arrived at by considering the operating conditions of the amplifiers in terms of Reynolds number and its effect on null shift and pressure gain. Power nozzle flow ranges which result in Reynolds numbers associated with transition from laminar to turbulent flow were avoided by proper selection of power supply level.

Two types of amplifiers, proportional and bistable, are used in the system. All control loops utilize proportional amplifiers from the sensor through the pulse width modulator summing stage. Bistable amplifiers are used for the remainder of the loop including the servo amplifier.

The proportional amplifiers selected for use in this system are of the beam deflection type. The amplifiers are chemically etched in copper beryllium. Cover plates are brass, and contain the necessary connection tubes. The amplifiers are fabricated in several configurations of impedance and number of input or control ports.

Most of the proportional amplifiers used in the system have power ports 0.010 inch wide and 0.005 inch deep. A high impedance input for the fluidic sensor signals is provided by this small size.

The two signal shaping networks, high pass and lead lag, were mechanized with the 0.010 by 0.005 inch amplifiers operating at supply level of 1.5 psig.

The bistable amplifiers used in the system are all aluminum filled epoxy cast devices. The power port width and depth vary from 0.015 inch and 0.020 inch to 0.040 inch and 0.10 inch, the largest being the final servo amplifier stage.

All three control axes use the same type Pulse Width Modulation (PWM) System to drive the cable-drum servo actuators. Each preamplifier cascade drives a Pulse Width Modulation cascade of bistable amplifiers. The preamplifier output biases a sawtooth feedback signal in the summing amplifier of the PWM cascade and the biased sawtooth signal controls the firing frequency and pulse duration of the bistable cascade output. The operating frequency of the PWM cascades is approximately 25 cps.

#### Amplifier Cascade Construction

The etched amplifiers selected were proportional stages of the regular single input configuration and the summing input configuration. The size of the sheet stock into which amplifiers are etched has a large effect on the output power capabilities of an amplifier. The thicker the stock is, the greater the amount of air flow and fluid power output. This system needed an amplifier etched on 0.010 inch stock, but successful amplifiers were only available on 0.005 and 0.008 inch stock. This condition forced the stacking of two 0.005 inch stock amplifiers to make a 0.010 inch summing amplifier.

The preamplifier cascade was made with individual modular stages connected together by short lengths of vinyl tubing. This method was used because it permitted gain and null investigation of individual stages. To provide test points, 1/16 inch brass tees were put into all the transmission lines between the stages. When not connected to a pressure transducer, these tees were capped.

The circuit board method provided easy access to the amplifiers for the purposes of transmission line connection, replacement of unsatisfactory stages, attachment of pressure transducer leads, and adjustment of amplifier nulls.

After initial cascading of the preamplifier, it became apparent that a null offset problem existed and that a method of nulling the entire system must be found. Null offsets in early preamplifier stages, for example, caused early saturation of the preamplifier output and thus cause a serious limitation in inputs possible before the system is driven hardover.

The reason for these undesirable null offsets is not completely clear. It has been found that a small shift of an amplifier plate with respect to its cover plates often makes large changes in null, linearity, and gain of the stage. These operation characteristics, however, can also be greatly changed by supply pressure variation, control flow ratio, and level ratio variation and downstream loading of an amplifier.

The method used in this development program to cascade amplifiers and reduce nonlinearity problems caused by null offset was successful but very time consuming. It involved a combination of adjustments of the factors known to affect null, including such trial and error methods as shifting cover plates. Nulling the system involved a step by step amplifier null adjustment, often requiring backtracking to a previously adjusted amplifier, because of loading effects. In the end, satisfactory operation was attained.

## COMPONENT DESIGN

Two vortex rate sensors are used in the system. The theory and operation of this device are adequately described in available literature. \*

In most rate sensor applications, the important performance characteristics are sensitivity, accuracy, and response time. Performance with respect to these characteristics depends upon several parameters, the most important being the dimensions of the vortex chamber and the flow rate through it. A large vortex chamber, a small outlet, and a low flow rate generally result in a larger and more stable vortex motion. This is conducive to a more sensitive and accurate output signal. However, this also results in a slow response, for the response time of the vortex rate sensor is dependent upon the chamber volume and flow rate through it. A sensor with a fast response requires a small chamber volume and a fast flow rate; sensitivity is sacrificed. Because of these two conflicting requirements, a tradeoff is generally necessary between size and power (flow rate) to obtain the best compromise between accuracy and response.

The major criteria for the design tradeoffs for this system's rate sensors were:

- Maximum flow rate of 1 SCFM at operating pressure of 4 psig
- Phase lag of 90 degrees at 2.5 cps (corresponds to a 0.100 second response time in the sensor)
- Impedance match sensor output with a 0.010 x 0.005 amplifier
- Maximize scale factor and threshold 0.1 degree/sec

\*For example - Fluid Technology - Paper dated August, 1965 - Subject: Applied Fluids Technology - Author R. A. Evans - Aerospace Division, Honeywell Inc.

Based on these guidelines, the initial design was generated from previously developed mathematical models. The resulting vortex rate sensors are 6 inches in diameter, 5/8 inch thick, and weigh 1.1 pounds. The scale factor when driving the pre amplifier is 0.066 inch of H<sub>2</sub>O per degree per second at sea level.

### Servo Actuator

The servo actuators are provided to convert system commands into force to move the aircraft control surfaces in response to corrective signals or pilot commands.

Three servos are required: one for roll, one for pitch, and one for yaw. The yaw servo, MG113C1, is a production MG113 from the Honeywell H14 autopilot without the electromagnetic valve assembly. The roll and pitch servos, MG113C2, are modified MG113 with larger (10 square inch) piston area.

This unit consists of two cylinders with pistons sealed against pressure loss by rolling diaphragms as shown in Figure 22. The piston rods are designed to drive against an output linkage which converts the linear force to torque introduced to the aircraft control system through the servo cable drum. When a control command is introduced, a differential pressure is developed in the two cylinders. One piston will extend while the other retracts, causing a rotational output of the linkage assembly. When the servo is disengaged, the cylinders are de-pressurized and vented to atmosphere.

The operating detail of the output linkage assembly is further illustrated in Figure 23. When the autopilot is disengaged, the links and piston shafts are retracted allowing 120 degrees free rotation of the output shaft which

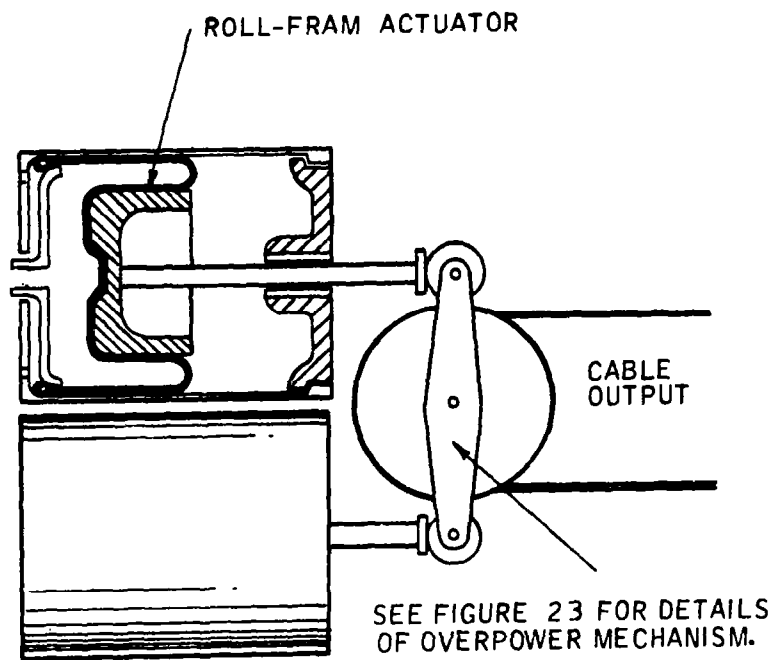


Figure 22. Servo Actuator Schematic

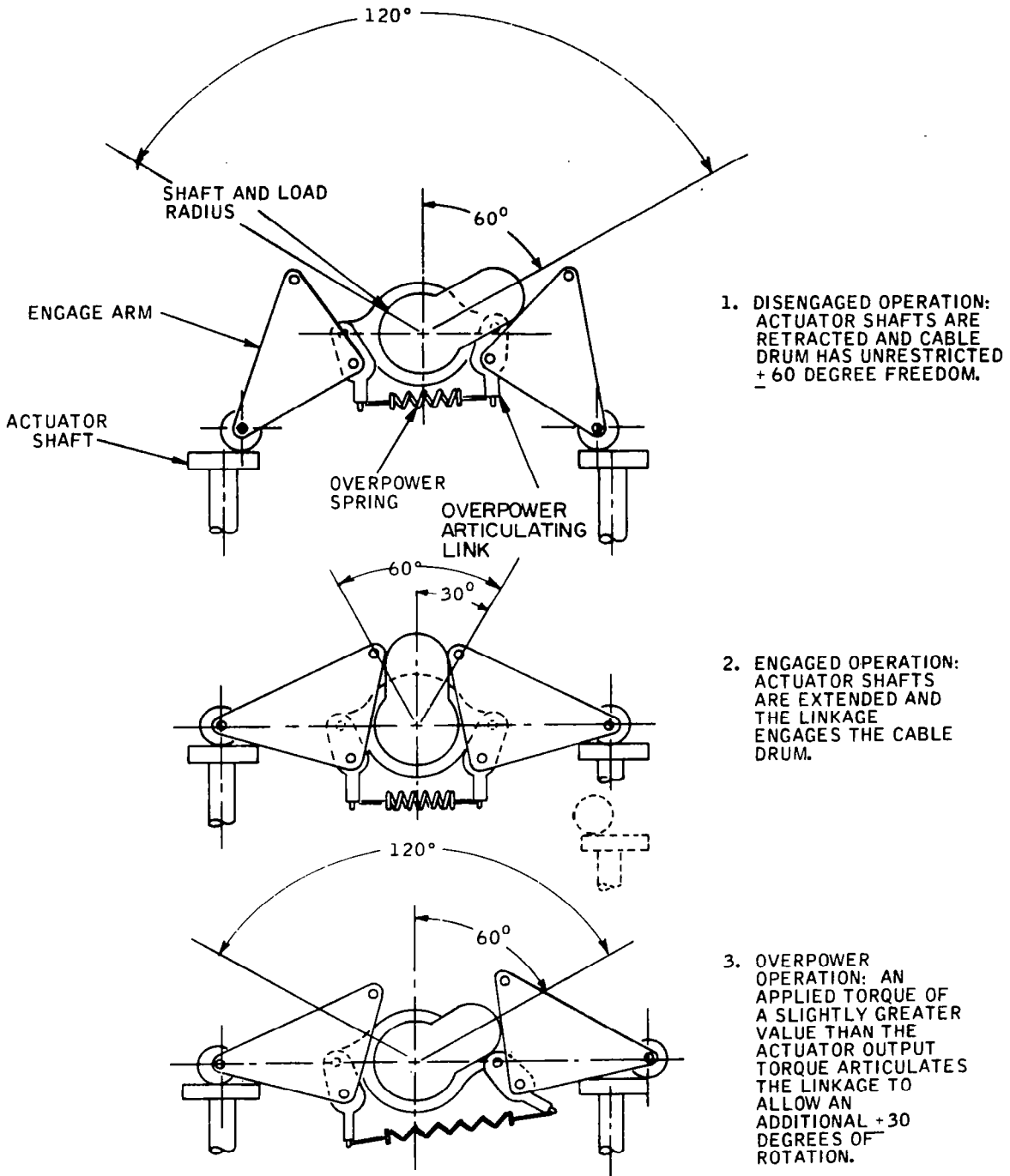


Figure 23. Servo Actuator Overpower Mechanism

follows control movement; no frictional load is added to the aircraft control system.

When the servo is pressurized upon engagement, the shafts and links slowly advance into contact with the output shaft arm which has a normal rotational authority of 60 degrees. Thus, the nominal command control authority does not exceed 50 percent of aircraft control authority, a significant flight safety advantage.

To provide full control travel for pilot overpower, however, the linkage assembly is articulated but normally held rigid by overpower springs. Application of over-power force allows deflection of the springs and provides an additional 60 degrees of servo rotation to the aircraft control system mechanical limits.

The roll servo has an 8-inch diameter output drum, Assembly No. Z944997-21.

The pitch servo has a 6.5-inch diameter output drum, Assembly No. Z944997-3.

The yaw servo has a 3-inch diameter output drum, Assembly No. Z944997-7.

### Function Selector

The function selector is located in the aircraft cabin for pilot operation and provides system turn on/off, control axis engage/disengage, mode selection, and 3-axis trim capabilities. Connections to the device are 28 vdc electrical power and 4 psig pneumatic power. Electrical switches and trim and turn knobs are off-the-shelf hardware. The flow dividers, trim indicators, and packaging were designed for this application.

The trim input devices used in the system caused considerable trouble due to binding and looseness. Looseness was a problem because vibration caused the thumb wheel and spool to rotate, changing the null of the system.

The null trim indicators worked very well. When they indicated null, the servo amplifier output was very close to null in all cases. A slight signal transport lag was present since the transmission lines were 20 feet long. The pilot's readability of the null conditions could be improved by removing the indicators from their present location in the map case compartment and placing them on the instrument panel. Also, the null indicator range of motion might be extended to give better resolution.

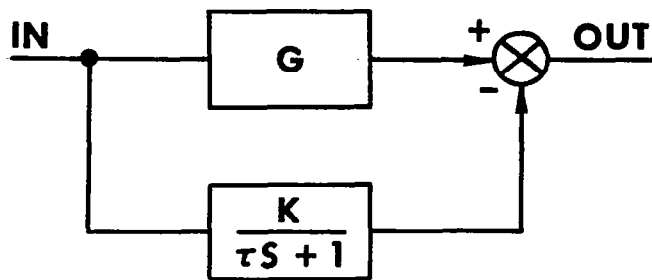
The Heading and Turn Control engagement solenoid valves were located inside the Roll-Yaw component assemblies. They were used to provide short circuit paths between transmission lines to sum either Turn or Heading Error Signal into the Roll axis preamplifier. The Turn solenoid was normally closed and the Heading was normally open. The Heading Select Switch energized both solenoids. Placement of the short-circuiting tees in the signal transmission lines from the Turn Control and Heading Control is important. If the tees are placed too close to the input ports of the summing amplifier, some of the short circuited signal will still reflect into the preamplifier and this undesirable signal will result in an output at the servo amplifier. This reflection problem was eliminated in this autopilot by leaving 6 inches of 1/16 inch transmission tubing between the short circuit tees and the summing amplifier. Also, the short circuit path lines were made with 1/8 inch tubing to reduce the short circuit impedance. This setup worked very well and no Turn or Heading signal could be transmitted to the preamplifier when the respective short circuits were made.

Transmission lines between the fluidic component assemblies and the servo amplifiers are important because their impedance has considerable effect on Pulse Width Modulation performance. For each axis, the last bistable stage within the component assembly has its output split so that it drives the pulse width modulator feedback as well as the first bistable stage of the servo amplifier. The input impedance of a bistable amplifier changes as it switches and this can cause a sharp change in the amount of flow that it demands from the previous stage. In the case of the pulse width modulator, a short transmission line of large diameter between the Pulse Width Modulator and the servo amplifier is undesirable.

The best transmission lines for these systems were 24 to 36 inches of 1/16 inch diameter tubing.

### High Pass Network

A two second high pass network was required for yaw damper signal shaping. Figure 24 is the block diagram and the resulting schematic mechanized. This network filters out low frequency signals by the canceling effect of the negative feed forward loop through amplifier A20. As the frequency of the signal increases the negative loop portion is dissipated in the RC circuit. This results in the high frequency signal passing directly through amplifier A12. The resistors in the RC circuit were set at 0.007-inch diameter and the capacitors set at 16 cubic inches. The feed forward loop was summed into the high gain ports of A12 because better linearity resulted. To decrease the gain and produce better linearity in the negative loop, negative feedback was used around amplifier A20. Figure 25 gives the desired frequency response characteristics and the actual measured frequency response.



WHERE  $G = K$

$$\frac{OUT}{IN}(s) = \frac{G\tau s}{1 + \tau s}$$

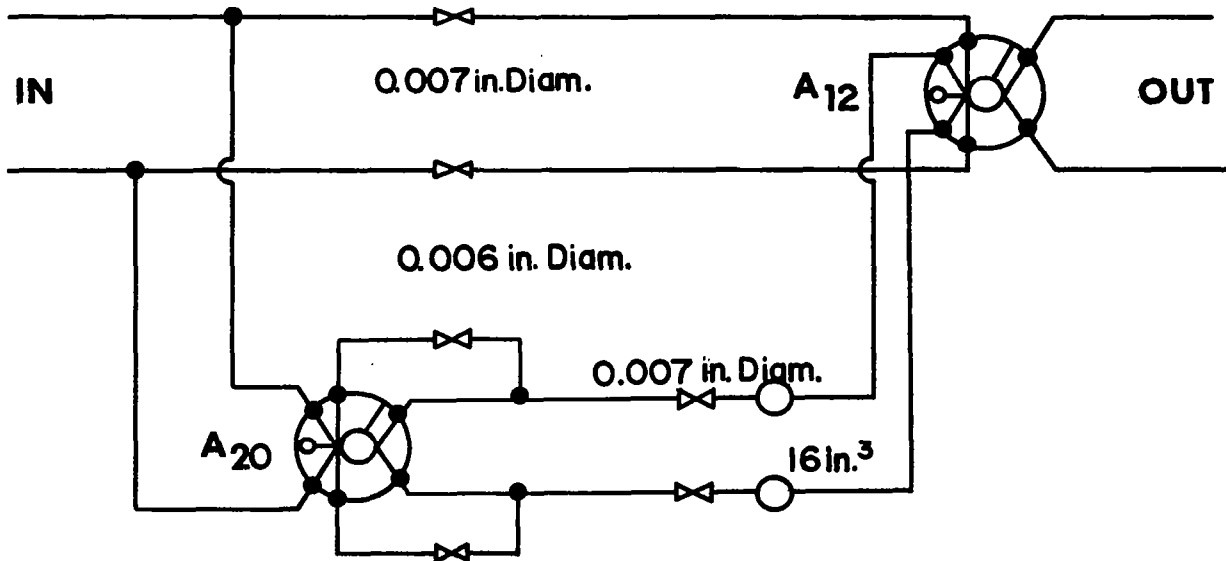


Figure 24. Mechanization of High Pass Network

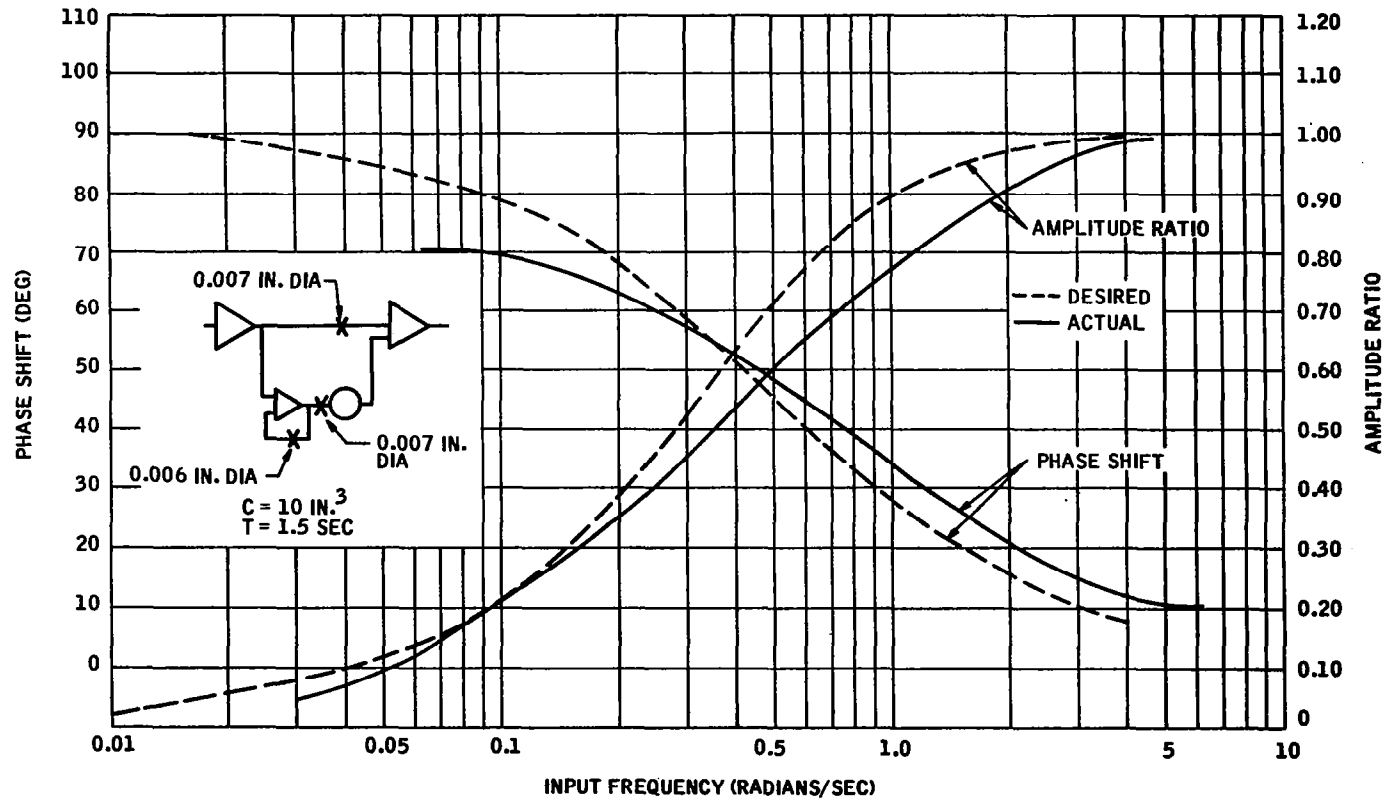


Figure 25. Frequency Response of High Pass Network

## Lead Lag Network

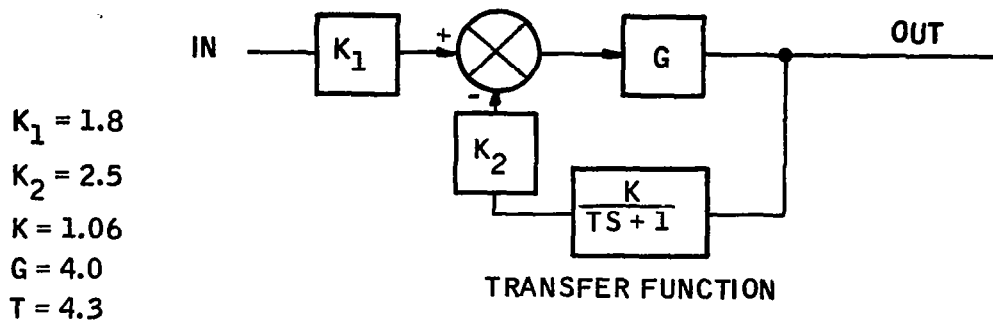
A 10 to 1 lead lag network was required for altitude error signal shaping. Figure 26 shows the block diagram and the schematic mechanized. In Figure 26, K1 and K2 represent the gain of the two sets of summing ports of amplifier A12. G represents the gain of amplifiers A13 and A14. K represents the cumulative gain across A15 and the time constant. The measured values for each of these parameters and the resulting transfer function are also given in Figure 26.

With the network as illustrated, frequency response data were obtained. These test data are plotted as discrete points on Figure 27. The desired frequency response is shown as a continuous line on the same figure. The input sine wave amplitude was held constant at  $\pm 1.1$  inches  $H_2O$  differential pressure through the 0.063 to 63 radians per second frequency range.

## Purchased Components

The directional gyroscope is air driven and has a pneumatic pickoff. Figure 28 functionally represents the pickoff device. The pickoff consists of a movable stator ring, a directional error cam, a manifold plate, and two adjustable orifices. The movable stator ring is geared directly to both the course select knob and course selector card. The directional cam is fastened to the gimbal of the directional gyro. By rotating the selector card with the selector knob, the stator can be aligned with the cam, commanding a desired heading.

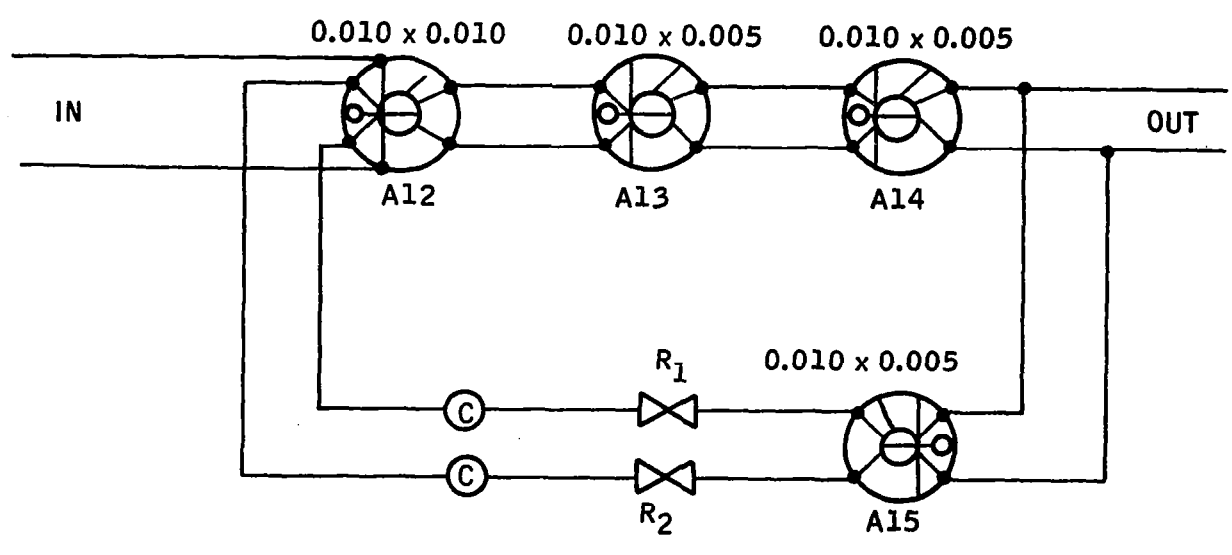
The heading scale factor is set by cross bleed orifices. The input/output relationship of the gyroscope is shown by Figure 29.



$K_1 = 1.8$   
 $K_2 = 2.5$   
 $K = 1.06$   
 $G = 4.0$   
 $T = 4.3$

TRANSFER FUNCTION

$$\frac{GK_1 (TS + 1)}{\frac{GKK_2 + 1}{\left(\frac{T}{GKK_2 + 1}\right) s + 1}} = \frac{0.65 (4.3S + 1)}{0.39S + 1}$$



POWER SUPPLY 1.5 PSIG  
 $R_1$  AND  $R_2$  0.006" DIA  
 $C$  17.5 IN<sup>3</sup>

Figure 26. Lead-Lag Block Diagram

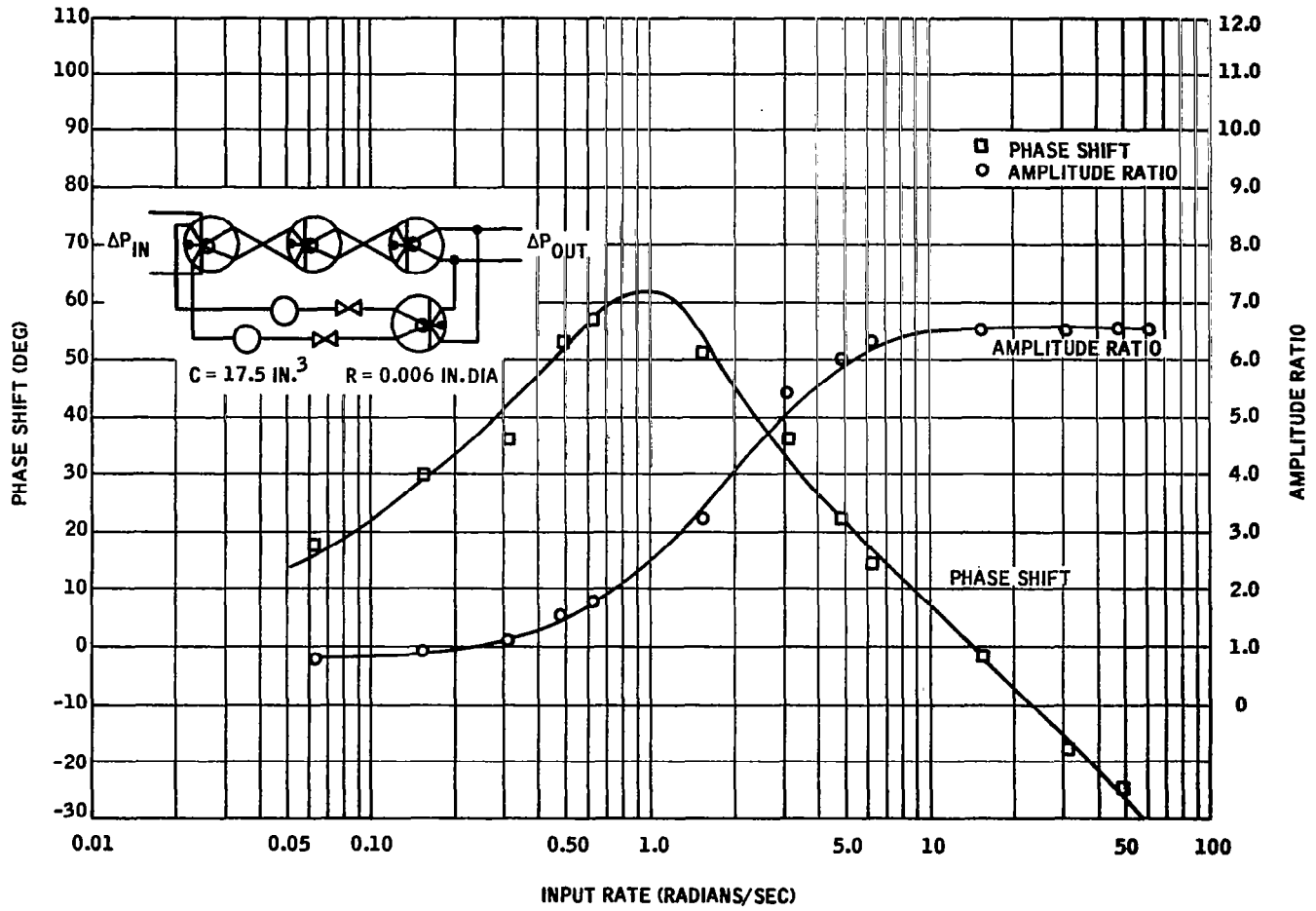


Figure 27. Frequency Response Lead Lag Network

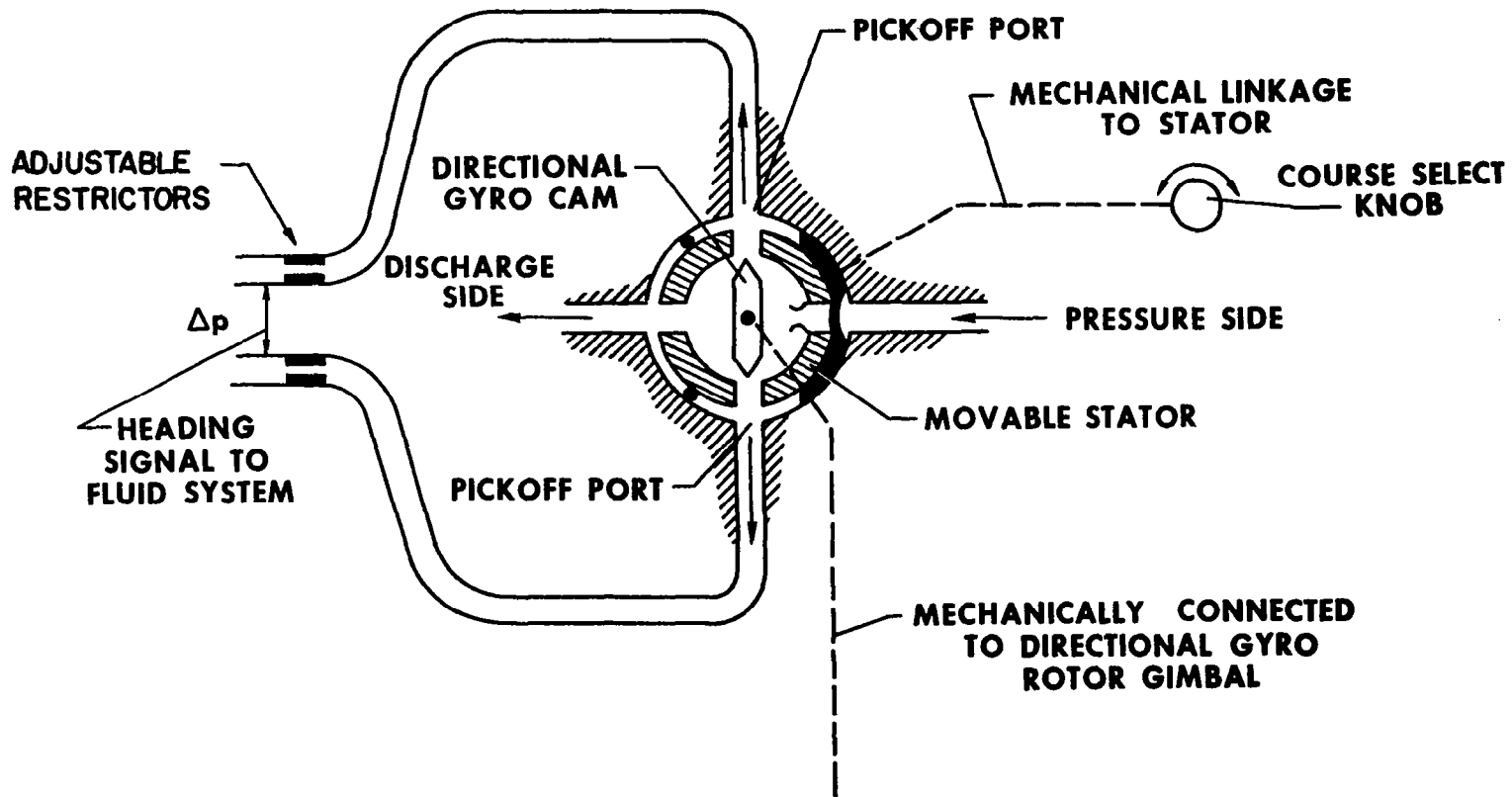


Figure 28. Directional Gyro Pickoff Schematic

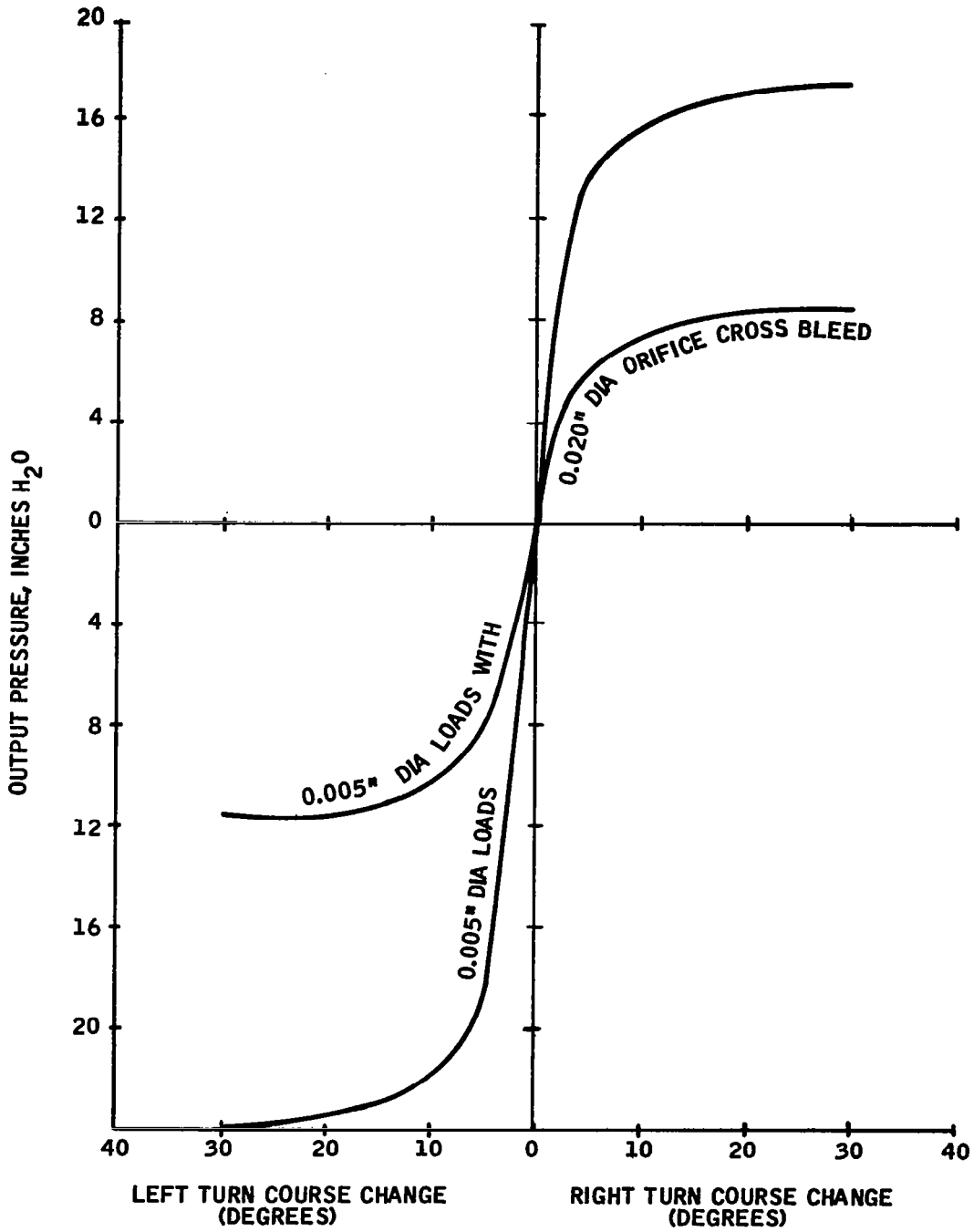


Figure 29. Directional Gyro Input/Output Relationship

The directional gyro rotor gimbal causes a differential signal pressure proportional to angular displacement up to approximately  $\pm 5$  degrees. From  $\pm 5$  to  $\pm 15$  degrees displacement, the signal becomes nonlinear, and beyond  $\pm 15$  degrees the maximum signal pressure is obtained. At 90 degrees of error, a phase reversal will occur.

The altitude-error sensor consists of a dual chamber with a mechanical flapper, as shown schematically in Figure 30. Both chambers are initially vented to ambient pressure. When altitude hold is commanded, the pressure in one chamber is trapped as a reference. As altitude changes occur, the differential pressure between the two chambers causes the flapper to be deflected accordingly. Flapper movement is used to create a differential signal pressure in proportion to altitude error. Unit threshold is approximately  $\pm 5$  feet of altitude. An electrically operated solenoid valve is used to trap the altitude air sample. The input/output relationship for the device used is shown in Figure 31. The X axis represents static ambient pressure which can be converted to feet by using the proper altitude pressure lapse rate for the reference altitude desired. The output of this device is fed into a 10 x 5 amplifier and then into the lead lag shaping network.

## DEVELOPMENTAL TESTS

A rate table was used to provide a rate signal for the fluidic rate sensor. A pressure transducer was used to monitor the rate sensor output and the signal was recorded on a Sanborn recorder. As the preamplifier cascade was built up, the gain of each stage in the cascade was plotted on an X-Y plotter using two pressure transducers to monitor input and output of the stage. Also, the gain of any continuous group of stages in the system cascade could be found using these transducers and the X-Y plotter. The most common gain curves plotted used the rate sensor signal as the X

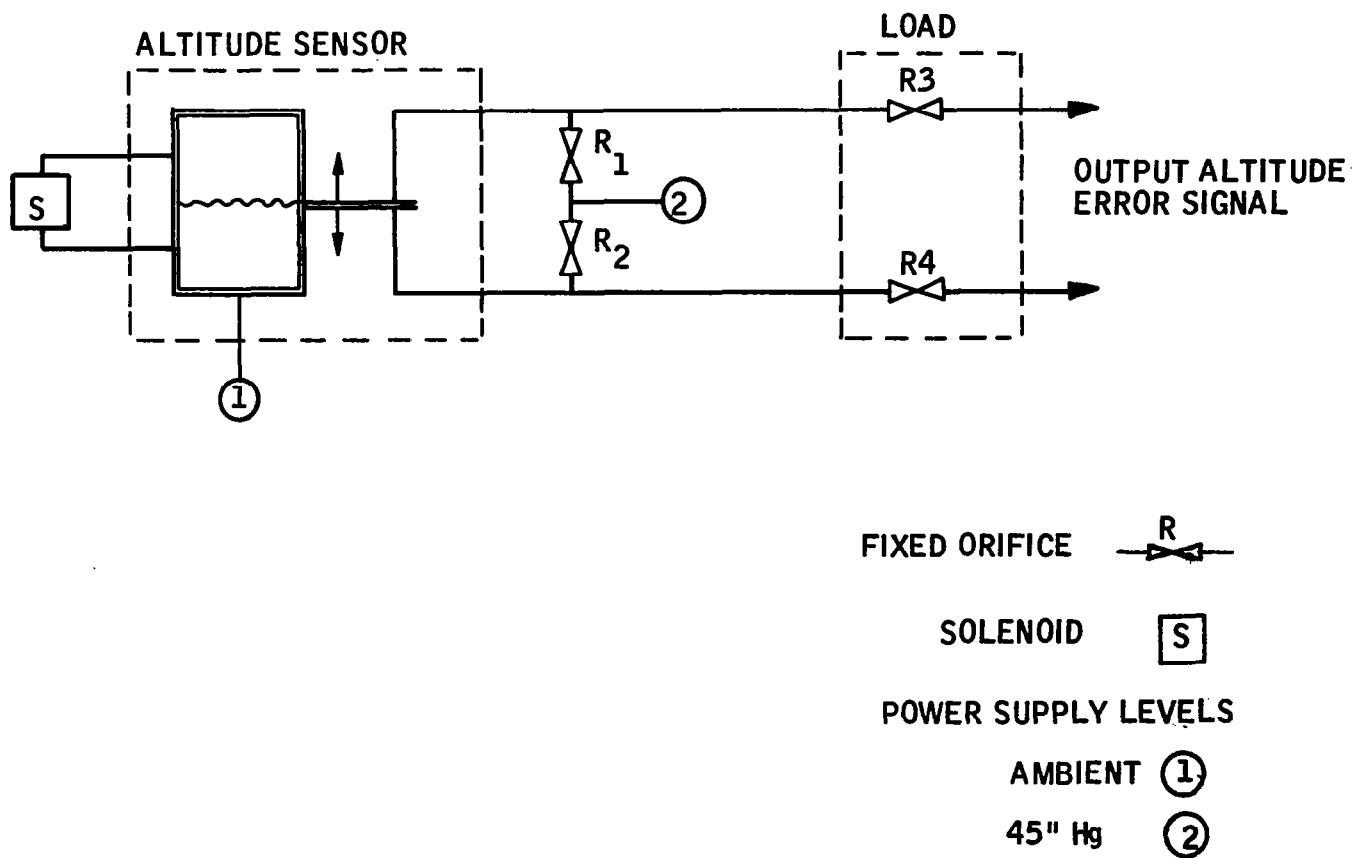


Figure 30. Altitude Sensor Schematic

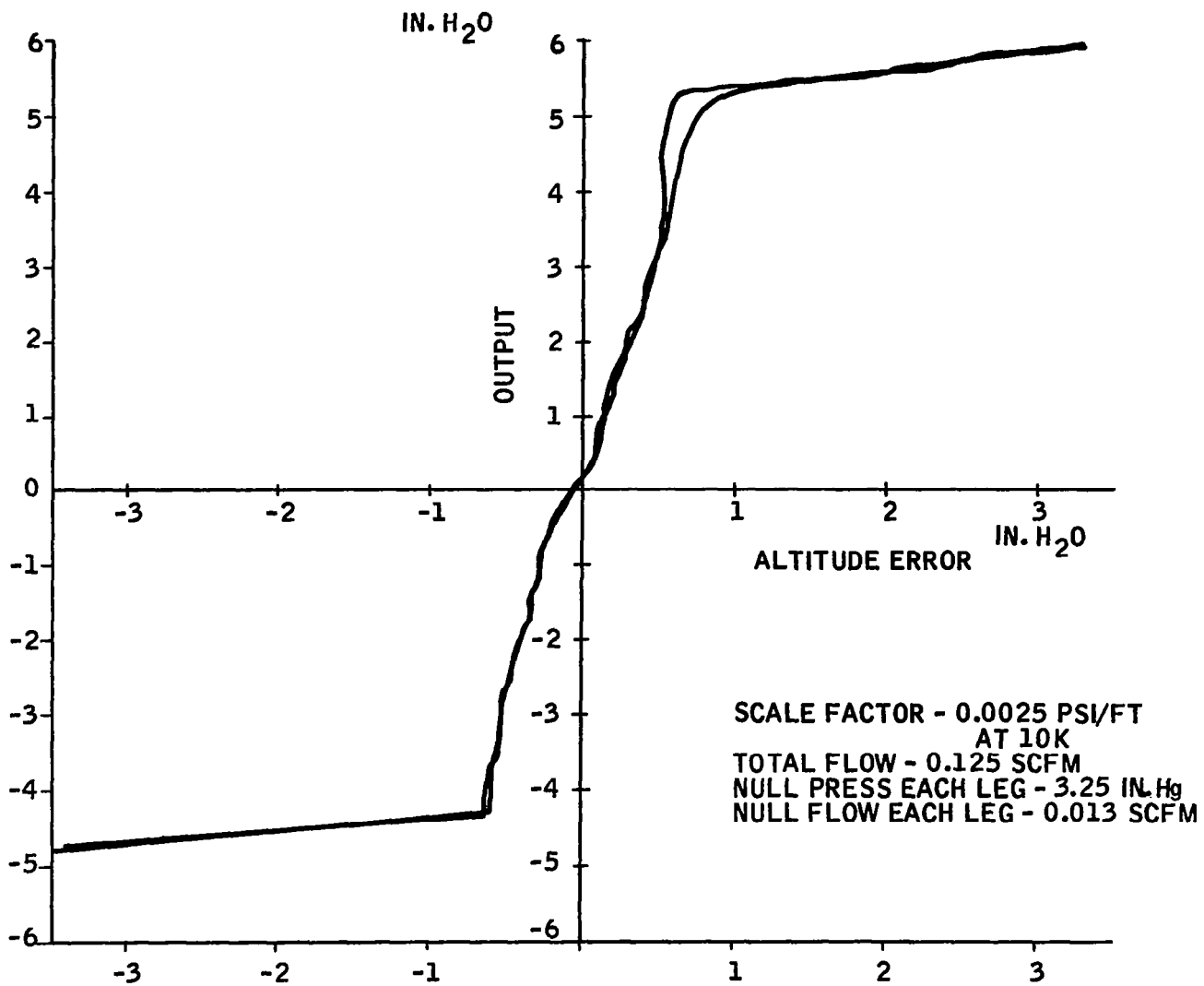


Figure 31. Altitude Sensor Input/Output Relationship

input and the output of each of the stages in the cascade as the Y inputs. This gives total cascade gain up to the output of the stage being investigated. These gain curves are very useful in detecting when the addition of a stage in the cascade causes nonlinear performance.

Figures 32, 33 and 34 are representative X-Y plots of the yaw, roll, and pitch axes, end to end, as obtained by the above described method.

The drum, cable and aircraft control surface loadings on the actuators were simulated in the laboratory. The test fixture consists of a torque arm, driven by the actuator output shaft, and pairs of springs which are stationed along the arm on both sides of the spindle to provide torque loading. The spring force/displacement constants and the spring attachment positions on the torque arm determine the torque loading on the actuator. A linear resistance potentiometer connected to the end of the torque arm monitors the position of the actuator. For the small angles of actuator motion (less than  $\pm 7$  degrees) encountered in the system, the linear output of the resistance potentiometer is effectively proportional to the angular output of the servo actuator cable drum.

The frequency response of each control loop in the system was found by placing the fluidic amplifier component assembly on a Genisco Oscillating Table (Model B-386) and adjusting the angular displacement of the table so the peak angular rate input to the rate sensor was held constant. The rates used were 1 degree/sec. from 0.1 cps to 1.5 cps and 3 degree/sec. from 1.5 cps to 4 cps. The table position, the rate sensor output, the servo amplifier output and the servo actuator position (using the actuator test fixture) were monitored and recorded on a Sanborn four channel recorder. These frequency response data were then analyzed for amplitude and phase relationships between angular input and system output.

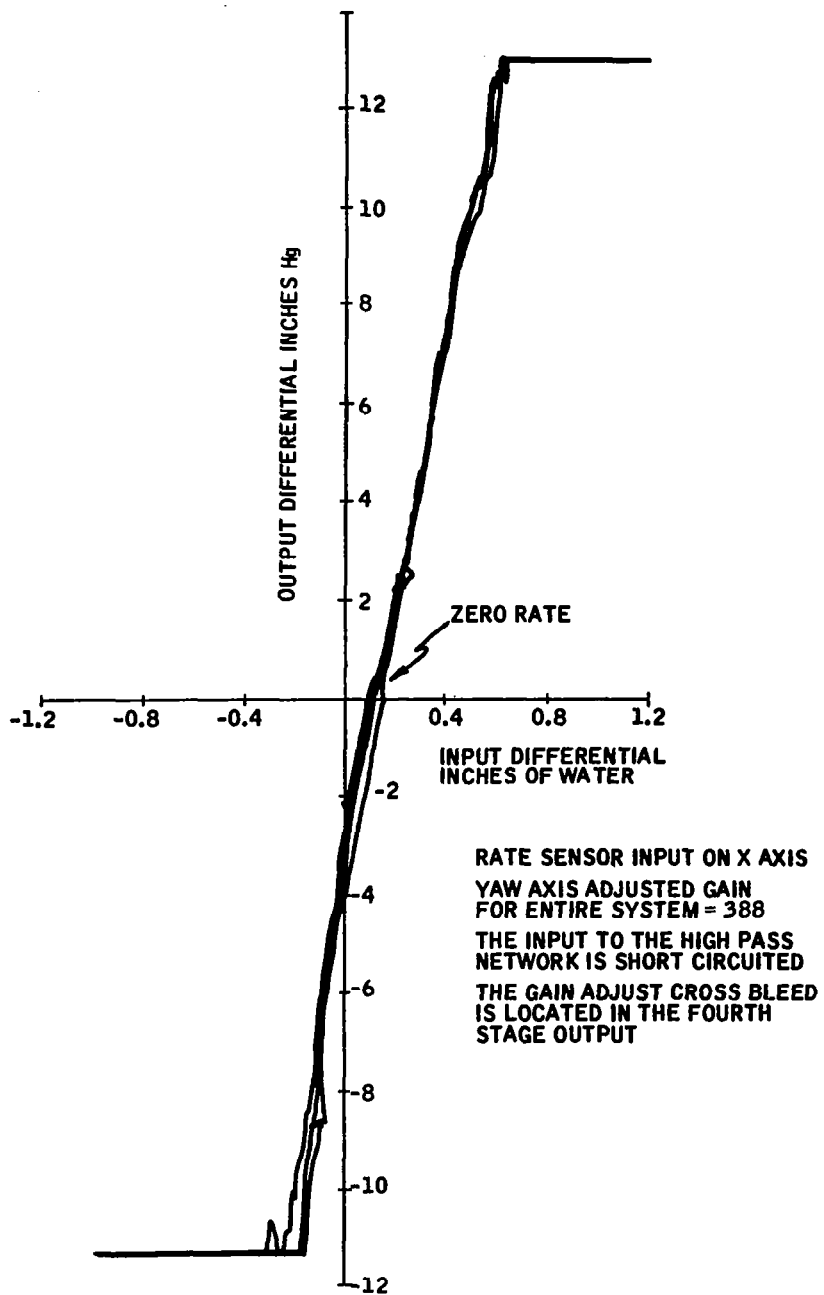


Figure 32. Yaw Axis Gain Curve

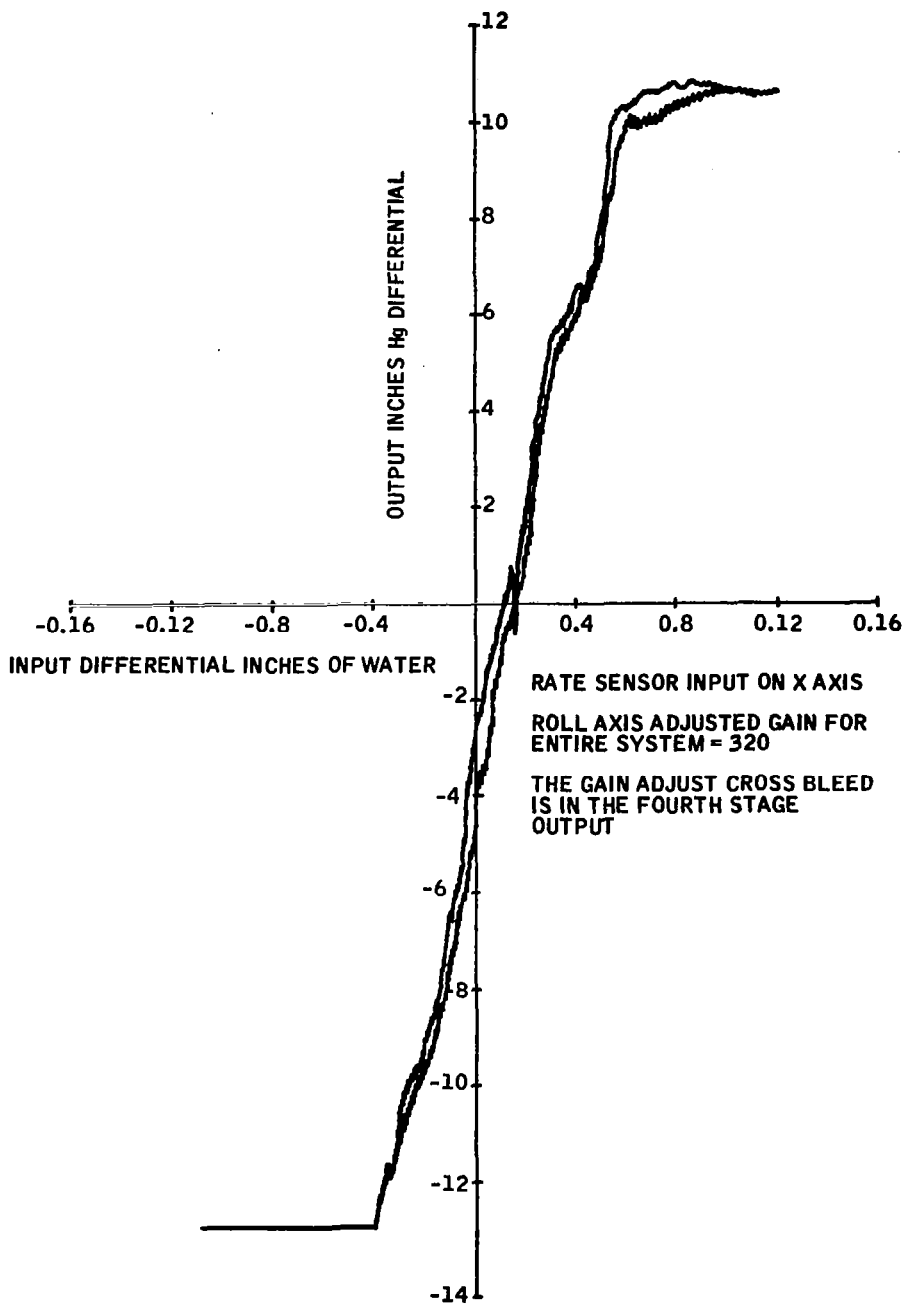


Figure 33. Roll Axis Gain Curve

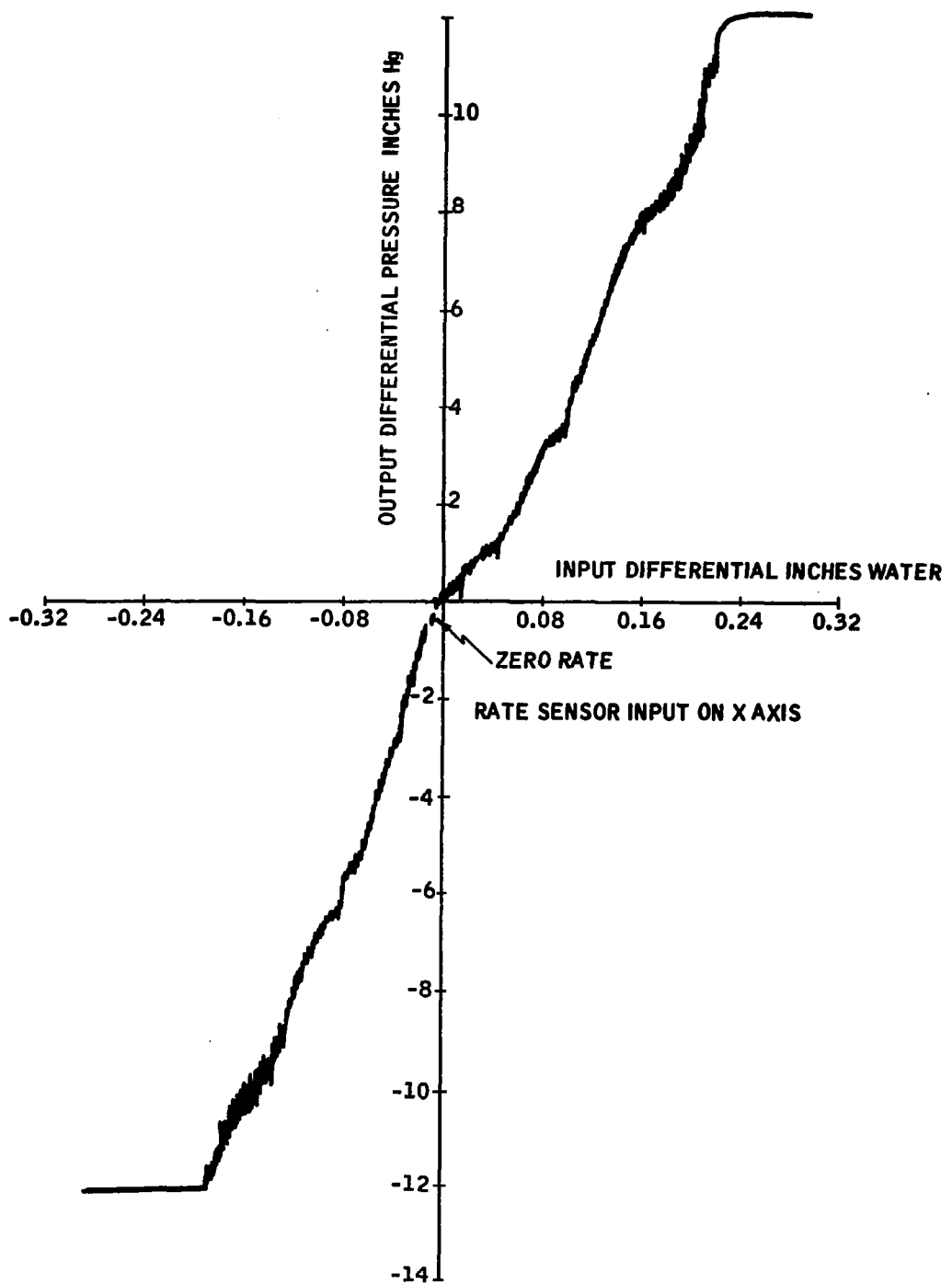


Figure 34. Pitch Axis Gain Curve

The frequency response of the altitude hold mode was found with the pneumatic sinusoidal function generator (bellows - vari-speed-drive device) supplying the varying altitude error signal to the altitude hold device. The amplitude of the input was  $\pm 30$  feet and the frequency range investigated was 0.01 cps to 5 cps. The sinusoidal input, the pitch axis servo amplifier output and the pitch axis servo actuator position were monitored and recorded on a four channel Sanborn recorder. These data were then analyzed for amplitude and phase relationships.

Frequency response checks were necessary during development of the amplifier, restrictor, and capacitor networks for the high pass filter in the yaw axis system and the lead-lag signal shaper in the altitude hold system. The inputs to these networks during frequency response tests were provided by the first stage of a hydraulic servo valve (Moog Valve Model 947) which has internal orifice modifications so it can control air flow. The first stage is an electrically positioned flapper valve which controls air flow through an orifice network so that a sinusoidal electric input signal will produce a sinusoidal air flow output signal. This device provided the necessary input to the filter and shaping networks to indicate what adjustments in restrictor sizes and capacitor volumes should be made to obtain the desired frequency response characteristics.

Figures 35 through 38 give the desired and actual frequency response of the altitude hold, yaw damper, wing leveler, and pitch damper modes of the system. Desired response is shown by lines; amplitude is continuous and phase is a broken line. Actual measured data are shown by discrete points.

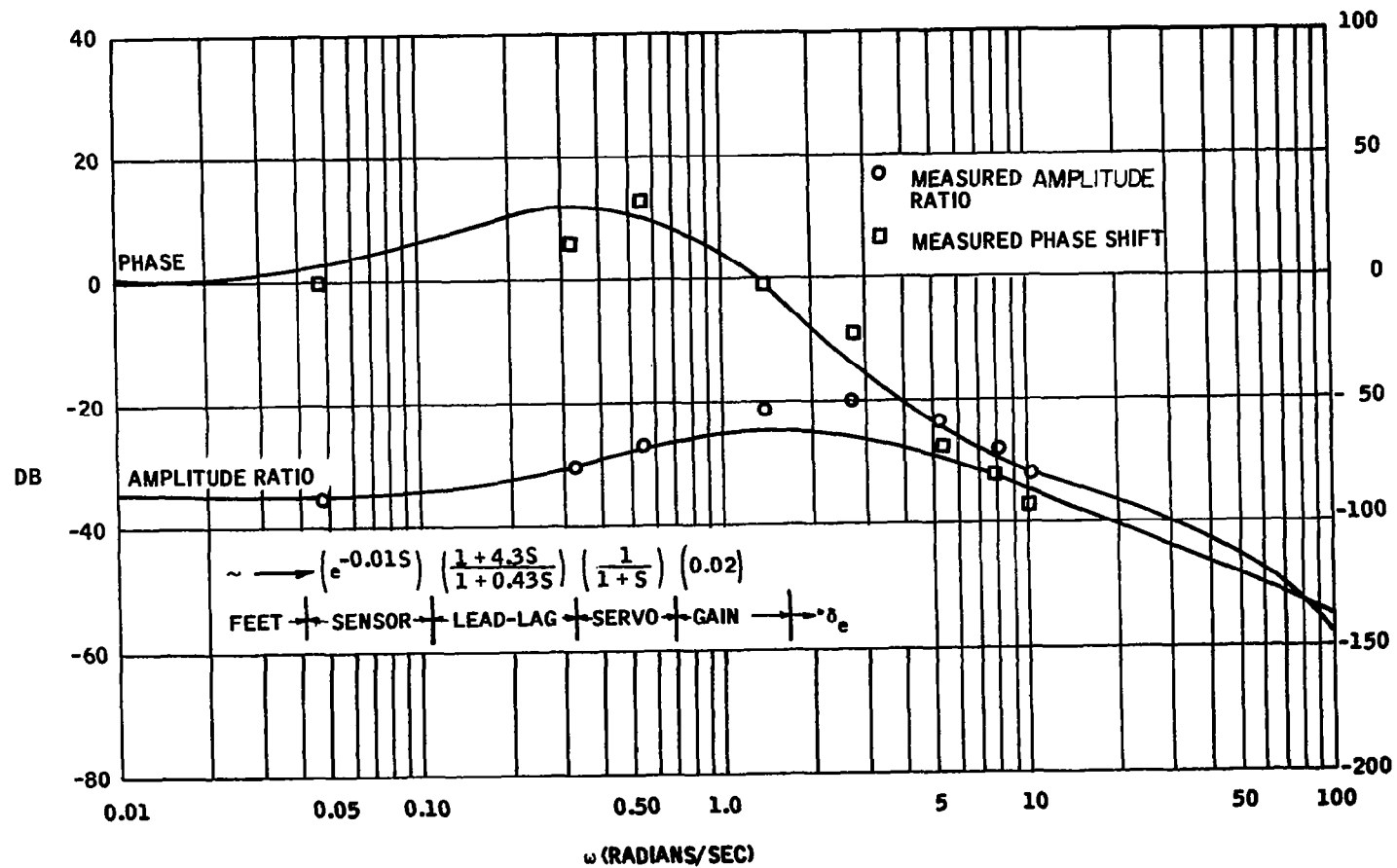


Figure 35. Altitude Hold Frequency Response

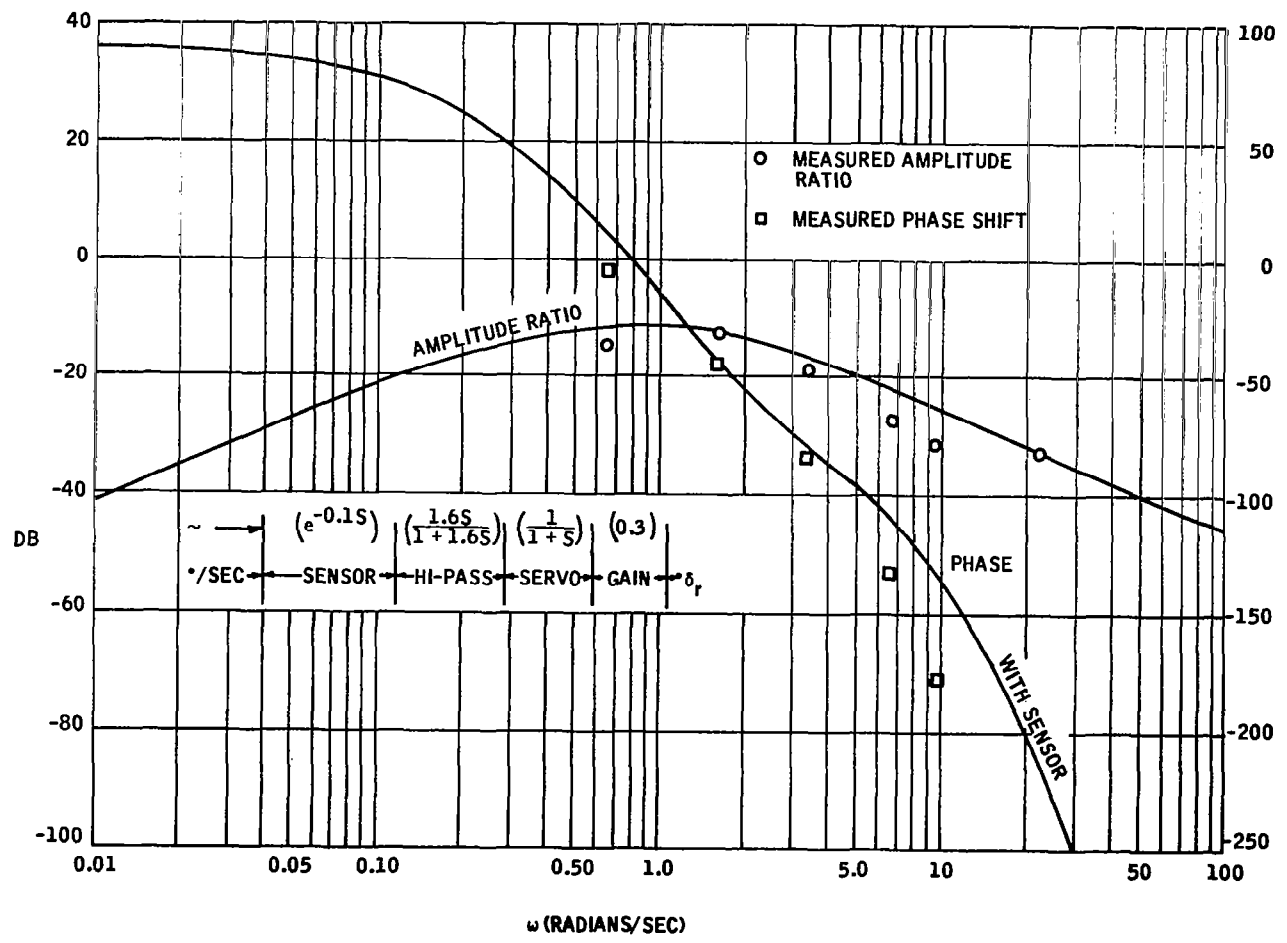


Figure 36. Yaw Damper Frequency Response

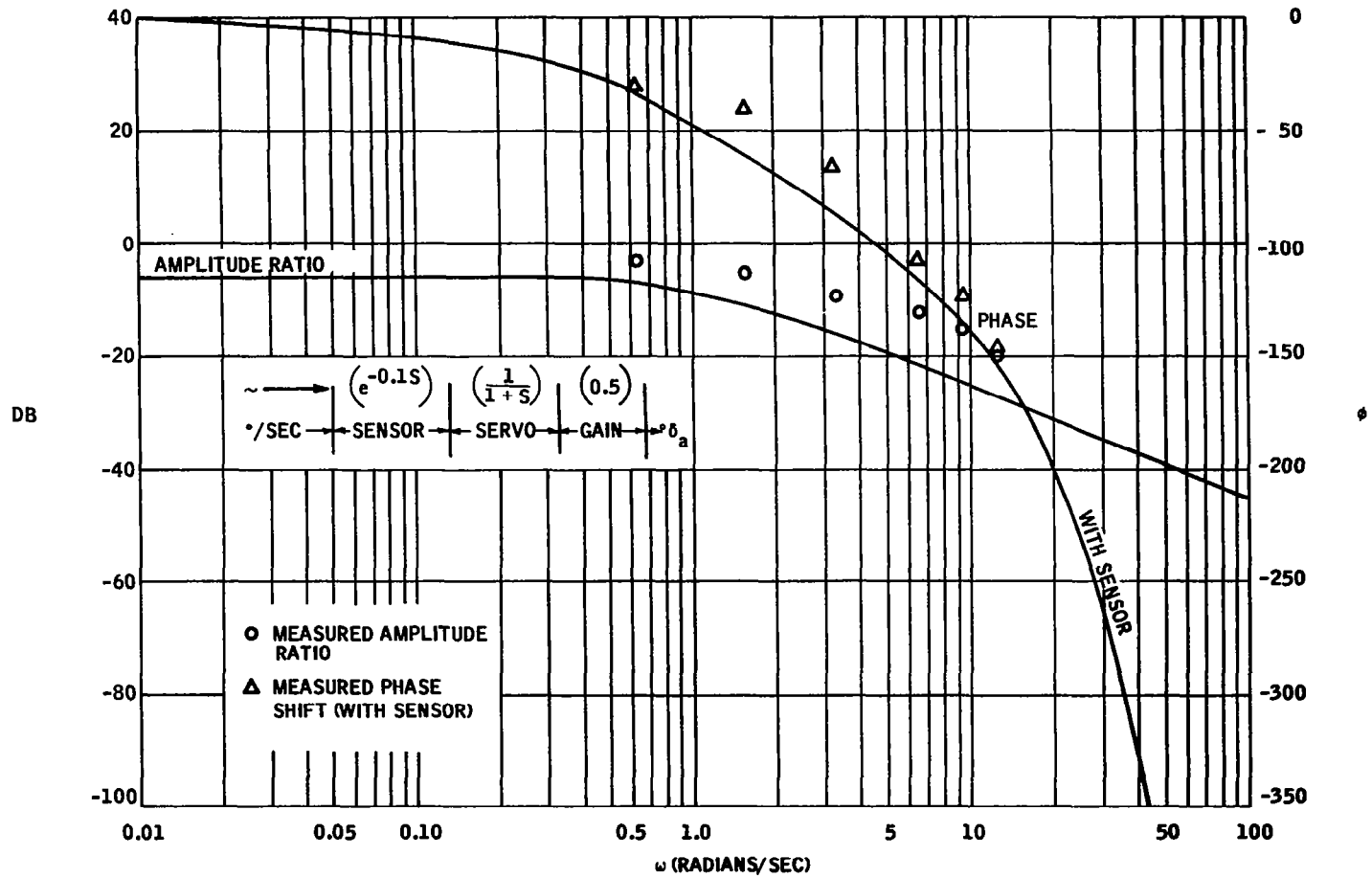


Figure 37. Wing Leveler Frequency Response

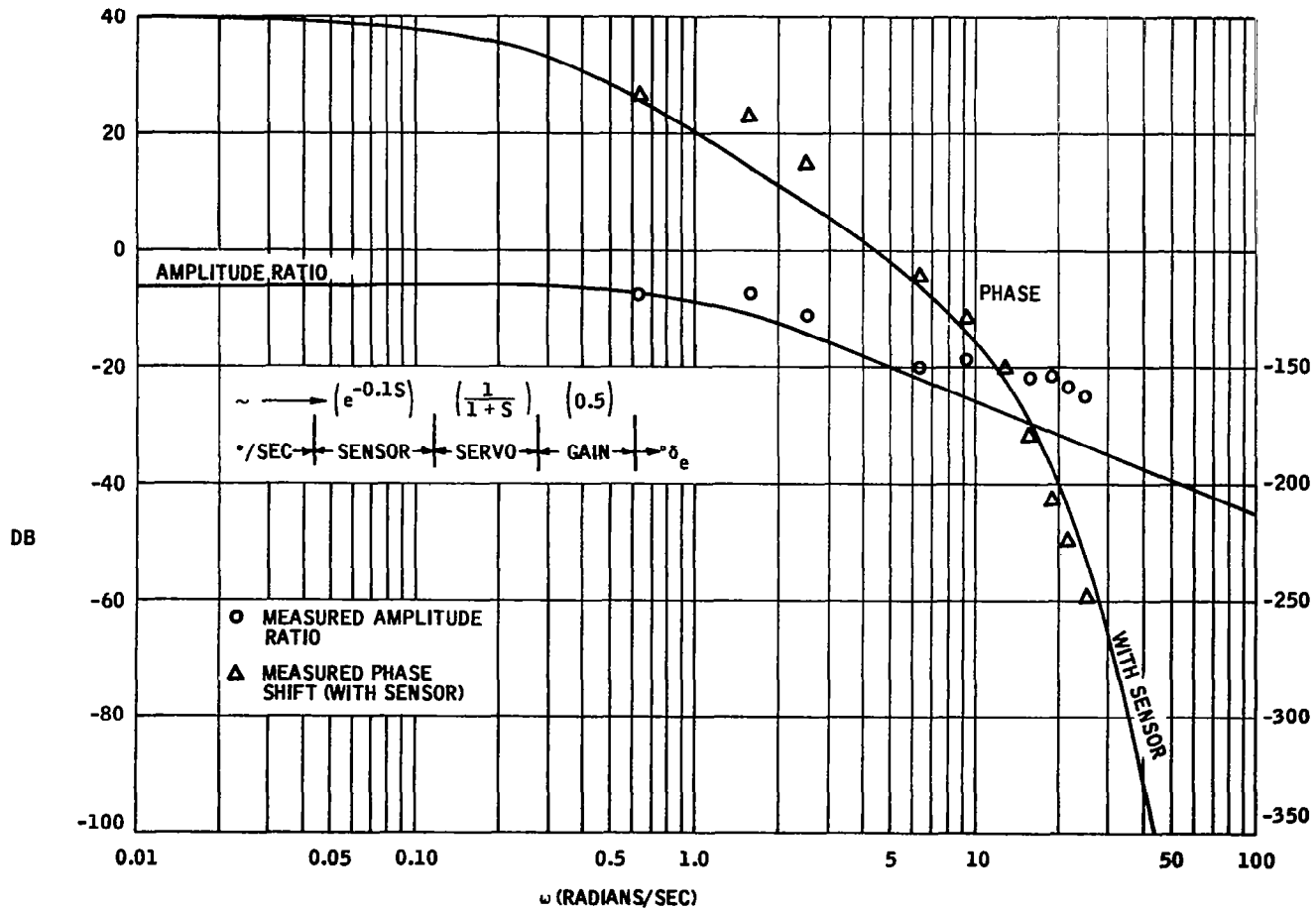


Figure 38. Pitch Damper Frequency Response

## ENVIRONMENTAL TESTS

Four groups of environmental tests were conducted:

In the first group all three axes were operated at 130 degrees F, room temperature and -30 degrees F, and the pitch axis was subjected to an additional test at 0 degrees F. Two-hour soak times were used in these tests.

In the second group, the system was operated in ambient pressures corresponding to operation at ground level, at 7,500 feet, and at 15,000 feet.

In the third group, cold temperature exposure was combined with altitude variations. The Pitch Axis Control System was tested both at 0 degrees F and -30 degrees F, while the Yaw and Roll axis control systems were only tested at -30 degrees F.

The fourth group consisted of vibration testing.

Description of the test setups is as follows:

The fluidic component assemblies, servo actuators mounted to their test fixture, and pressure regulators were placed inside the environmental chamber. Cockpit devices, i. e., Function Selector and Directional Gyro, were left outside the chamber at room conditions. The control flow outputs of the Function Selector and the Directional Gyro and the pressure inputs to the null indicators were fed through 20 foot lengths of 1/16 inch diameter plastic tubing to the fluidic component assemblies inside the chamber. Air power for the Function Selector came through 20 feet of 1/8 inch diameter tubing from a regulator inside the chamber. Air power for the Directional Gyro came through 20 feet of 3/8 inch diameter tubing from a regulator inside the chamber.

Supply pressures were monitored by Mercury manometers inside the chamber.

The following operation parameters were monitored with pressure transducers during environmental testing:

- (a) Rate sensor output
- (b) Trim device output
- (c) Turn device output
- (d) Directional gyro output
- (e) Servo amplifier output
- (f) Altitude error input

Actuator position was monitored with the linear potentiometer mounted on the actuator test fixture. All of the monitored information was recorded on two four-channel Sanborn recorders. The altitude error input was provided with a screw driven bellows. A Hass Electric Read-Out Mercury Manometer was used for making accurate adjustments of the altitude error signal. Supply pressure changes, Trim authorities, null shifts, Turn input capabilities, Heading Hold and Select capabilities, and Altitude Hold capabilities were checked during the environmental tests.

The vibration tests were conducted as follows:

The fluidic component assemblies and the function selector assembly were mounted on the vibration exciter and subjected to 2g, 15 minute vibration scans from 0 cps to 500 cps and back to 0 cps. All assemblies were subjected to these scans in three axes.

The control systems being tested were operating during vibration and the following operation parameters were monitored:

- (a) Rate sensor output
- (b) Trim device output
- (c) Servo amplifier output
- (d) Altitude hold output
- (e) Actuator position output
- (f) Turn device output

A strobe light was used during vibration to observe the structural integrity and flightworthiness of the packaging. Observation of all input devices during vibration was made to detect null shifts, leaks, and any other unsatisfactory operation characteristics.

The environmental tests were accomplished with the intent of duplicating the actual system operational environment and usage.

The yaw/roll FCA operated satisfactorily at all test conditions except the combination test (low temperature/high altitude). An operational failure occurred in this environment as a result of the simulated pressurized cabin configuration.

The cabin pressurization system on the aircraft can maintain a 3 psi differential above the atmosphere. This differential results in the function selector and directional-gyro (D. G. ) pickoff being at a vacuum with respect to the cabin. The D. G. leaks at the pickoff, caging knob, and course select knob.

When the cabin differential pressure results in a vacuum, these leaks result in the ingestion of warm, humid air which freezes in the transmission lines where the lines enter the low temperature areas. The freezing causes loss of input capability from the pilot's control devices. The basic autopilot devices located in the unheated chamber were not affected.

The function selector devices were reworked to prevent leaks. The D. G. pickoff operating pressure was raised to 2.25 psig. However, the cabin differential of 3 psig leaves a net vacuum of 0.75 psi on the D. G. The D. G. leaks are difficult to prevent completely since this device was not intended to be hermetically sealed.

Vibration testing of the yaw/roll FCA, pitch FCA, and function selector consisted of separately vibrating each component in three axes through a scan of 0.018 inch double amplitude to 45 cps and 2 g's to 500 cps. The rate sensor output, trim output, turn output, altitude output, and servo amplifier output were recorded.

The yaw/roll FCA operated satisfactorily; however, the amplifier holding brackets required strengthening to improve the slight resonant deflections that were noted.

Function selector modifications which were required for vibration qualification included: (1) greater squeeze on the roll and yaw trim controls to prevent movement, (2) stiffening brackets between the front and back panels; and (3) securing the cover on top and bottom to reduce cover motion.

Pitch FCA vibration tests produced the following malfunctions which were corrected as noted:

1. Rate Sensor Output Hardover

Cause - Pickoff lock screw loosened.

Correction - Replaced pickoff blade and provided nyloc screws for the pickoff lock screws. Provided a more rigid mounting bracket.

2. Altitude Hold Output Variance With Vibration Frequency

Cause - Resonance motion of flapper-nozzle assembly.

Correction - Modified mounting bracket and installed vibration isolators.

3. Excessive Resonant Displacement Amplitudes of Capacitor Cans and Amplifier Brackets.

Correction - Added two mounting screws and braces to capacitor cans. Provided added stiffening to amplifier brackets.

During the initial low temperature tests, the altitude hold loop control range decreased by 56 percent at 0 degree F and 84 percent at -30 degrees F. Modification of the altitude circuit orifice network, adjustment of the altitude sensor nozzle-flapper, and addition of an amplifier stage improved both linearity and control range such that no decrease in range occurred down to 0 degree F.

At the combination of low temperature and altitude (-30 degrees F/15,000 feet), the pitch servo amplifier output signal went hardover with a very small input in one direction. This condition was caused by an insufficient control signal differential and was corrected by increasing the diameter of the transmission line between the pitch FCA and pitch servo Amp from 1/16 inch to 1/8 inch.

**System performance at high temperature, 130 degrees F, was similar to performance at room temperature. Slight amounts of rate-sensor drift occurred, but the offset was easily trimmed out by using the function-selector controls.**

**System performance at low temperature, -30 degrees F, varied from axis to axis. All axes developed null offsets because of an increase of mass flow and required manual retrimming. Loop gain increased as the temperature decreased. The altitude-error sensor was found to have an erratic output when operated at temperatures below 0 degree F. Small transient temperature variations when the unit was at -30 degrees F resulted in large changes in altitude-sensor output.**

**System performance at altitudes from sea level to 15,000 feet was found to be satisfactory if pilot retrimming about wings-level was acceptable. The pilot trimming was necessitated by null shift with altitude in the sensors.**

## SECTION IV FLIGHT TEST

### SUMMARY

The flight test work of the program consisted of the installation and ground check-out of the fluidic system and instrumentation, contractor flight checkout, and the NASA flight test program. All of the flight test work was accomplished at the NASA Flight Research Center, Edwards, California.

Installation started March 21, 1966, and was completed May 31, 1966. The first contractor checkout flight was June 2, 1966; the last contractor checkout flight was June 24, 1966. A total of nine flights were made. The system was accepted by NASA and the contractor checkout phase concluded June 24, 1966. The installation and contractor flight checkout was scheduled for 10 weeks and 10 flights. The actual program took 13 weeks and nine flights.

The most limiting problem encountered in flight testing the fluidic system was in obtaining flight data on pressure signals in the system. This problem was never satisfactorily resolved, since at the end of the program only three fluidic signals could be simultaneously recorded in flight.

Performance of the system is acceptable in all modes except the altitude hold mode. Altitude hold mode performance is good at altitudes up to 7,000 feet. At 7,000 feet and greater altitudes, the altitude hold mode is unstable; as altitude is increased, stability decreases. The reason for this is believed to be decrease in pitch rate gain with altitude increase. The gain decrease results from the cumulative fluidic amplifier and rate sensor gain losses with altitude.

## **INSTALLATION**

Five weeks were scheduled for installation of system, instrumentation, and ground checkout. Installation started March 21, 1966. The aircraft was taken off flight status and all seats, cabin right side upholstery, and carpeting were removed. This was necessary to determine the best routing for fluidic transmission lines through the pressure bulkhead and forward through the cabin to the function selector, for instrumentation and servo installation.

The following items of work were accomplished:

### **A. Modified Aircraft Pneumatic System**

1. Replaced existing vacuum pump on each engine by contractor supplied pumps. Three Airborne Manufacturing Company 423CC pumps were provided for this purpose, one of which is a spare.
2. Removed existing primary oil separator located in each engine nacelle and replaced by contractor supplied filter.
3. Added AFCS pneumatic tee fitting between deicer regulator separator valve and deicer distributor.
4. Added deicer cut-off solenoid.

Items 3 and 4 were particularly arduous since access to the rear fuselage was by the battery access door which is approximately 24 inches by 12 inches. In addition, the space between the deicer regulator and distributor was too short to allow straight line addition of the cut-off solenoid and tee, so extra plumbing was required.

## **B. Installed AFCS Components**

1. Installed yaw, roll, and pitch servo actuators and pulley bracket in baggage compartment.
2. Installed fluidic AFCS directional gyro on instrument panel.
3. Installed yaw/roll chassis and pitch chassis in baggage compartment.
4. Installed AFCS controller in cockpit map case.
5. Purged pneumatic pressure lines.
6. Installed controller wiring. Master AFCS switch was put in series with deicer such that pilot selection of deicer interrupts electrical power to AFCS.
7. Installed AFCS plumbing and regulators.

To accomplish item 2 above required removal of the copilot's flight instrument panel and fabrication of a new panel to provide space for installation of the directional gyroscope.

The steps listed below were followed to accomplish ground checkout of the system as installed.

### **Ground Check Pneumatic System Operation**

1. Run aircraft engines while checking correct operation of:
  - Instrument Panel Vacuum Pressure Gauge
  - Flight Instruments
  - Deicer Operation

- **Pump Relief Valve Setting and Operation**
- **Electrical Load and Condition**

### **Ground Check AFCS Operation**

**Using hangar air supply as a power source, the following checks were performed:**

**1. AFCS Mode Selection Operation -**

- **Yaw/Roll Axis Engaged**
- **Heading Engaged**
- **Turn Control**
- **Yaw Trimming**
- **Roll Trimming**
- **Pitch Axis Engaged**
- **Pitch Trimming**

**2. Manual Control System Operation -**

- **Check for full free control cable travel**
- **Check cable friction levels compared with friction levels prior to servo installation**
- **Check servo actuator engage and disengage feel**
- **Yaw, roll, and pitch servo actuator overpower operation.**

**3. AFCS Loop Gains -**

- **Power regulation by AFCS regulator and deicer regulator separator valve.**
- **Rate sensor operation**
- **Loop pressure gain check**
- **Signal phasing checks.**

#### **4. AFCS Operation with Aircraft Engines Running -**

- **Pressure Levels**
- **AFCS Interface Operation Including Servo Overpower Check.**

No configuration changes were made in the power supply during flight checkout. Honeywell print C13089-7 accurately depicts the layout as it is in the aircraft. Three Moore pressure gauges were added in the aircraft baggage compartment. These gauges together with the proper operating pressures are indicated in Figure 39.

The servos were sized based on 5 psid inputs. The nominal servo amplifier power supply level was set at 15 psig in order to meet the 5 psig servo requirement assuming 0.33 recovery. The servo amplifier recovery is approximately 0.4 of the power level. This would allow the servo amplifier level to be 12.5 psig.

However, 12.5 psig is too low for the Moore regulators to function properly. The regulator minimum is 13 psig to obtain 4 psig regulated. So the lowest the servo amplifier pressure can be is 13 psig.

The Bendix deicer regulator was then adjusted until 13.5 psig was obtained at the servo amplifiers. This pressure resulted with line losses and the pump running at 18.5 psig.

The existing vacuum systems are maintained unchanged at 5 inches Hg vacuum on the aircraft.

All work on the equipment was done at the aircraft with the equipment installed. A rate table was placed under the wing next to the baggage compartment door and the FCA's were unbolted from their mounting brackets and placed on the rate table. Gains were checked then by actual rates into the FCA's.

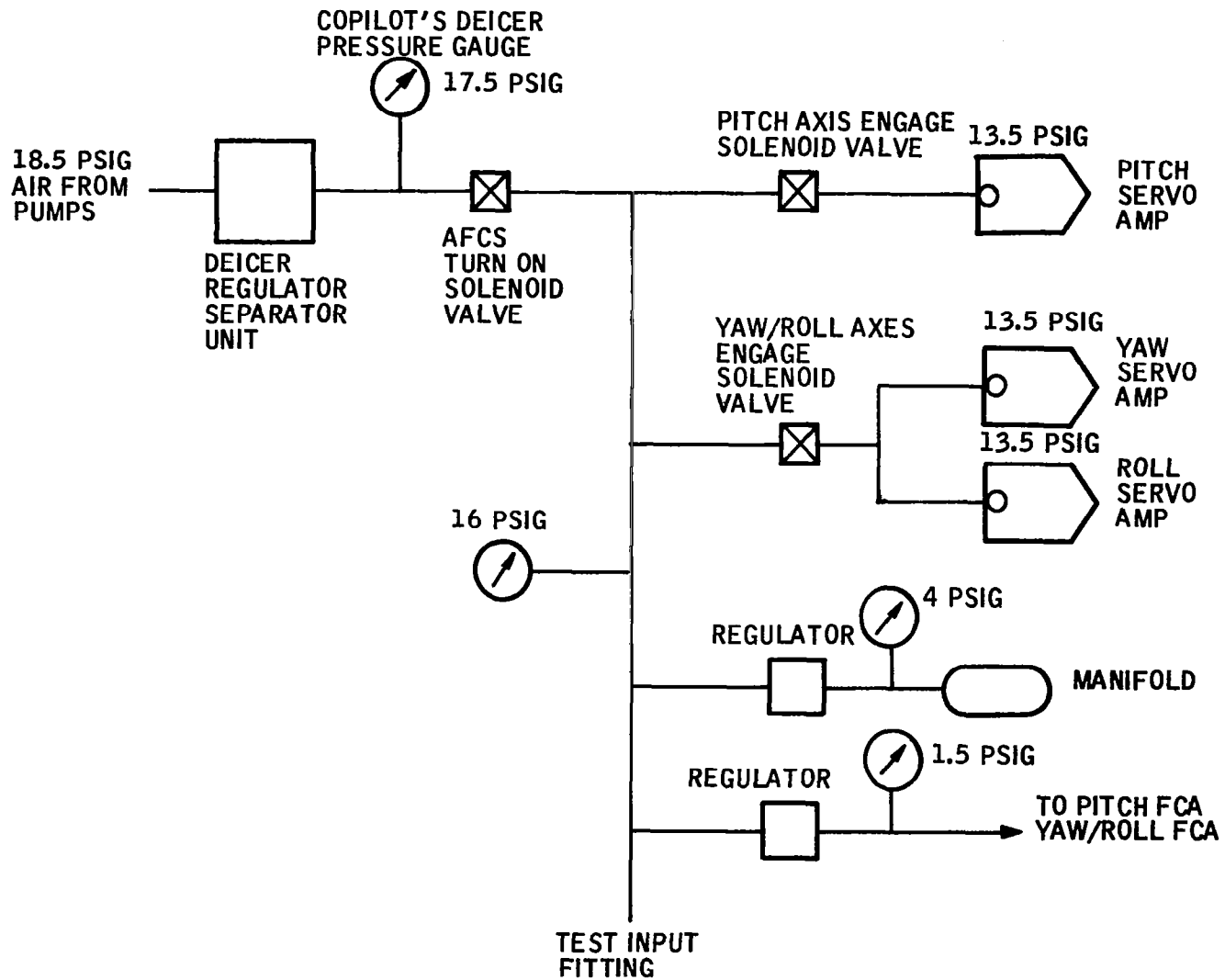


Figure 39. Power Supply Pressure Level

The pressure levels to the trim devices were all adjusted to give acceptable trim gain to the pilot.

The pressure gains were set up as follows for the first flight.

- Roll Axis

$$G_{\delta a_r} = 375; \frac{\text{Aileron Servo Amplifier Output}}{\text{Yaw Rate Sensor Output}}$$

$$G_{\delta a_{\text{Turn}}} = 70; \frac{\text{Aileron Servo Amplifier Output}}{\text{Turn Control Output}}$$

Heading: 10°  $\psi$  Select    3 deg/sec CW  
          345°  $\psi$  Select    3 deg/sec CCW

- Yaw Axis

$$G_{\delta r_r} = 390; \frac{\text{Rudder Servo Amplifier Output}}{\text{Yaw Rate Sensor Output}}$$

- Pitch Axis

$$G_{\delta e_{\dot{\theta}}} = 590; \frac{\text{Elevator Servo Amplifier Output}}{\text{Pitch Rate Sensor Output}}$$

$$G_{\delta e_h} = 170; \frac{\text{Elevator Servo Amplifier Output}}{\text{Altitude Sensor Output}}$$

## FLIGHT TEST INSTRUMENTATION

An instrumentation package was fabricated in Minneapolis to fit the seat mounting rails in the aircraft. The package contained the following devices:

**One 8-channel flight recorder**  
**One 8-channel recorder amplifier**  
**One 8-channel a-c calibrator**  
**One vertical gyroscope**  
**Three rate gyroscopes**  
**One normal accelerometer**  
**One self-balancing thermocouple readout**  
**Three pressure transducer amplifiers**

**These devices provide the following 12 aircraft parameters for recording:**

**Pitch attitude**  
**Roll attitude**  
**Yaw rate**  
**Roll rate**  
**Pitch rate**  
**Normal acceleration**  
**Rudder position**  
**Aileron position**  
**Elevator position**  
**Three selectable pressure signals**

**The a-c calibrator is the main control and calibration panel as well as the junction point for all the interconnecting system cabling.**

**All the instrumentation is 400 cps single phase a-c power. This power is provided by a 750 va single-phase inverter installed in the baggage compartment for this purpose.**

**Three control position transmitters were installed in the aircraft to measure aileron, elevator, and rudder position.**

**Two thermocouples were installed -- one in each engine driven pump output.**

Three pressure transducers were wired from the baggage compartment where the Fluid Component Assemblies are, to the pressure transducer amplifiers, and then to the flight recorder.

The power required by the instrumentation setup as described above is:

- Recorder (1 each)

115 vac	3.25 amps	400 cps	1 $\phi$
27.5 vdc	1.8 amps dc		

- Vertical Gyro (1 each)

115 vac	0.43 amps Starting	400 cps	1 $\phi$
	0.2 amps Running		

26 vac	0.4 amps Running	400 cps	1 $\phi$
--------	------------------	---------	----------

28 vdc	1.0 amps Maximum		
--------	------------------	--	--

- Rate Gyro (3 each)

115 vac	0.35 amps Starting	400 cps	1 $\phi$
	0.13 amps Running		

The instrumentation set up is convenient and adequate for the task, except for pressure signals. The recorder is the hot wire, direct recording type, so no processing of the recordings is necessary. It is cabin installed, and tests may be repeated until desired recording results are obtained. The limitation is that only 8 channels may be recorded simultaneously and a capability of 12 parameters exists. Therefore, prior to performing a test, the proper parameters must be selected.

The major instrumentation problem is recording transduced pressure signals from the fluidic system. The output from the strain gage pressure transducers is very small. For the PM131TC transducers, the scale factor as used is approximately 90 microvolts per inch of H<sub>2</sub>O pressure. It is required to record signals in the order of hundredths of an inch of H<sub>2</sub>O. The flight recorder will not satisfactorily record such small signals, needing at least a gain of 300. To solve this problem, procurement of special amplifiers was required. Three instrumentation amplifiers were purchased by NASA for this purpose. Another problem associated with pressure transducer use in operating systems is the added time constant and resulting change in circuit performance. It was found that the PM5TC Statham transducers have sufficient volume to prohibit their use in operating circuits because of the added phase lag.

## CONTRACTOR CHECKOUT

The purpose of this phase of the flight testing was to verify the flightworthiness of the AFCS installation and check lateral and longitudinal axis operation. Nine contractor checkout flights were made between 2 June and 24 June 1966. Figure 40 is a summary of these flights.

One of the first problems of the flight test program was that the pneumatic pump output temperature was higher than expected and output pressure/flow consequently lower. Pump temperature is a function of load which means as more axes of the system are engaged, altitude is increased and engine rpm increased pump temperature goes up. Initially it was found with all modes engaged at cruise flight conditions at 10,000 feet altitude, 2,600 rpm, 160 knots indicated airspeed pump temperatures were approximately 450°F and pressure was 12 psig instead of 17.5 psig. This problem was somewhat alleviated by adding 1-1/2 inch diameter tubes which direct impact air from the front of the engine nacelle to the pump for cooling. This dropped pump temperatures about 100°F. However, to obtain adequate pressure required 2800 rpm where 2600 rpm was the minimum cruise under these conditions.

Flight No.	Date	System Configuration	Objective	Result
1	June 2, 1966	$G_{\delta_{a_r}} = 375$ Heading $10^\circ 3''/\text{sec. r}$ $G_{\delta_{r_r}} = 390$ $G_{\delta_{e_q}} = 590$ $G_{\delta_{e_h}} = 170$	Operational check of all modes.	Power supply pressure loss and $475^\circ\text{F}$ temperature at altitude. Ground checks found filter leaks.
2	June 3, 1966	Same as Flight No. 1	Power supply checks. Operational check.	Increased RPM will provide pressure. Wing leveler mode gain too low. Altitude mode unstable.
3	June 6, 1966	$G_{\delta_{a_r}} = 1100$ (maximum) $G_{\delta_{r_r}} = 390$ $G_{\delta_{e_q}} = 590$ Altitude mode disabled; pitch damper only.	Wing leveler operation; pitch damper operation.	Wing leveler gain too high. Pitch damper functioning. Yaw damper phased wrong. Altitude circuit tube found pinched.
4	June 9, 1966	$G_{\delta_{a_r}} = 544$ Yaw damper; phasing corrected $G_{\delta_{r_r}} = 475$ $G_{\delta_{e_q}} = 680$ Altitude mode $G_{\delta_{e_h}} = 180$ Re-activated with aft fuselage static source Ram air pump cooling added.	Wing leveler mode, yaw damper, and altitude mode operation.	Wing leveler, turn, and yaw damper satisfactory. Pump temperature max $340^\circ\text{F}$ . Altitude mode unstable.
5	June 13, 1966	$G_{\delta_{a_r}} = 544$ Altitude shaping circuit worked on. $G_{\delta_{r_r}} = 475$ $G_{\delta_{e_q}} = 1100$ $G_{\delta_{e_h}} = 150$ $G_{\delta_{a_\psi}} = 34$	Heading mode operation. Altitude mode operation.	Heading limit cycle $\pm 4^\circ 40$ sec. period.  Altitude mode stable at 5,000 feet by operation on linear portion of altitude curve.
6	June 15, 1966	$G_{\delta_{a_r}} = 544$ $G_{\delta_{r_r}} = 900$ $G_{\delta_{e_q}} = 1100$ $G_{\delta_{e_h}} = 150$ $G_{\delta_{a_\psi}} = 11$	Yaw damper, heading, and altitude mode operation.	Pitch trim flow divider malfunction. Yaw trim flow divider loose. Heading hold solenoid open because of function selector mechanical interference. Heading gain too low. Yaw damper improved. Altitude performance similar to Flight 5.
7	June 21, 1966	$G_{\delta_{a_r}} = 544$ Altitude shaping circuit worked on. $G_{\delta_{r_r}} = 900$ $G_{\delta_{e_q}} = 1100$ $G_{\delta_{e_h}} = 170$ $G_{\delta_{a_\psi}} = 34$	System operation; emphasis on altitude control.	Wing leveler and turn good at 5,000 and 10,000 feet. Heading hold good at 5,000 but has limit cycle at 10,000. Altitude has limit cycle at 5,000 and is unstable at 10,000.
8	June 22, 1966	$G_{\delta_{a_r}} = 544$ $G_{\delta_{r_r}} = 900$ $G_{\delta_{e_q}} = 1100$ $G_{\delta_{e_h}} = 82$ $G_{\delta_{a_\psi}} = 30$	Altitude Hold	Altitude has limit cycle at 5,000 feet and unstable at 10,000 feet.
9	June 24, 1966	$G_{\delta_{a_r}} = 544$ Altitude shaping circuit $G_{\delta_{r_r}} = 900$ linearized $G_{\delta_{e_q}} = 1100$ $G_{\delta_{e_h}} = 82$ $G_{\delta_{a_\psi}} = 30$ Independent pitch damper and altitude mode capability added.	Altitude Hold	5,000 feet altitude limit cycle period. 18 seconds $\pm 0.6^\circ/\text{sec}$ . 10,000 feet altitude mode diverges.

Figure 40. Control Flight Summary

Several changes were made in gain and work was done on the altitude shaping network. To document these changes, each control loop will be considered separately and discussed below.

Yaw rate to aileron was flown initially with a pressure gain of 375. This was found to be too low. The maximum gain of 1100 was tried and it was found to be too high. The compromise gain of 544 was selected. The  $G_{\delta a_r} = 544$  gave a loop gain of  $1.0 \text{ } ^\circ \delta_a / \text{sec } r$  at 10,000 feet. This gave satisfactory performance.

The turn control gain was set such that  $\pm 3$  deg/sec turn rate was obtained in the  $\pm$  mechanical travel midpoint of the turn knob. This was found acceptable to the pilot.

The heading gain was initially set such that 10 degrees heading select would command 3 deg/sec turning rate. This proved to be much too high a gain. The gain was tried at various levels and left at  $0.1 \text{ degree } \delta a / \psi$ , the nominal value. A pressure gain of 30 was required to achieve the nominal heading gain. The higher heading gains were tried in an attempt to make the heading select more useful. The directional gyro has a maximum output at  $\pm 15$  degrees heading error. For good heading select utility, the aircraft should have at least a standard turn rate capability. The ratio of the heading to aileron gain,  $\delta a_\psi = 0.1$ , to the yaw rate to aileron gain,  $\delta a_r = 1.0$ , is  $0.1^\circ / \text{sec } r / 1^\circ \psi$  as set up in the flight checkout. The directional gyro heading error signal is limited to a maximum yaw rate of  $\pm 1.5$  deg/sec. At cruise airspeeds, the resulting maximum bank angle is about 15 degrees. The result of setting the heading gain at  $0.1^\circ \delta a_\psi$  is that heading select is slow because turning rate commanded is slow and is limited by the directional gyro's maximum heading error capability of  $\pm 15$  degrees.

The yaw rate to rudder pressure gain was initially set at 390. Flight testing found this to be low so it was increased to 900. This gave a

damping ratio of about 0.4 and was considered acceptable. Some difficulties were encountered during the first 2 flights in that an amplifier was accidentally phased wrong in the yaw damper circuit. This resulted in opposite rudder motion to that desired. The amplifier phasing was corrected by routing the signal tubes properly.

The pitch rate to elevator pressure gain was initially set at 590. Pitch axis performance was unsatisfactory because of the altitude hold mode. In an effort to improve altitude hold performance the pitch rate pressure gain was increased to 1100, the maximum obtainable.

The altitude error to elevator pressure gain was initially set at 170. Flight performance was poor because gain increased by a factor of four for altitude errors below reference altitude. This was caused by mechanization problems in the altitude lead circuit. Much effort was expended in making the altitude to elevator gain linear. This required four circuit changes which were:

1. Move the gain adjust flow divider from across the output of the altitude error sensor to across the output of amplifier A16.

This change provided a linear altitude error into the lead network. The gain adjuster was put across the altitude sensor to provide gain adjusting capability and to lower the scale factor at that point in the circuit. The gain adjuster introduced a non-linearity when put across the altitude sensor.

2. Amplifier A-11 was loaded with a 10 x 5 amplifier, i. e., A11 drives a loading amplifier as well as amplifier A-12.

This change lowered the scale factor back to the point it had been with the gain adjuster but in a linear fashion.

3. Null lead network amplifiers, A-13, A-14 and A-15. This was done to permit the full range of possible altitude error signals to pass through the network.
4. Rephase the summing inputs to A4. This was done because A4 summing inputs had different input impedances and matching the inputs with A16 outputs provided a more linear curve.

After the lead network was linearized a pitch trim problem became apparent. The pitch axis is mechanized such that selecting pitch on the pilot's function selector feeds both pitch rate and altitude error into the elevator. It was found that when the pitch axis was engaged a pitch transient resulted. To determine the cause of the transient a temporary additional switch was added. The function selector pitch switch engaged the pitch rate feedback and the added switch engaged the altitude feedback.

The pitch transient was found to be due to inability of the pilot to trim the pitch axis to zero. This is caused by poor visibility and indication of the pitch trim indicator. Once trimmed to zero, engagement of the altitude mode was smooth and satisfactory.

Altitude hold mode performance was stable at 5000 feet. At 10,000 feet, however, it is divergent. Further work during the NASA flight test program was planned to make it acceptable.

The loop gains established during Contractor Checkout were:

- Lateral Axis

$$\text{Yaw rate to aileron, } \delta_{a_r} = 1.0 \frac{\text{°Aileron (Differential)}}{\text{°/sec yaw rate}}$$

$$\text{Heading to aileron, } \delta_{a_\psi} = 0.1 \frac{\text{°Aileron (Differential)}}{\text{°Heading Error}}$$

$$\text{Yaw rate to rudder, } \delta_{r_r} = 0.6 \frac{\text{°Rudder}}{\text{°/sec}}$$

- Longitudinal Axis

$$\text{Pitch rate to elevator, } \delta_{e_q} = 0.7 \frac{\text{°Elevator}}{\text{/sec}}$$

$$\text{Altitude error to elevator, } \delta_{e_h} = 0.01 \frac{\text{°Elevator}}{\text{Foot}}$$

The block diagrams of the lateral and longitudinal axes are given in Figures 1 and 2, respectively. The values shown on the diagrams are the design nominal values.

The changes in loop gain were made during the flight-contractor checkout period to improve performance. Further changes were expected to be made during the NASA flight test program to optimize the gains.

#### Final System Configuration

A number of hardware changes were made in the system during the flight checkout. These changes are documented by the list below:

1. R7 "Yaw Trim Pressure Level" orifice in the Yaw Roll FCA changed from 0.005 to 0.004 in.
2. R9 "Roll Trim Pressure Level" orifice in the Yaw Roll FCA changed from 0.006 to 0.0047 in.
3. R10 "Turn Pressure Level" orifice in the Yaw Roll FCA changed from 0.005 to 0.0049 in.
4. R1 and R2 "Roll PWM Time Constant" orifices in Yaw Roll FCA changed from 0.010 to 0.009 in.

5. R14 "Yaw Axis Pressure Gain" adjustable orifice in Yaw Roll FCA removed.
6. Adjustable orifice added to turn circuit in Yaw Roll FCA between connections 11 and 12.
7. Adjustable orifice added to pitch trim circuit in Pitch FCA between connections 5 and 6.
8. 0.0059 orifice added to Heading Circuit in system tubing across connections 13 and 14 of the Yaw Roll FCA.
9. R5 "Pitch Axis Pressure Gain" adjustable orifice in Pitch FCA removed.
10. Adjustable orifice added to altitude circuit in Pitch FCA across the output of A16.
11. Adjustable orifice across the input to A-11 in Pitch FCA removed.
12. Low Impedance 10 x 5 amplifier added in parallel with A-12 in Pitch FCA. A-11 now drives two amplifiers, A-12 and added amplifier.

Figures 41 through 55 are examples of flight performance of the system. The recordings are representative of system performance with the final gains, and the configuration as shown on Figures 1 and 2. All of this series of recordings was obtained on Contractor flights 8 and 9. Flight conditions represented are cruise:

- Condition 1 - 5,000 feet, 160 knots indicated airspeed, 2600 RPM. Severe turbulence was present in all recordings at this flight condition.

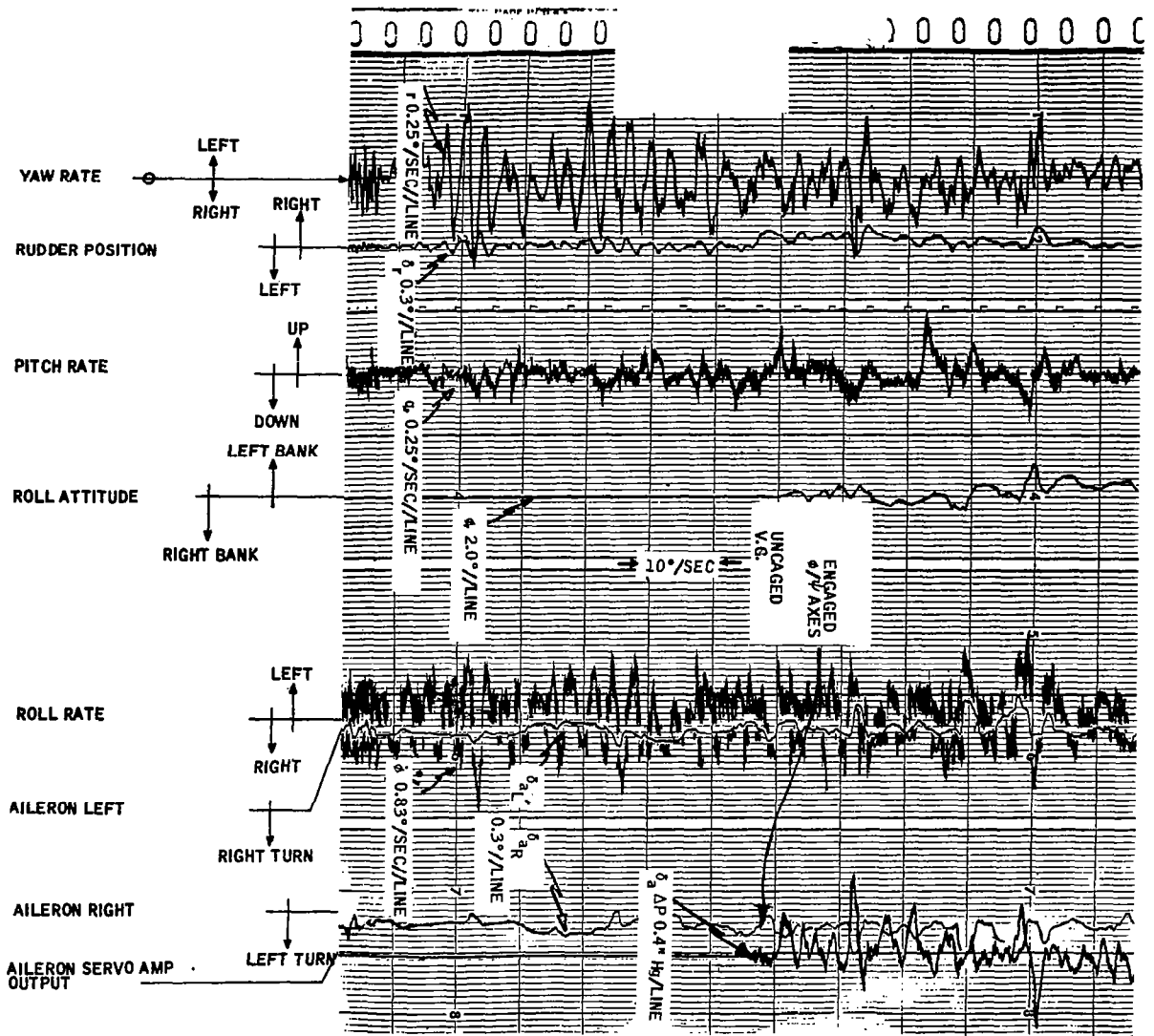


Figure 41. Performance During Contractor Flight Checkout

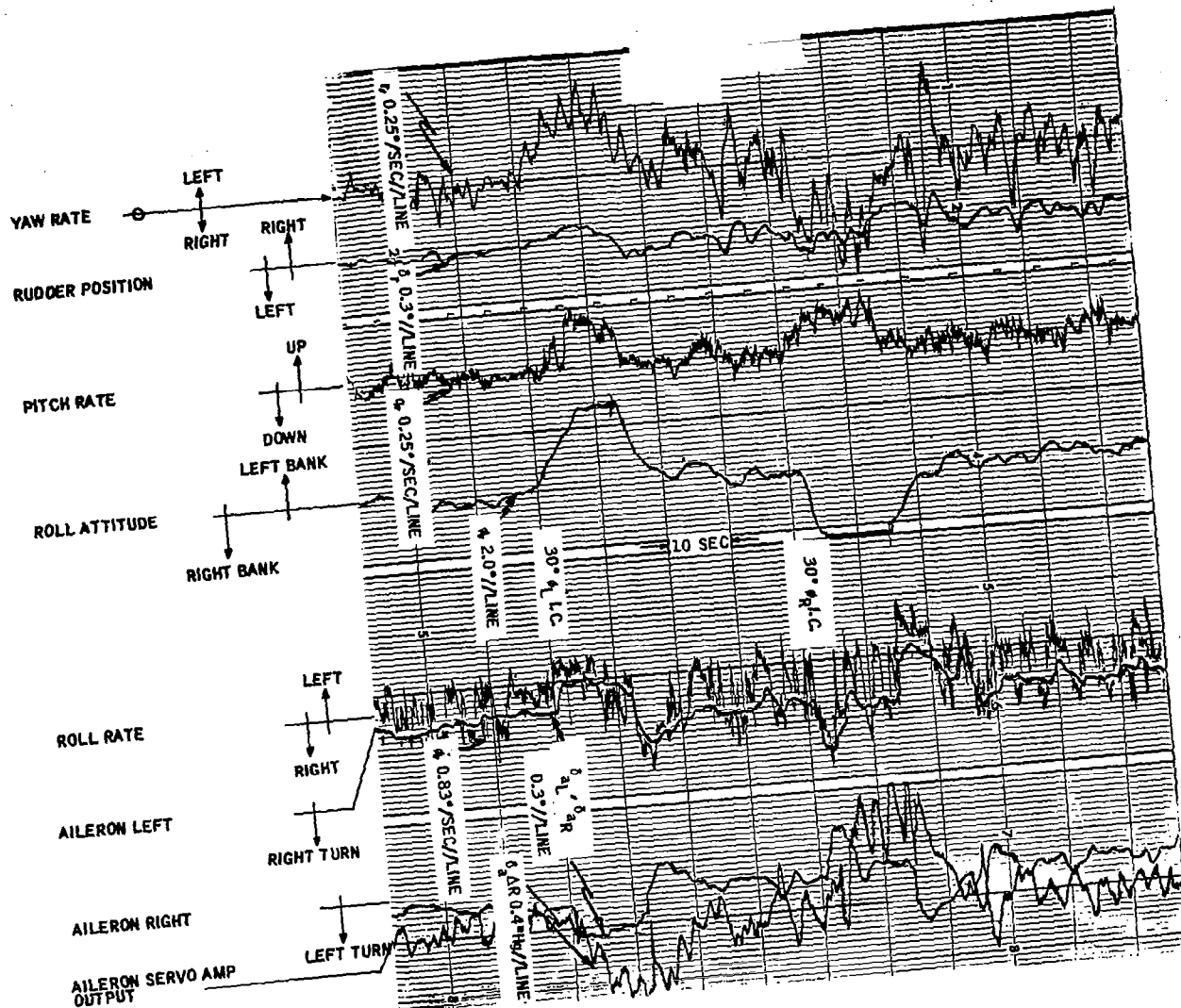


Figure 42. Performance During Contractor Flight Checkout

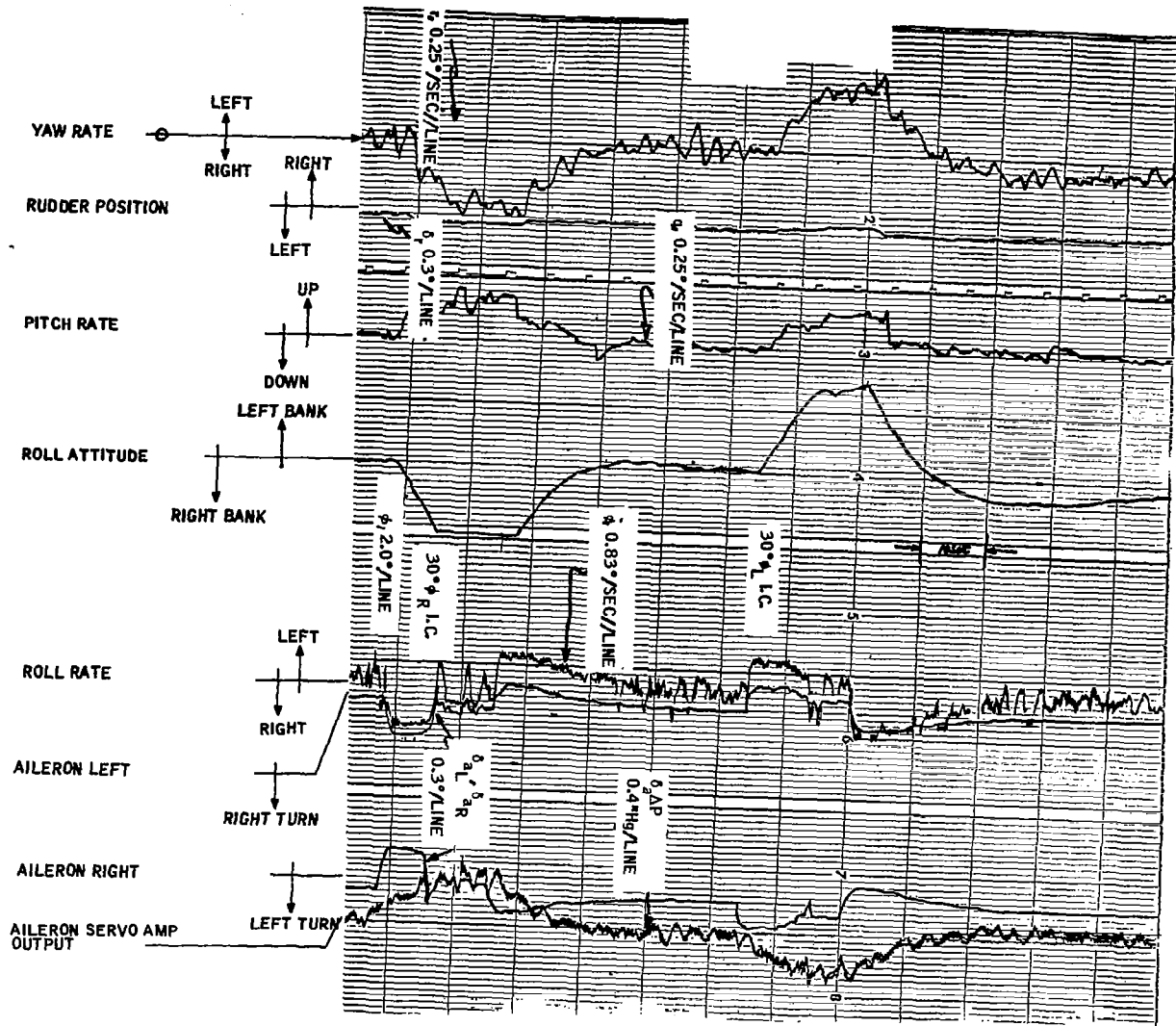


Figure 43. Performance During Contractor Flight Checkout

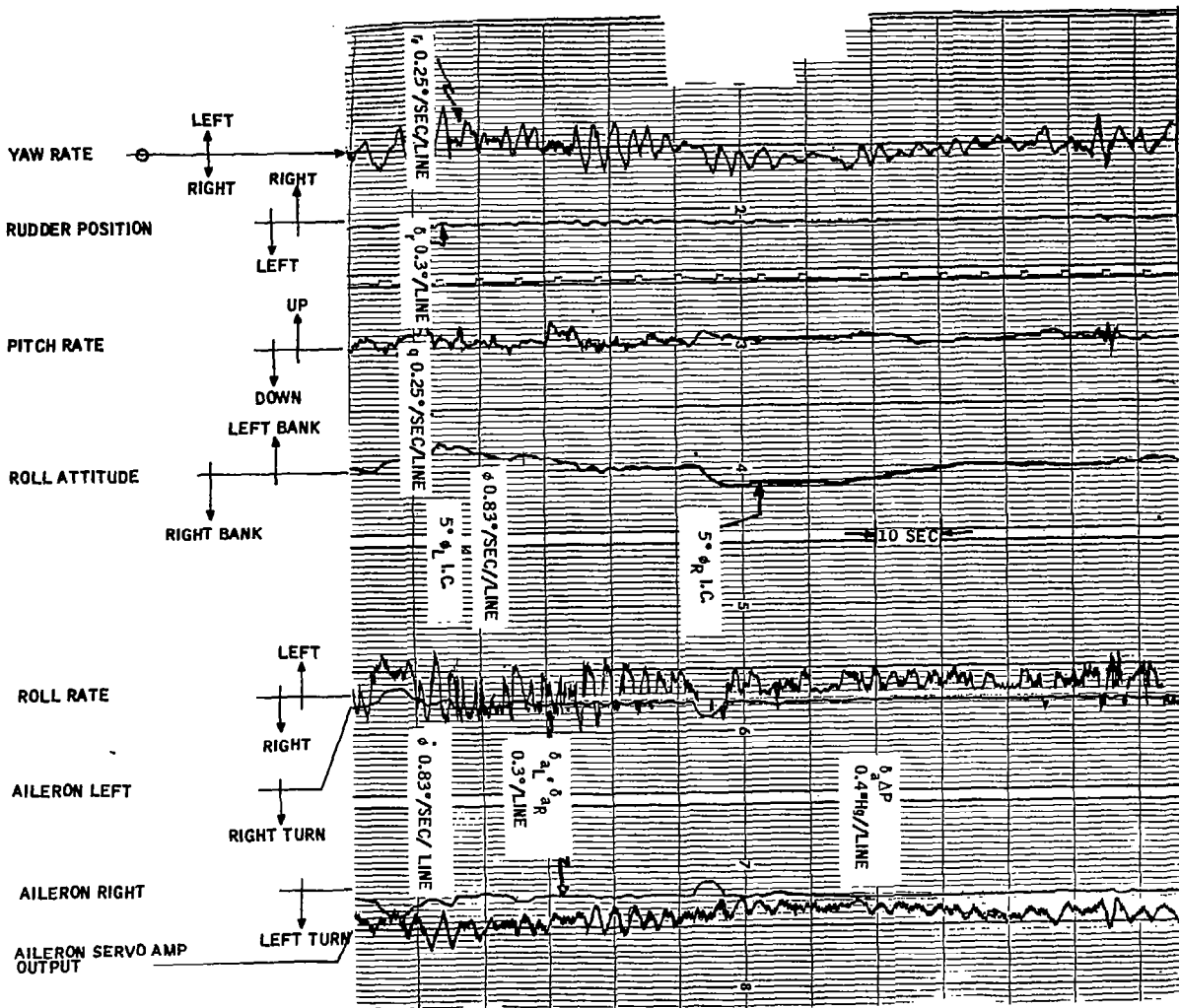


Figure 44. Performance During Contractor Flight Checkout

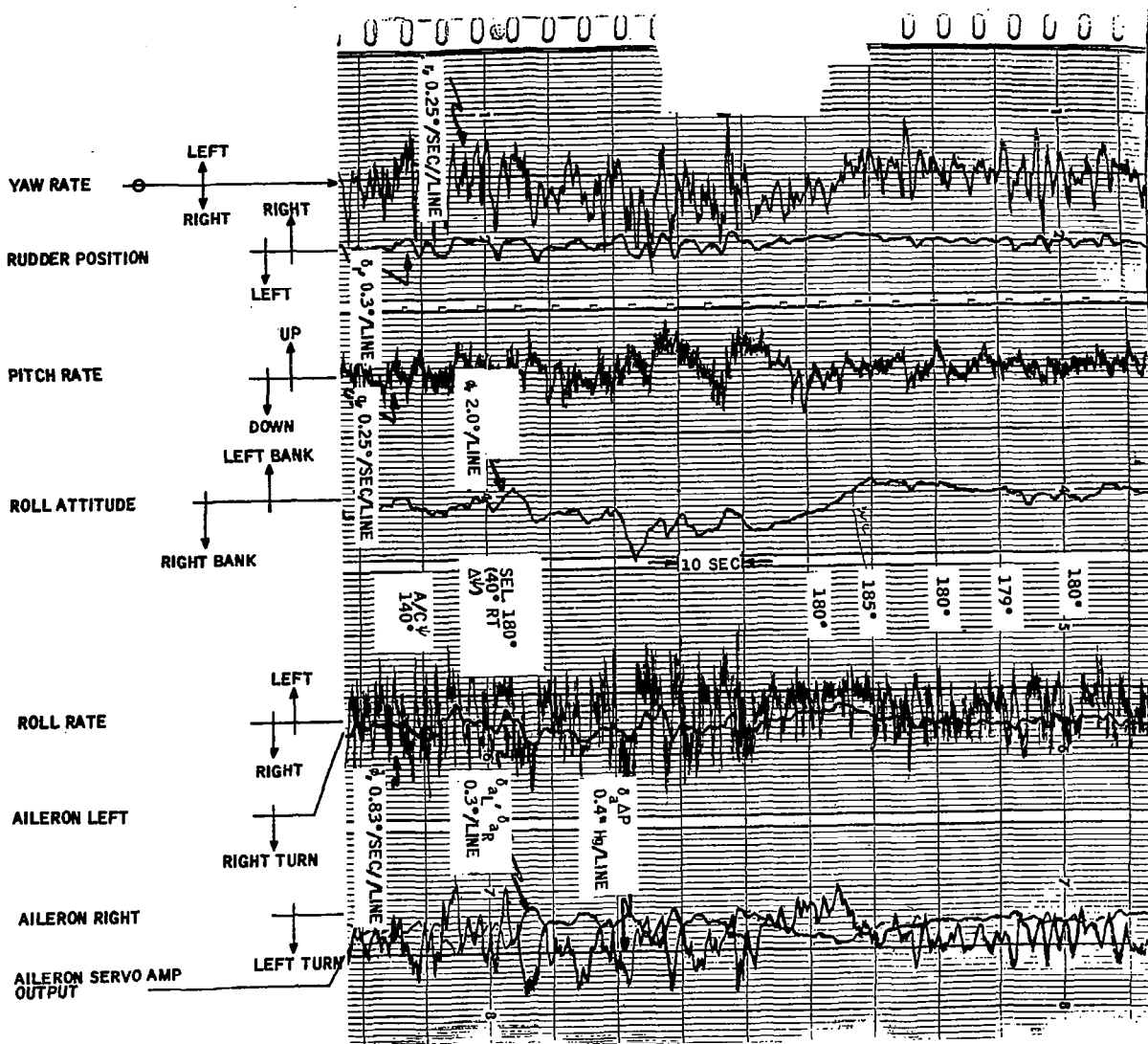


Figure 47. Performance During Contractor Flight Checkout

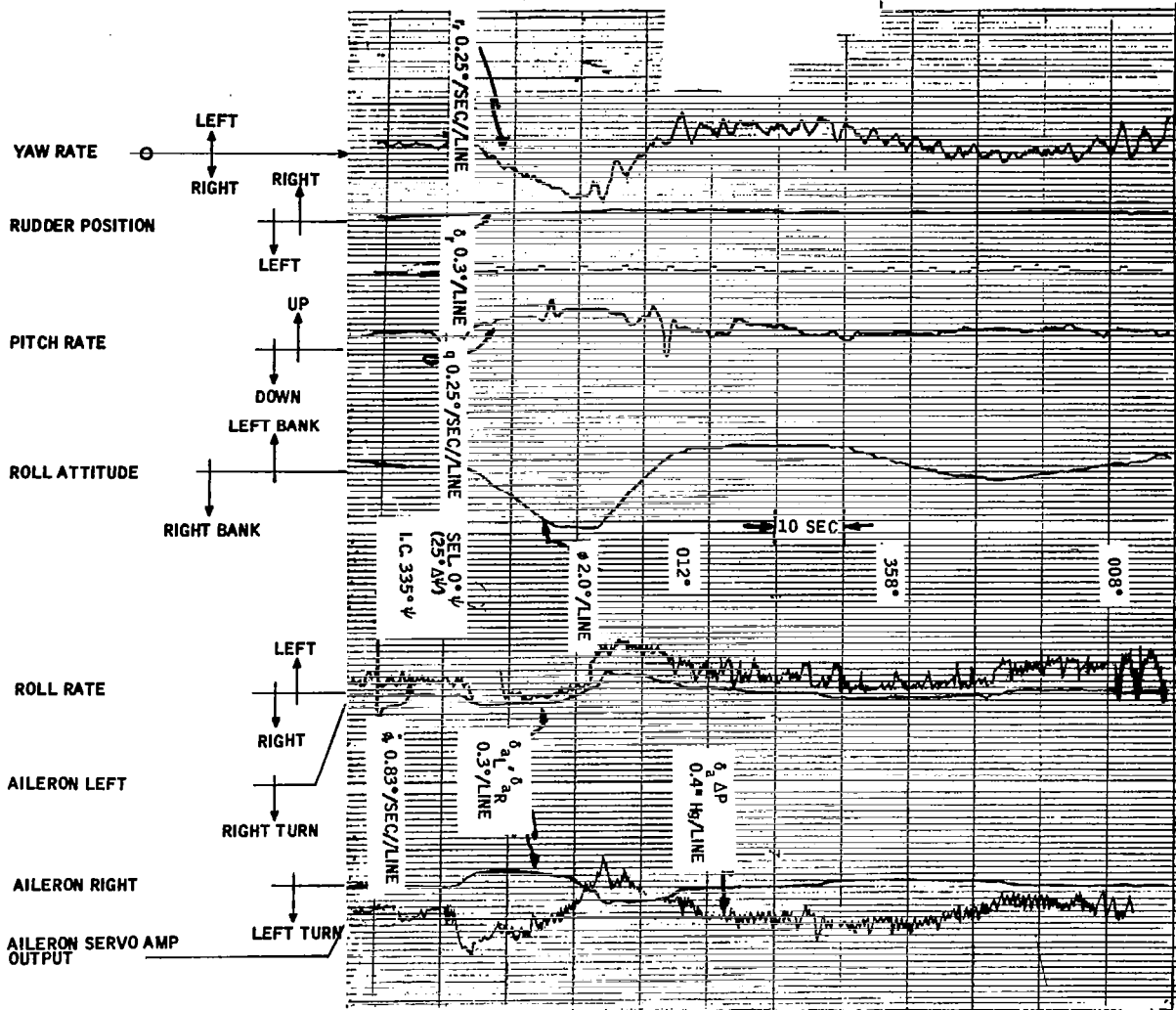


Figure 48. Performance During Contractor Flight Checkout

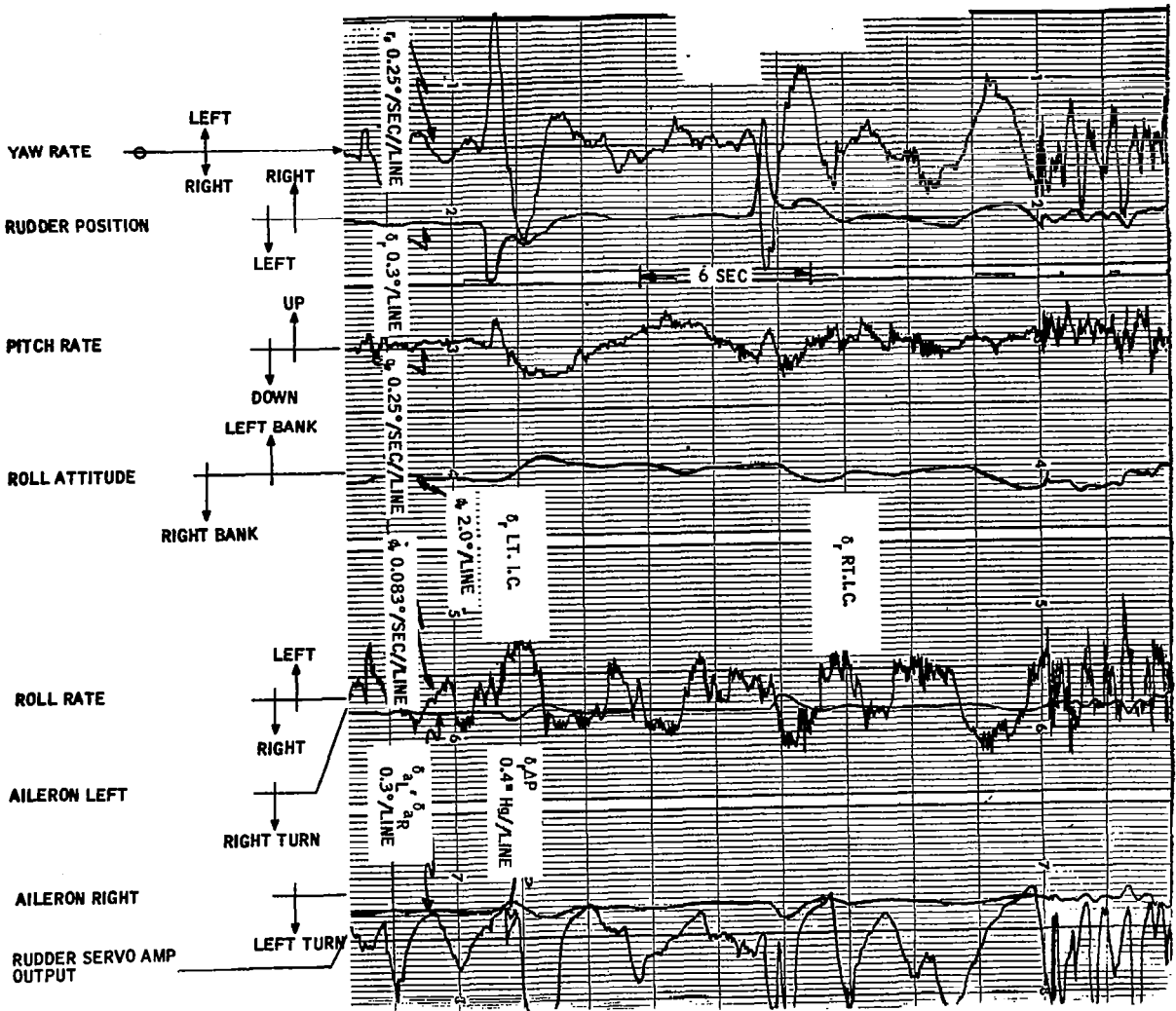


Figure 49. Performance During Contractor Flight Checkout

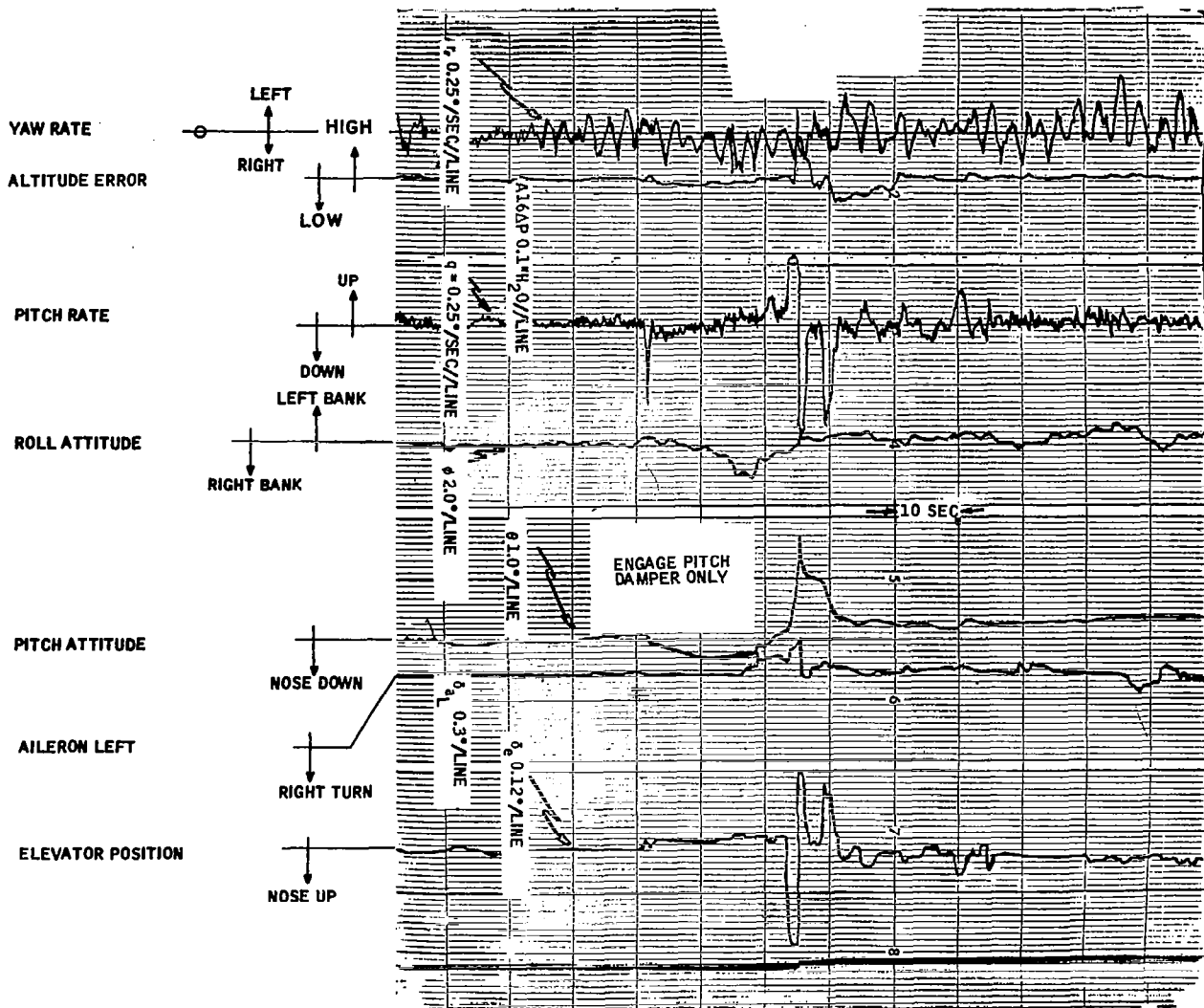


Figure 50. Performance During Contractor Flight Checkout

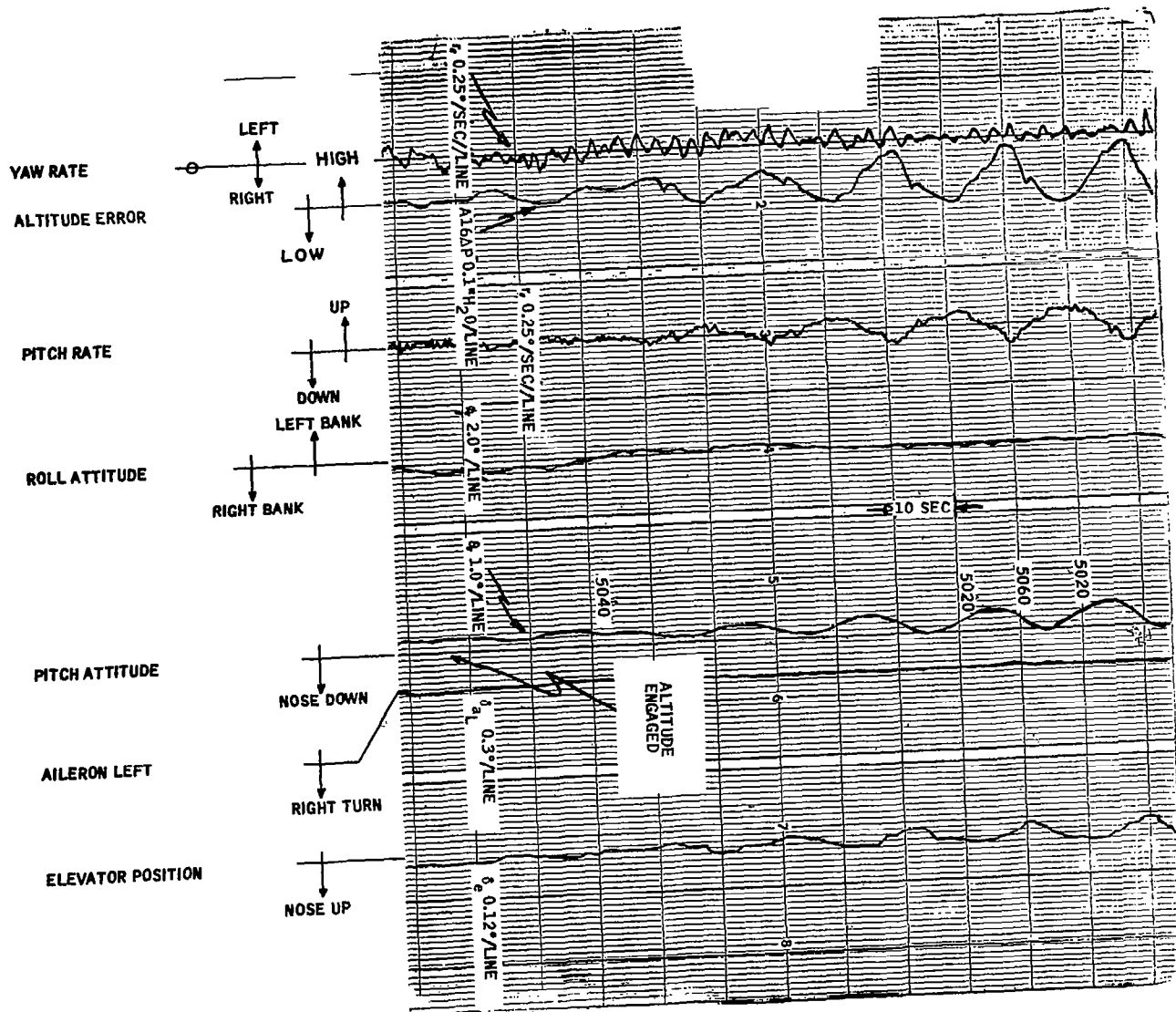


Figure 51. Performance During Contractor Flight Checkout

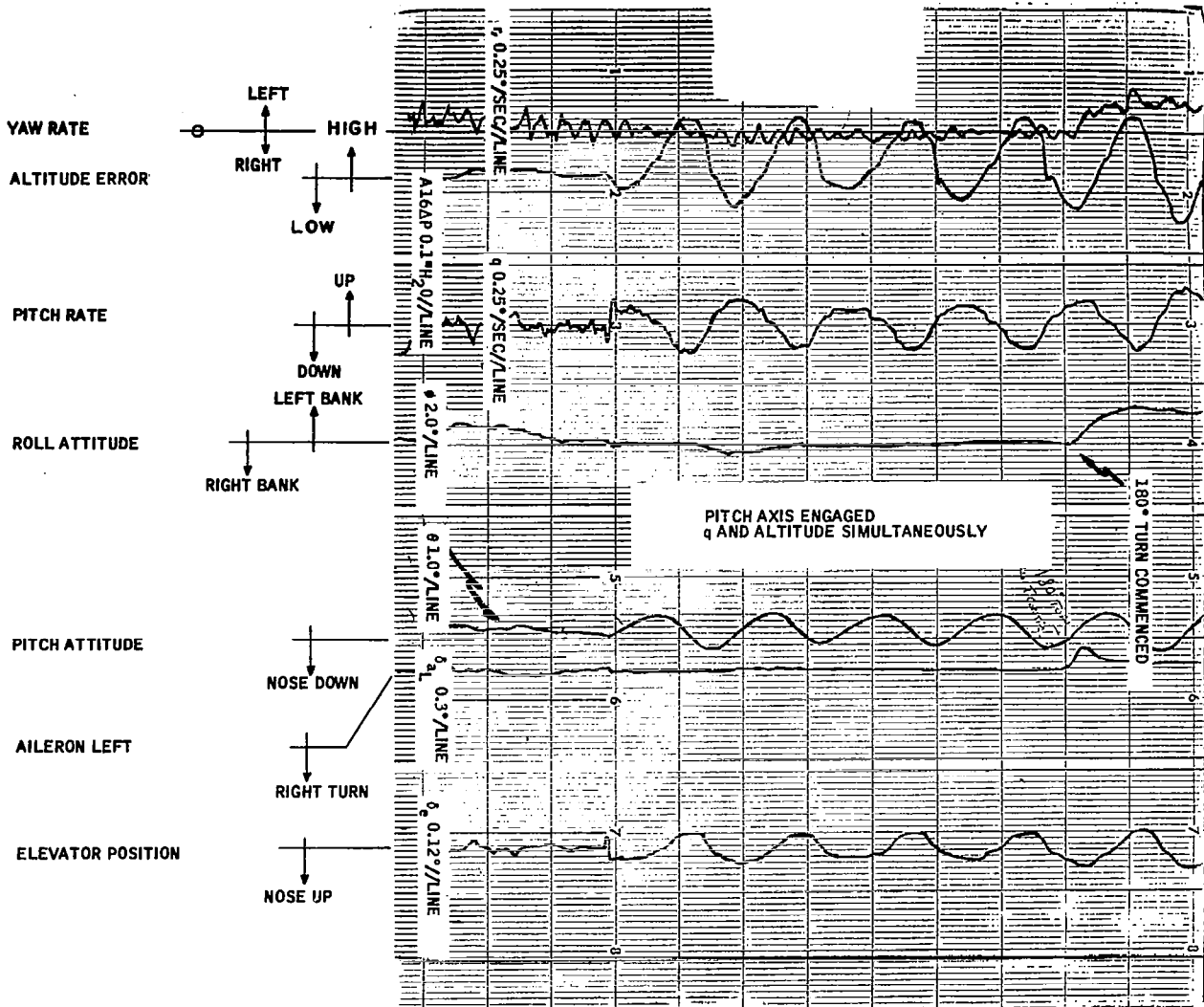


Figure 52. Performance During Contractor Flight Checkout



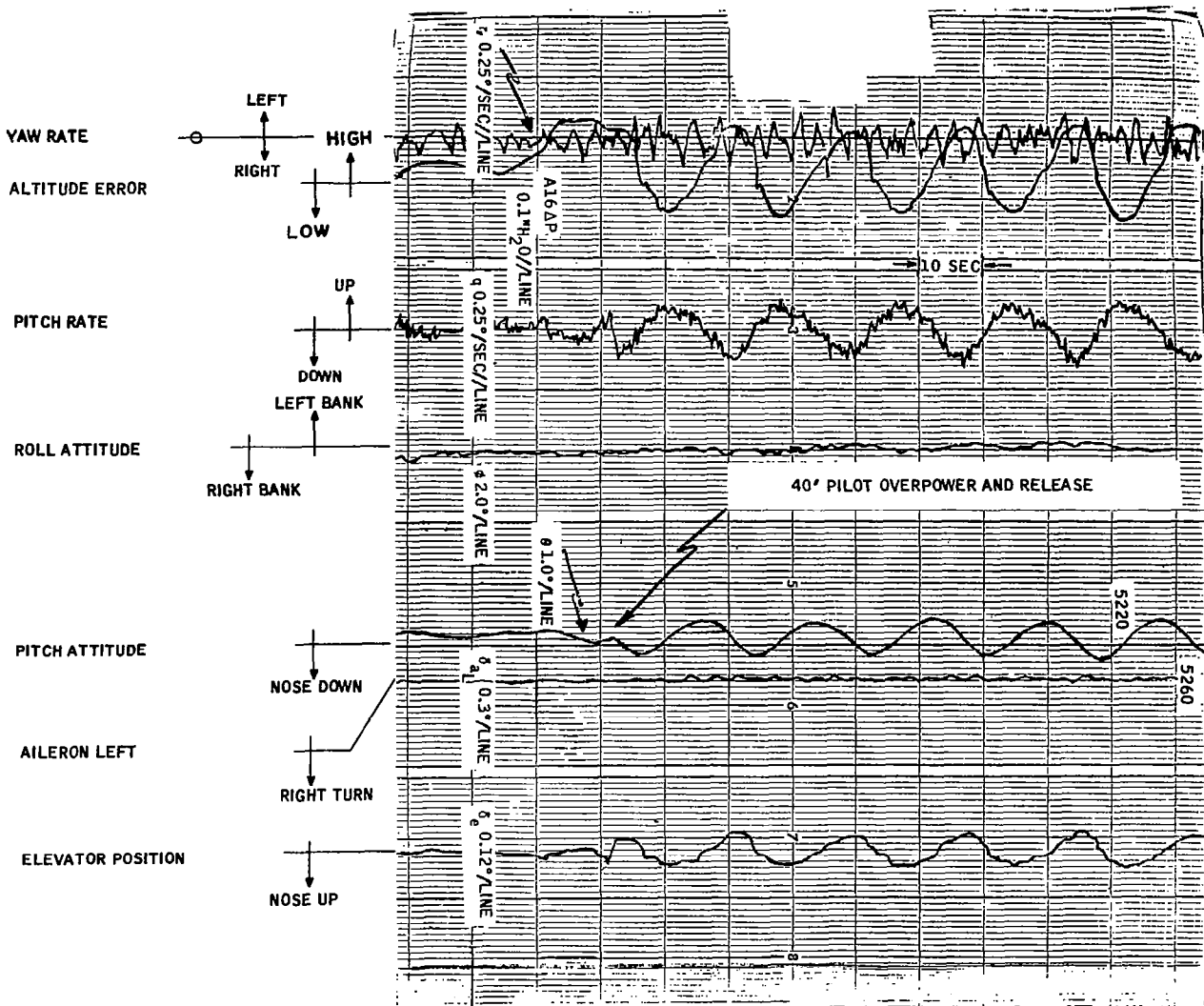


Figure 54. Performance During Contractor Flight Checkout

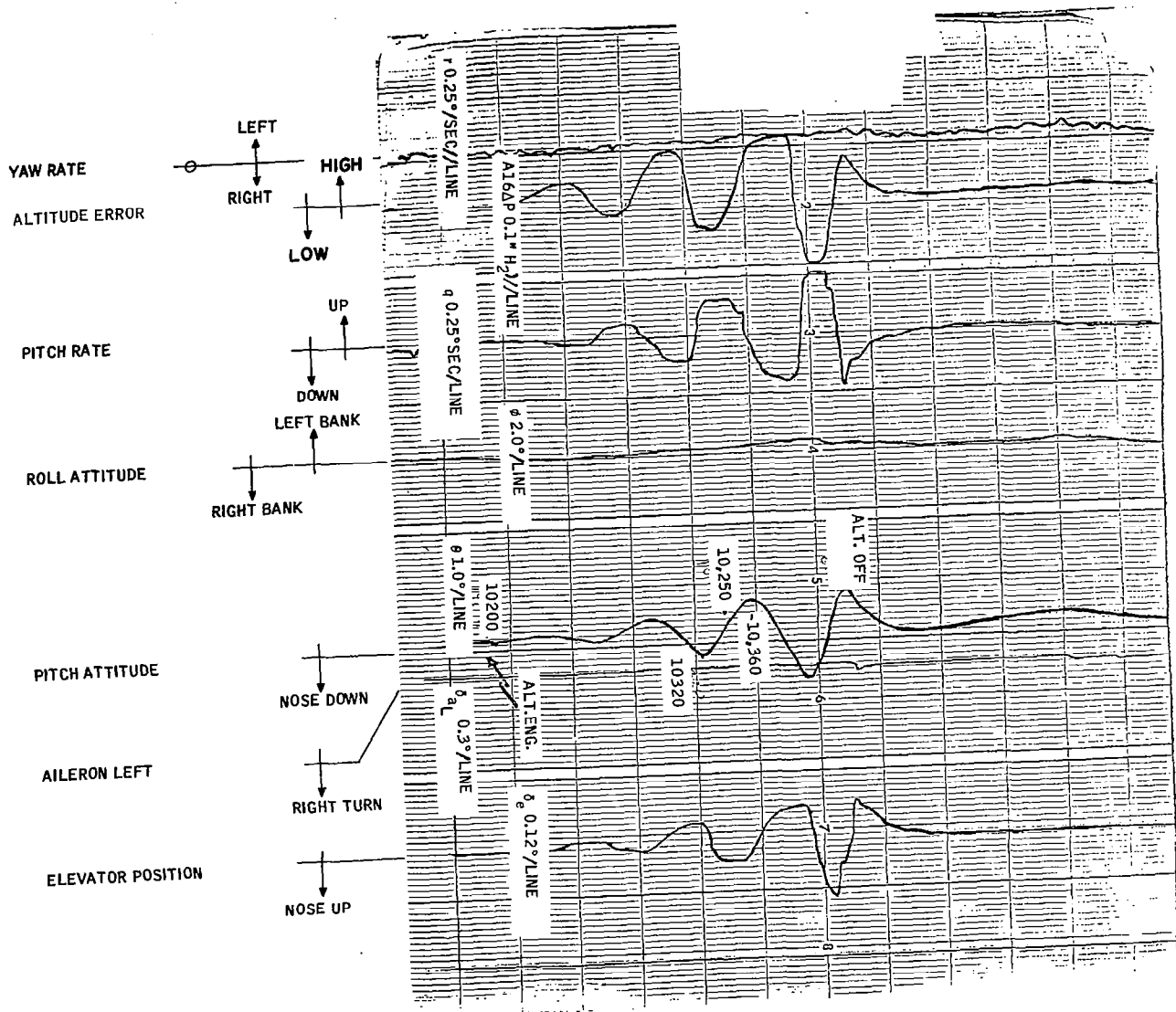


Figure 55. Performance During Contractor Flight Checkout

- **Condition 2 - 10,000 feet, 160 knots indicated airspeed, 2800 RPM.**  
**Air conditions varied from smooth to light turbulence.**

The recorded parameters are listed with appropriate scale factors on the recording. The signals are all recorded from instrumentation sensors except for channel 8,  $\delta_a \Delta P$ , aileron differential pressure. This is the fluid system aileron servo amplifier output which drives the aileron servos.

Figure 41 is at cruise condition 1 and shows engagement of the roll and yaw axes. Severe turbulence is present at this flight condition as shown by the free aircraft recording prior to engagement of the control system. Yaw rate excursions due to turbulence are reduced when the system is engaged. The instrumentation vertical gyro was not uncaged (inadvertently) until about three seconds after engagement.

Figure 42 shows system performance at flight condition 1 when subjected to  $\pm 30^\circ$  roll attitude initial conditions. When released the aircraft is rolled to wings level in approximately eight seconds. It will be noted that at this flight condition the responses to right and left initial bank angle conditions are nearly identical. Excursions about the wings level position are due to air turbulence.

Figure 43 shows wing leveler performance at flight condition 2 when subjected to  $\pm 30^\circ$  roll attitude initial conditions. When released the aircraft is rolled to wings level in approximately 15 seconds with 2 to 6 degrees roll attitude overshoot. The overshoot in roll attitude from a left bank is greater than from a right bank. This difference in apparent damping is thought to be due to differences in aircraft control cable friction.

This difference is not seen at flight condition 1 where the air turbulence effectively "dithered out" the effects of aircraft control system friction levels. The smooth responses of Figure 43 are an effective illustration of the air turbulence effects.

Figure 44 shows wing leveler responses at flight condition 2 to  $\pm 5^\circ$  roll attitude initial conditions. Again, there is a noticeable difference in the solution time to wings level between left and right banks. The aircraft tended to hold or hang off on the  $5^\circ$  bank right initial condition - apparently due to higher control system friction level in that direction.

Flight performance to turn commands is shown in Figures 45 and 46. The commands were inserted using the function selector turn control. Figure 45 is at flight condition 1; Figure 46 is at flight condition 2.

Heading select performance is shown in Figures 47 and 48. The maximum heading signal is obtained for a  $20^\circ$  heading error. Since both figures show heading selections of greater than  $20^\circ$ , the only difference in response should be flight condition. The presence of air turbulence obscures the comparison of the two flight conditions. The aircraft heading was not recorded but was written in from pilot call outs of aircraft heading read from his compass.

Yaw damper performance is shown by Figure 49. The aircraft was given left and right rudder kicks. Damping ratio is approximately 0.3 at this flight condition.

Channel 8 records system rudder servo amplifier output which drives the rudder. Note that the time scale has been changed by speeding up the paper.

Figures 50 through 55 document pitch axis performance. The pitch axis has two feedback signals, pitch rate and altitude error. The system is mechanized such that engagement of the pitch axis engages both feedbacks simultaneously. It was found that when the pitch axis was engaged a pitch transient resulted. To determine the cause of the transient a temporary additional switch was added. The function selector pitch switch engaged the pitch rate feedback and the added switch engaged the altitude feedback. After resolving some lead network mechanization problems it was found that the pilot had difficulty trimming the pitch axis to zero inputs to the servo. The resulting mistrim caused the pitch transient.

The roll and yaw axes are also engaged throughout the sequence of Figures 50 through 54. Channel 5 has been changed to pitch attitude. Channel 7 has been changed to elevator position. Channel 8 is inoperative. Channel 2 is the output of pitch FCA amplifier 16 which is the altitude error after being shaped by the lead network. This signal is summed with pitch rate and is then the elevator control signal.

Figure 50 is an engagement of the pitch rate feedback only. The initial nose down pitch motion is probably caused by the mistrim present at engagement. The pilot then overpowered and trimmed the system until zero aircraft motion was present.

Figure 51 follows Figure 50 chronologically in flight sequence and shows engagement of the altitude feedback. Aircraft altitude is not available as a recorded signal. The pilot called out altimeter readings at peak altitudes and these were written on the recordings. After engagement of the altitude feedback, a limit cycle with an 18 second period and  $\pm 20$  feet amplitude developed. The pitch attitude limit cycle amplitude was approximately  $\pm 2.0$  degrees.

Figure 52 shows both pitch rate and altitude being engaged at the same time. This engagement is after trimming had been accomplished as shown in Figures 50 and 51.

Figure 53 shows performance in turns which were commanded by the Turn Control. The limit cycle is still present, with less amplitude. This performance was considered acceptable by the pilot.

Figure 54 shows a pilot overpower initial condition of 40 feet high altitude error. The aircraft response was to correct the error and resume the limit cycle.

**Figure 55 is at flight condition 2, 10,000 feet altitude. At this flight condition the altitude hold is divergent. It is expected that the flight test program will result in optimization of gain and phase lead required on the altitude signal such that 10,000 foot altitude performance will be satisfactory.**

## SECTION V

### CONCLUSIONS AND RECOMMENDATIONS

**This program demonstrated that a fluidic flight control system for light aircraft is possible. System performance is as good, in most cases, as similar conventional systems; in some cases it is better. Excellent system reliability was demonstrated. In spite of the breadboard nature of the system, no failure has been experienced since flying started. Significant developmental and operational experience with fluidic systems has been obtained. This operational system serves both as a demonstrator and as a test bed for future work.**

**A continued program is desirable to optimize system performance, particularly with respect to the altitude hold mode, and to refine the breadboard hardware.**

- **The function selector flow dividers used for trim control do not present the proper feel to the pilot and some sensitivity to vibration was experienced in flight.**
- **The altitude hold mode performance is being adversely affected by insufficient error signal range and linearity in both the altitude error sensor and altitude shaping circuit.**
- **The pitch damper gain appears to be inadequate for providing the required tight inner loop for satisfactory altitude hold above 6,000 feet.**
- **Better yaw rate damping could be achieved if more gain were available in the yaw axis.**
- **The present fluidic servo amplifiers recover approximately 40 percent of their power supply. A greater recovery amplifier would reduce the load on the aircraft pneumatic system.**

*"The aeronautical and space activities of the United States shall be conducted so as to contribute . . . to the expansion of human knowledge of phenomena in the atmosphere and space. The Administration shall provide for the widest practicable and appropriate dissemination of information concerning its activities and the results thereof."*

—NATIONAL AERONAUTICS AND SPACE ACT OF 1958

## NASA SCIENTIFIC AND TECHNICAL PUBLICATIONS

**TECHNICAL REPORTS:** Scientific and technical information considered important, complete, and a lasting contribution to existing knowledge.

**TECHNICAL NOTES:** Information less broad in scope but nevertheless of importance as a contribution to existing knowledge.

**TECHNICAL MEMORANDUMS:** Information receiving limited distribution because of preliminary data, security classification, or other reasons.

**CONTRACTOR REPORTS:** Scientific and technical information generated under a NASA contract or grant and considered an important contribution to existing knowledge.

**TECHNICAL TRANSLATIONS:** Information published in a foreign language considered to merit NASA distribution in English.

**SPECIAL PUBLICATIONS:** Information derived from or of value to NASA activities. Publications include conference proceedings, monographs, data compilations, handbooks, sourcebooks, and special bibliographies.

**TECHNOLOGY UTILIZATION PUBLICATIONS:** Information on technology used by NASA that may be of particular interest in commercial and other non-aerospace applications. Publications include Tech Briefs, Technology Utilization Reports and Notes, and Technology Surveys.

*Details on the availability of these publications may be obtained from:*

SCIENTIFIC AND TECHNICAL INFORMATION DIVISION  
NATIONAL AERONAUTICS AND SPACE ADMINISTRATION

Washington, D.C. 20546